Properties of Enhançons in Supergravity

Apostolos A. Dimitriadis

A Thesis presented for the degree of
Doctor of Philosophy

Centre for Particle Theory
Department of Mathematical Sciences
University of Durham
England

December 2003

Στους Γονείς μου και στον αδερφό μου Κωνσταντίνο.

Properties of Enhançons in Supergravity

Apostolos A. Dimitriadis

Submitted for the degree of Doctor of Philosophy
December 2003

Abstract

A certain class of naked singularities, related to $\mathcal{N} = 2$ pure super Yang–Mills theory, are resolved in string theory with the enhançon mechanism. We study the properties of the enhançon in supergravity. Initially we consider the stability of the supergravity solutions. We study small perturbations of these solutions, constructing a sufficiently general ansatz for linearised perturbations of the non-extremal solutions, and show that the linearised equations are consistent. We investigate linearised perturbations of the horizon branch and the extremal solution numerically. We show that these solutions are stable against the perturbations we consider. This provides further evidence that these latter supergravity solutions are capturing some of the true physics of the enhançon. We show that the shell branch solutions violate the weak energy condition, and are hence unphysical. We extend the investigation of nonextremal enhançons, finding the most general solutions with the correct symmetry and charges. There are two families of solutions. One of these contains a solution with a regular horizon found previously; this previous example is shown to be the unique solution with a regular horizon. The other family generalises a previous nonextreme extension of the enhançon, producing solutions with shells which satisfy the Weak Energy Condition. We argue that identifying a unique solution with a shell requires input beyond supergravity.

Declaration

The work in this thesis is based on research carried out at the Centre for Particle Theory, the Department of Mathematical Sciences, the University of Durham, England. No part of this thesis has been submitted elsewhere for any other degree or qualification and it all my own work unless referenced to the contrary in the text. Chapter 4 of the thesis is based on a joint research with my supervisor Dr. Simon F. Ross, published in reference [1]. Sections 5.1–5.3 of Chapter 5 are based on a joint research with Dr. Simon F. Ross, published in reference [2], while Section 5.4 of the same chapter contains independent unpublished results. Chapter 6 is based on a joint research with Dr. Simon F. Ross, Dr. Amanda W. Peet and Geoff Potvin, published in reference [3]. References to other people's work are given as appropriate throughout the text.

Acknowledgements

Ad Majorem Dei Gloriam

I wish to take this opportunity to thank all the people who have helped me all these years and contributed to the completion of this work.

First of all I would like to express my deepest gratitude to my supervisor Dr. Simon Ross. His patience, understanding, encouragement and guidance during all the stages of the preparation of this work have been invaluable.

Since this is my last act as a student, I would like to thank people who have been my teachers and shaped my understanding of the cosmos. I would like to thank all staff members of the Mathematics Department of Durham University and of the Physics Department of Aristotle University of Thessaloniki. I am indebted to Dr. Nikolaos Vlachos, Prof. Georgios Gounaris, Dr. Dimitrios Papadopoulos and Dr. Douglas Smith for everything that they taught me, for their advices and their interest. I am indebted to Dr. Ruth Gregory and Dr. Nick Evans for their suggestions and critical comments on this thesis.

Dr.s Babis Anastasiou, Christos Charmoussis, Ioannis Floratos and Georgios Tzamtzis were usually among the first people to ask for advice. They have all helped me a lot and part of this can be seen in this thesis. I would like to thank Dr Kostas Kokkotas for various comments and suggestions.

I would like to thank Amanda Peet and Geoff Potvin for the collaboration that resulted in the sixth chapter of the thesis.

Jessica Barrett and Paul Bostock had tons of patience, sharing an office with me. I learnt from discussions with them. I would also like to thank Dr. James Gregory, who helped me at the initial stages of the numerics, Daniel Bundzik, Dr. Laur Järv, Dr. Mark Hale and Emily Hackett–Jones for nice discussions.

Professors George Zoupanos and Elias Kiritsis managed to fund my participation in two conferences–schools that they were organising. I am indebted to both them. EPSRC has funded my studies by paying for my tuition fees and for a string theory school in Trieste, plus travelling expenses for the previous mentioned schools. I am also funded by the University of Durham for my living expenses and I must thank Professor Wojciech Zakrzewski for securing this funding for me.

My thanks go also to all the people who made my stay in Durham a very enjoyable one. I would like to thank Ioanna Sotiropoulou, Ioannis 'The Vampire' Rodios, Leonidas Tzonis, Christos 'Blondie' Evangelidis, George Georgiou, Kostas Mpotsialas, Michael Abson, George Tzamalis, Dyanne Zimmerman, George Filis, Lena Bakatsi, Stephanie Fehr, Caroline Loutre, Dr. Ioannis Platis and Dr. Christos Spanos for being good friends and for helping me whenever I was in need. I would also like to thank Kelly, Manolis, Stauros, George K., Nikos, Barbara F., Barbara D., Amel, Sonia, Matthias, Chantal, Aggelos, Pepe, Christina, Lena, Aristea, Christos C., Dimitris G., Dimitris B., Vaggelis, Manapol, Aimilios, Litsa, Thani, Matthew, Andreas, Kostas P. and Stelios T.

In addition I would like to thank my colleague and very good friend for almost a decade Konstantinos Kyritsis. His enthusiasm and clear thinking were enough to understand a lot in every aspect of my life, academic or otherwise.

Last but not least I would like to thank my Parents and my brother Konstantinos. Their love, support and encouragement have been overwhelming and no words of gratitude can ever be enough.

Contents

List of Figures

Chapter 1

Introduction

Our current understanding of the physical laws governing nature is based on two main theoretical frameworks. One is Quantum Mechanics and its sibling Quantum Field theory, which describes the microcosm with great accuracy. Electromagnetic, weak and strong forces are described by Quantum Field Theories, and their success in explaining physics of molecules, atoms, nuclei and elementary particles is tremendous [4]. The other one is Einstein's General Relativity which describes the macrocosm. This is a geometrical theory of gravity which explains very well phenomena of cosmological scale down to one millimetre [5, 6]. It expanded our understanding of the universe and its expansion, of its constituent galaxies, stars and their evolution.

Gravity is a very weak force compared with the other three, so we do not in general take it into account when studying phenomena in the microcosm. There is a point though, where gravity becomes important. For length scales of the order of the Planck length $l_{Planck} \sim 10^{-35}$ m, gravity as a force becomes significant to the description of physical phenomena and must be taken into account. This is also the regime when gravity ceases to function as classical theory. We need a quantum theory of gravity in order to describe the physics correctly.

Since gravity is more relevant to much larger scales do we really need such a description? There are two physical arguments in favour. The first is that classical GR is not a complete theory. It allows spacetime singularities which can be found inside black holes and of course the initial singularity in the Big–Bang theory [7–

9]. Quantum gravity is needed in order to understand their physics. The second argument is that it is expected that all the forces of nature can be described by a unified theory. There is already a successful electroweak model in quantum field theory and various suggestions to incorporate the strong force[1], but as long as a quantum theory of gravity eludes us we can not have a complete understanding of fundamental physics.

There are various approaches towards a quantum theory of gravity. There are many difficulties trying to merge quantum mechanics and general relativity. The usual methods of quantum field theory do not apply in this case.

One of the main candidates is string theory. String theory is a theory of one–dimensional extended objects. It contains gravity and one can see that it can be quantised using the perturbative methods of quantum field theory. It also contains gauge bosons in the spectrum with a gauge group large enough to include the currently known interactions (electromagnetic, weak and strong). On top of that it knows how to treat certain kind of singularities. Unfortunately these theories live in more than four spacetime dimensions and there are five of them (superstrings) which are consistent at the quantum level.

In the last ten years there was a great advance in understanding string theory. There is a unified way to look at the theory, connecting the existent five theories together with eleven dimensional supergravity through various dualities. It was found that there are new objects, D–branes, which are very important [12]. D–branes opened a window to the non–perturbative regime of string theory. They helped understand the properties of black holes and spacetime, by describing mechanisms of singularity resolution.

These are the first steps in order to understand the quantum structure of spacetime. There are still difficulties and open questions but the road is open although not very clear.

[1]For more details, standard textbooks on Quantum Field Theory [10, 11], can be consulted.

1.1 Classical gravity

Gravity is the force that is binding the universe together and governs the dynamics of the various objects in it. It is its driving force. It is very weak, its range is infinite and because in large scales the net charges are zero, it is the dominant force in the universe.

Gravity is very well described by Einstein's General Relativity[2]. General Relativity is based on two principles. The first principle is the equivalence principle which states that all bodies are influenced by gravity and they fall precisely the same way in a gravitational field. The second is Mach's principle which states that it does not make sense to speak about an accelerating mass in an empty, absolute space.

The theory Einstein derived from these principles states that the intrinsic and observer–independent properties of spacetime are described by a spacetime metric. The curvature of this metric causes the physical effects ascribed to a gravitational field. The curvature of spacetime is caused by the existence of matter (or energy) and the relation is given by Einstein's equations. In simpler words matter tells spacetime how to curve and spacetime dictates to matter how it should move.

Although this theory has given many predictions which have been found to be with agreement with experiment, it is not complete. There appear solutions containing curvature singularities, where curvature is infinite. Classical curvature singularities are defined through geodesic incompleteness: a test particle will reach in finite proper time regions of spacetime beyond which its evolution is not defined. There are theorems due to S. Hawking and R. Penrose [7–9] which prove that singularities are inevitable and they are generic features of cosmological and collapse solutions.

An important goal in extending General Relativity is to understand the resolution of singularities. This can be done by classical extensions of the theory. Some of these singularities can be resolved by adding higher curvature interactions in the Einstein–Hilbert action, or higher derivatives of the metric and matter fields. These have a negligible contribution for ordinary gravitational fields but become important

[2] [13, 14] for more full presentations of the theory.

in regions of large curvature, modifying the nature of the solutions. This happens because adding these extra terms spoils some of the local energy conditions needed in order to prove the singularity theorems so one may hope that a singularity free theory of gravity may be constructed [15, 16]. There are also examples of singular solutions which become regular if they are thought of in terms of higher dimensional theories [17].

1.2 Quantum gravity

The above treatment uses entirely classical tricks to avoid singularities. When space-time curvature is of the order of the Planck length, the nature of gravity changes. This happens because quantum phenomena related to gravity are important and must be taken into account. The formation of singularities can not be correctly described by classical gravity. One needs a quantum formulation of gravity in order to understand the physics for curvature scales smaller than the Planck length. One could draw an analog with the renormalisation program of quantum field theory, and say that there might be quantum corrections which smooth out the singularities.

Not all singularities can be resolved by quantum gravity. In [18] it was shown that there are certain kind of singularities whose resolution would lead to contradiction. In the example in [18] the negative mass Schwarzschild is studied. This solution does not have a horizon, so the singularity is naked. If quantum gravity smooths out the singularity and replaces it with another finite–sized object, then this object should have negative mass. This would render the vacuum unstable.

Unfortunately one can not obtain quantum gravity by straightforwardly merging of quantum mechanics and general relativity. The theory can not be formulated perturbatively in a way similar to the program of quantising (gauge) field theories [19–21]. It is non–renormalisable, meaning that we have to add infinite counterterms in the action to cancel resulting infinities, thus losing predictability.

One can extend general relativity using supersymmetry, writing down a supergravity theory [22]. In general, supersymmetric theories have bosons and fermions related to each other through supersymmetry. It is well known that in supersymmetric theories boson loops are cancelled by fermion loops[3] and this improves the convergence of the perturbations series. Although perturbative quantum supergravity has milder problems than general relativity, it remains a non–renormalisable theory [23, 24].

A definite proof is still missing, mainly because of the very complicated algebraic structure of the Feynman rules for quantum supergravity, but it is today widely believed that perturbative quantum field theory approaches to quantum general relativity, or its supersymmetric extensions, are not going to provide us with a theory that we can entirely trust.

Although a quantum extension of general relativity is not available, there are some glimpses of the world of quantum gravity. S. Hawking showed using semiclassical techniques[4] that black holes, objects that have a gravitational field so strong that even light can not escape, radiate [25]. Hawking radiation is a result of quantum particle pair creation in the vicinity of a black hole. One of the two falls in the black hole while the other may escape and reach an observer at infinity. The energy of this particle comes from the black hole and gradually the black hole may evaporate[5]. There was also a proposition by Bekenstein that a black hole has an entropy which is proportional to the area of its horizon [27–29][6]. This is a very interesting result because entropy is in a way a measure of the degrees of freedom of a theory. In ordinary quantum field theory entropy scales with the volume of space. It seems that in quantum gravity the entropy scales with the area of the boundary of space, so the degrees of freedom of the theory are characterised by a field theory with one fewer space dimension[7].

There are various approaches to quantum gravity. A widely pursued approach is loop quantum gravity or quantum geometry reviewed in [36–38], euclidean quantum

[3] Infinities come from calculations of quantum loop corrections.

[4] Spacetime is treated classically, while matter fields quantum mechanically.

[5] There are some issues concerning unitarity and information loss not compatible with quantum mechanics, [26] for a review.

[6] [30, 31] for reviews.

[7] This is the idea of holography elevated to a principle by G. t'Hooft [32] and L. Susskind [33], [34, 35] for reviews.

gravity [39,40], lattice quantum gravity [41] and other more unorthodox approaches like Topos theory [42], Twistor theory [43] and Causal Sets [44].

1.3 String theory

There is another approach to quantum gravity, which is more widely accepted than the others. It started in the late 60s as a candidate for a theory of strong interactions, eventually dropped because of the advent of Quantum Chromodynamics and reappeared because it included gravity. The theory of one dimensional extended objects, strings[8].

In order for string theory to be consistent one has to include supersymmetry[9]. Bosonic strings suffer from the existence of a tachyonic state in their spectrum, which renders the vacuum unstable. There are five distinct superstring theories type I, IIA/B and the two heterotic theories with gauge groups $SO(32)$ and $E_8 \times E_8$ [48,49]. One of the nice features of string theory is that their spectrum contain gravity and Yang–Mills interactions, unifying these two types of theories in the same object.

After 1994 it was realised that all five superstring theories and eleven dimensional supergravity are related to each other by various dualities. This led to the conjecture that there is a fundamental theory, called M–theory. The five known superstring theories and eleven dimensional supergravity are just effective perturbative descriptions near different inequivalent vacuum solutions of this mysterious theory [50–52][10].

String theory contains gravity in two ways. Massless string excitations include among others a spin two particle (the graviton). Consistent propagation of the strings requires the spacetime to satisfy supergravity equations at low energy. Actually the effective low energy limits of the five superstring theories are described by their respective supergravities [55].

One can quantise string theory in a flat spacetime background using the pow-

[8] For a fuller treatment we refer the reader to [45, 46].

[9] [47] and Vol. 3 of [10] for a review of supersymmetry.

[10] [53, 54] for reviews.

erful techniques of conformal field theory. There is also a consistent perturbation expansion to study interactions. The corresponding Feynman diagrams are finite at least at first order but this result is expected to hold at all orders. This is due to the nature of the fundamental objects which are now extended and not point–like particles. Since string theory contains gravity, this means that string theory is a consistent quantum theory of gravity.

1.4 Singularities in perturbative string theory

Since string theory is a consistent theory of quantum gravity, it should give us some insight in the problem of curvature singularities [56]. The first thing to note is that spacetime singularities differ from general relativity, even in the classical level. In general relativity we use particles to test geodesic incompleteness. In string theory the fundamental objects are strings so these are the test objects that we should use. If there is a singular space and a string propagating in that space and its physics is not singular, then this singularity does not really matter. The spacetime metric is simply a lower energy manifestation of the stringy physics and the singularity is a sign that some degrees of freedom were omitted at that approximation of the full theory.

An example of this is the propagation of strings on orbifolds [57,58]. An orbifold is a quotient of spacetime by a discrete group. We will use an orbifold of flat space as an example. It has vanishing curvature everywhere but it is geodesically incomplete; there is a conical singularity at the origin. Although the propagation of particles on this space is problematic, this is not the case with strings. In string theory new light states, the twisted states, are present. They are confined at the conical singularity. Taking these additional states into account the physics of the propagating strings is non–singular and consistent.

There are also examples of curvature singularities that are resolved by string theory (flops [59–61] and conifolds [62–64]). These occur in compactifications of string theory on Calabi–Yau manifolds. It is possible that the metric of the compact Calabi–Yau manifold varies slowly leading to a change in topology. This can be viewed as topologically non–trivial S^2 or S^3 spheres shrinking or growing. When they shrink to zero area a curvature singularity is formed. At this point new degrees of freedom become massless and if included in the analysis, the physics becomes non–singular.

The fact that there is a certain class of singularities that are resolved[11] by string theory is encouraging, since this is a property that we expected from a quantum theory of gravity. It would be nice if one could extend this to other classes of singularities such as Big–Bang or Big–Crunch like setups. There has been some work towards this direction [69–84], but we will not pursue it further.

1.5 D–branes and gauge/gravity correspondence

There are also other extended objects in a string theory. These are the D–branes [12]. A Dp–brane is a p–dimensional object which sweeps a p+1–dimensional worldvolume as it moves in time. Dp–branes are the natural charges of the R–R $C_{(p+1)}$ fields in string theory. They have a very important property namely that open strings can end on them. D–branes are dynamical objects and their dynamics are dictated by the open strings attached to them. Their low energy effective action is the gauge theory that lives on the worldvolume of the branes.

D–branes conserve half of the supercharges of the initial background and they are BPS objects. This means that the net force between various parallel D–branes is zero and we can move them around without spending energy, if this procedure is slow enough.

There are black p–brane solutions of the low energy supergravity actions [85] which in the extremal limit have the properties of N Dp–branes sitting at the origin. They carry N fundamental Dp–brane charge. These solutions have non–trivial metric, dilaton and R–R $(p + 1)$–form field.

Supergravity solutions can be described as being made by D–branes. One can combine them in various ways, such as intersecting them [86], wrapping them on

[11]There is also an article [65] discussing the problem from the string field theory [66–68] point of view.

compact manifolds, to 'create' spacetimes with various fields and amounts of conserved supercharges[12].

We gave two descriptions of D–branes. One based on open strings ending on them and another one as objects with non–trivial spacetime curvature described by a supergravity solution. The supergravity description is valid when the curvature is weak. For this regime it should be $g_s N \gg 1$, where g_s is the string coupling constant and N is the number of the branes. In this regime open string perturbation theory breaks down[13]. The supergravity p–brane is the correct description. When $g_s N \ll 1$ the curvature is very large and supergravity is not valid. Here one can use the D–brane description, with the effective gauge theory on the worldvolume.

There is a complementarity between the two descriptions. From the supergravity point of view, the equations of motion are found from string perturbation theory $g_s < 1$ so we can work with the supergravity p–brane solution with the assumption that N is large, such that the curvature is small. In the BPS case, one can work with arbitrary N, use the D–brane description in weak coupling and extrapolate at strong coupling. Then one can compare with the curved supergravity solution. This can be done because of the BPS property. In case some supersymmetry is preserved, there are non–renormalisation theorems which apply, and protect quantities like charge and tension from quantum corrections[14].

1.5.1 Gauge/gravity correspondence

These two descriptions of the dynamics of a D–brane (gauge theory on the world volume and from closed string theory lower energy effective action) can be used in order to get information from the one concerning the other. This is the basis for a gauge/gravity correspondence. One example in which the supergravity descrip-

[12]Sometimes this technique is not entirely trustworthy. We will see later that this naive way of construction may ignore extra light degrees of freedom coming from the full string theory and give the wrong result.

[13]A typical string diagram has a factor of $g_s N$ and there is a trace over N Chan–Paton factors.

[14]One can successfully calculate the entropy of a black hole by counting microstates using this technique [87]. [88–92] for reviews.

tion decouples completely from the gauge theory description and there is a duality between the two, is the AdS/CFT conjecture [93–95][15].

In the prototype example by Maldacena [93], type IIB string theory is considered with N parallel D3–branes sitting together. Taking a low energy limit[16], the theory describing the physics of the D3–branes is pure $\mathcal{N} = 4$ supersymmetric Yang–Mills in $3 + 1$ dimensions, with gauge group $U(N)$, which is known to be a conformal field theory. From the point of view of the D3–branes as massive objects having a spacetime solution, in the appropriate limit[17], their geometry is $AdS_5 \times S^5$. The conjecture states that when the Yang–Mills is in the limit ($N \to \infty$, $\lambda = Ng_{YM}^2$ large[18]) it is equivalent to classical type IIB supergravity theory on $AdS_5 \times S^5$.

The remarkable result from this conjecture is that one can do calculations in the classical, weakly coupled supergravity theory and have results about the strongly coupled gauge theory.

1.6 The correspondence and singularities

The prototype example by Maldacena is very interesting in its own account, but the gauge theory ($\mathcal{N} = 4$, $U(N)$ SYM) is preserving too much supersymmetry and is not very relevant to the Standard Model Physics. We need to study theories with less supersymmetry and non–conformal, which have more interesting properties, such as confinement and chiral symmetry breaking, using the correspondence.

Supergravity backgrounds have been found by deformations[19] of $AdS_5 \times S^5$ and by considering the near horizon limits of supergravity solutions constructed by more complicated D–brane configurations. The supergravity solutions dual to gauge theories preserving less supersymmetry are generically singular in the interior, corresponding to the infrared regime of the gauge theory[20].

[15] [96–98] for reviews.

[16] Keeping the energy and all the dimensionless parameters fixed while sending $\alpha' \to 0$.

[17] This is the near horizon limit which focuses on the region near the brane.

[18] This is the form of the correspondence most accessible to the calculation techniques that are available.

[19] This is dual to adding relevant perturbations in the $\mathcal{N} = 4$ gauge theory.

[20] For reviews of the gauge/gravity correspondence in less supersymmetric backgrounds [99, 100].

It is important to understand which of these singularities are acceptable [101]. It is expected that there is a mechanism coming from the full string theory which explains why these singularities are not really formed. This comes as a hint from the dual gauge theory picture; the infrared regime in the gauge theory is the weak coupling regime and the behaviour is known to be non–singular.

Such resolution mechanisms are known to exist, covering a range of singular spacetimes. In the case of $\mathcal{N} = 1^*$ Yang–Mills theories, obtained by mass deformations of the $\mathcal{N} = 4$ gauge theory, the supergravity dual contains a singularity. In [102] Polchinski and Strassler resolved this naked singularity using a manifestation of the Myer's dielectric effect [103]. Very naively the D3–branes used to construct the geometry are polarised to a D5–brane, because of a five–form flux present. The final spacetime is not singular, although we do not know its exact metric.

Another $\mathcal{N} = 1$ ([104] for a review) example is the resolution of a naked singularity [105] in the Klebanov–Tseytlin spacetime [106]. In this setup supersymmetry is broken by putting D3–branes on a conifold and conformal symmetry is broken by adding fractional D3–branes. This supergravity solution suffers from a naked singularity. In [105] it was found that the naked singularity is resolved by deforming the conifold. Similar approaches to the Polchinski–Strassler and Klebanov–Strassler where used in [107, 108].

In the case of $\mathcal{N} = 2$, supergravity duals have been found in different ways such as by mass deformation of the $\mathcal{N} = 4$ theory [109–112] fractional branes at orbifold singularities [113–121], M5–branes wrapped on Riemann surfaces [122, 123], five–branes wrapped on non–trivial two–cycles of a Calabi–Yau manifold [124–126] and by wrapping D–branes on $K3$ [127]. All these descriptions are related to each other by duality transformations [128]. The naked timelike singularities that arise, seem to be resolved by the enhançon mechanism [127].

1.7 The enhançon mechanism

Supergravity duals of certain $U(N)$ gauge theories conserving eight supercharges, have a naked singularity known as the repulson. A brane configuration with such a supergravity solution was first considered in [127]. This singularity is not compatible with the physics of the gauge theory and should be unphysical. One can use D–branes as probes of the geometry and try to construct it using a large number of the constituent objects. This procedure shows that, in the case of wrapping D$(p+4)$–branes on $K3$ manifolds, the branes used to construct the geometry cease to be localised at the enhançon locus and expand out into a $(4-p)$–sphere surrounding the would be singularity. This is due to extra massless degrees of freedom from string theory which are not included in the supergravity effective action. These enhance the gauge symmetry, hence the name enhançon. The interior geometry is excised and replaced by flat space[21].

It is quite remarkable that, although supergravity can not describe the physics of the enhançon correctly, it supports the excision. The source at the excision surface behaves exactly as a shell of wrapped branes [129]. We will see later on that the enhançon is stable under a particular set of linear perturbations. This is something expected from supersymmetry, since we are dealing with BPS objects and it adds to the validity of the construction from the point of view of supergravity.

The enhançon physics is known to be connected to monopole physics in the case $p = 2$ [130], [131], [132]. There are also solutions of enhançons with non–spherical shapes [133] and of rotating enhançons [134]. One can also include orientifolds leading to cases with $SO(2N+1), USp(2N), SO(2N)$ gauge groups [135]. The enhançon is also crucial to black hole physics. In certain cases the enhançon mechanism prevents branes that would reduce black hole entropy from entering the horizon [134, 136, 137][22].

There are many related studies of the enhançon in the literature. The setup of D–branes on $K3$ is T–dual to fractional D–branes [139, 140]. The enhançon mechanism can be seen, for the fractional brane picture, for non–compact orbifolds $\mathbb{C}^2/\Gamma$ [114–116, 119, 120, 141] and on the compact orbifold limit $T^4/\mathbb{Z}_2$ of $K3$ [142]. It is also considered on a conifold [141] and in heterotic string theory [143]. Some analogues of the enhançon mechanism have been considered in the context of com-

[21]We will provide more details about the mechanism later in the thesis.

[22]For a review of the above [138].

pactifications of eleven dimensional supergravity on Calabi–Yau spaces [144] and in a non–supersymmetric setup [145, 146]. There is also a study of the enhançon mechanism incorporating from the beginning non–abelian fields and the monopole physics in [147].

1.8 Non–extremal enhançon

Generally, one of the simplest questions to consider from the bulk spacetime side of the AdS/CFT correspondence is the finite-temperature behaviour of the theory. One would expect that the theories with reduced supersymmetry should have interesting phase structures. At high temperatures, one would expect to find that the partition function is dominated by a black hole solution, and there may be some symmetry-breaking phase transitions as the temperature decreases. Attempts to investigate these issues by studying black hole solutions on the AdS side were made in [148–154]. Since the enhançon provides an example where there is a simple supergravity solution describing the singularity resolution, it is interesting to study these issues in this case.

Regarding the non–extremal enhançon generalisation of the enhançon, it was found in [129] that it has two branches of solutions. One has a horizon and it appears at a finite value of the non-extremality parameter. We call this the horizon branch. The other always has a shell of branes outside the horizon and in the extremal limit give the known extremal solution of [127]. This is the shell branch. A similar structure is found in the case of fractional branes [155].

The shell branch of solutions has a few peculiar properties. First of all it depends on a free parameter which we can not set to a particular value without some extra information from the physics of the full string theory on the background. This is too difficult to do, because we do not know the behaviour of string theory in non–extremal, or equivalently in this case, finite–temperature situations. Another problem slightly more important is that, in the case of wrapped D6–branes on $K3$, taking the compactification volume to infinity does not give the usual non–extremal D6–brane.

The two branches of solutions seem to be valid in different regimes of the non–extremality parameter. Shell branch is valid for small non–extremality, while the horizon branch is definitely the solution for large non–extremality. This suggests that there might be an instability in the two solutions signalling a phase transition in the gauge theory side.

Part of the motivation for the research described in this thesis was based on trying to find such an instability. The horizon branch was found to be stable throughout the range of the non–extremality parameter. The shell branch on the other hand was found to be unphysical. By excising the interior to the enhançon radius, singular region, replacing it with smooth geometry and by matching to a smooth exterior over a shell, this shell has negative energy density, thus violating the Weak Energy Condition.

This is all from the supergravity point of view and it seems that although supergravity could grasp some of the physics of the extremal case, it fails for the non–extremal case. Further support is given from finding the families of general enhançon solutions, extremal and non–extremal. Here, again using supergravity, we find that the extremal solutions and the horizon branch of solutions are unique and are completely determined from the boundary conditions we impose to the general solutions. When it comes to the shell branch of solutions, there is a family of generalised solutions, which can help overcome the problem of Weak Energy Condition violation. Unfortunately from supergravity alone we can not decide which of these solutions describe the correct physics of the shell branch. In order to do that we have to know explicitly the degrees of freedom describing the physics of the shell, which is beyond the supergravity regime. As long as this is lacking we can not model the shell correctly.

We must stress here that using supergravity to model the thin shell in the extremal case, we succeed in describing the physics of the shell, especially when we studied its stability under linear perturbations. We expected that we would be equally successful with the non–extremal case, but unfortunately after we found the more general solutions, we realised that supergravity is still very limited in cases which break all supersymmetry.

1.9 Outline of the thesis

We will study the physics and the properties of enhançons using supergravity techniques. The plan of the thesis is as follows. In Chapter 2 we will review some essential tools necessary for our study. We will give a brief overview of string theory and we will focus on D–branes. We will describe how one can use D–branes to construct spacetime solutions.

In Chapter 3 we give a review of the enhançon mechanism. We will use the case of wrapped D6–branes on $K3$ as an example. Since we are interested on the supergravity description we will discuss the consistency of the excision in some detail. This will be useful in our calculation later. We also present the non–extremal generalisations and describe what happens when one adds extra D2–branes.

In Chapter 4 we study the perturbation ansatz we use in order to study the stability of the enhançon solutions under linearised perturbations. We write down the ansatz and find the differential equations that the perturbation modes are satisfying, using some diffeomorphism invariance left. Before we continue in the study of stability we give an example with a mode that is uncoupled and we can study the problem analytically.

In Chapter 5 we study the stability of the extremal enhançon. We use the model of wrapped D6–branes as a thin shell in order to calculate the boundary conditions at the shell. Again some diffeomorphism invariance left, helps us in simplifying the problem considerably. Finally we give a brief description of the numerical technique used, and study the problem. We find that the extremal enhançon is stable under the perturbation ansatz we used. Although this ansatz is very restricted, we believe that the extremal enhançon is stable on the ground that it is supersymmetric.

In Chapter 6 we extend the program to the non–extremal enhançon. We find that the shell branch of solutions is unphysical because it violates the Weak Energy Condition. The horizon branch is stable throughout the range of parameters. This is the expected behaviour for it, since it looks like a Schwarzschild black hole for very large mass and we know this to be stable.

In Chapter 7 we try to find more general solutions of the enhançon, solving supergravity equations. In the extremal case we find that the solution is the one we had before, once we specify the model for the shell and its constituents. We also find that the horizon branch of solutions is the unique solution. When it comes to the shell branch of solutions, we find a family of them. There is a way to avoid the violation of the Weak Energy Condition by adding 'hair' in the solutions but this needs extra information from the string theory that we do not have.

Finally in the Appendices in the end of the thesis, we present some facts about the $K3$ manifold, type IIA supergravity equations of motion in Einstein frame, a more detailed description of the numerical method we used for the stability analysis and a more detailed analysis of the calculation of the temperatures of the black hole in the two branches of the non–extremal enhançon solution.

Chapter 2

Strings and branes

This chapter will provide some introductory material concerning string theory. It is not meant to be a full review but just provide the reader with the essential information in order to understand the main subject of the thesis.

We will start with a brief discussion of string theory. In the bosonic case, we will write down the action and describe the spacetime field content of the theory for open and closed strings. Then we will expand this discussion to the case of the superstring.

Next we give a brief discussion on D–branes. We sketch their string theory origin and write down the action that governs their dynamics. We will also have a quick look over anomalous couplings that are the result of non–trivial curvature.

Next we will talk about supergravity p–branes and how they connect with D–branes. We will give the non–extremal solutions of p–branes and discuss the extremal limit which we will connect to D–branes. Due to their nice properties we can use them as building blocks to construct a supergravity solution.

2.1 String theory

We will give a very brief introduction to string theory. We will present an overview of the formulation and the field content of the theory, since we are mainly interested in D–branes[1].

2.1.1 Bosonic strings

We will start with the bosonic case. A one dimensional object will sweep out a two dimensional worldsheet, which can be described by a set of two parameters τ and σ. The simplest invariant action is proportional to the area of the worldsheet. This is the Nambu–Goto action:

$$S_{NG}[X] = -\frac{1}{2\pi\alpha'}\int_\Sigma d\tau d\sigma \left(-det\left(\partial_a X^\mu \partial_b X_\mu\right)\right)^{1/2}. \tag{2.1}$$

α' is the universal Regge slope parameter. It has dimensions of [length]^2 and it is the only dimensionful parameter in string theory. It is related to the fundamental string tension $T = (2\pi\alpha')^{-1}$ and it also sets the string length $\alpha' = l_s^2$. The coordinates τ, σ parametrise the string worldsheet Σ. X^μ are the D–dimensional spacetime coordinates of the string and are treated as fields from the worldsheet point of view.

We can simplify the Nambu–Goto by introducing an independent world–sheet metric $h^{\alpha\beta}$ which depends on τ, σ. The action for a string moving in flat spacetime is

$$S_P[X,h] = -\frac{1}{4\pi\alpha'}\int_\Sigma d\tau d\sigma \sqrt{-\det h}\, h^{\alpha\beta}\partial_\alpha X^\mu \partial_\beta X^\nu \eta_{\mu\nu} \tag{2.2}$$

This is the Polyakov action [159]. The equivalence to the Nambu–Goto action can be seen by varying (2.2) with respect to the metric h^{ab}

$$\delta_h S_P[X,h] = -\frac{1}{4\pi\alpha'}\int_\Sigma d\tau d\sigma \sqrt{-\det h}\,\delta h^{ab}\left(\partial_a X^\mu \partial_b X_\mu - \frac{1}{2}h_{ab}h^{cd}\partial_c X^\mu \partial_d X_\mu\right). \tag{2.3}$$

Setting this variation equal to zero, we can use it to eliminate h^{ab} from the Polyakov action. The result is non other than the Nambu–Goto action[2].

This Polyakov action has symmetries which we can use in order to gauge fix and get simple equations of motion. These are spacetime Poincarè invariance, worldsheet (two–dimensional) diffeomorphism invariance and Weyl invariance. After gauge fix-

[1] More complete reviews can be found in [45, 46, 156–158].

[2] More details can be found in the string theory reviews mentioned earlier.

ing, the equations of motion that we get for the spacetime fields are

$$\frac{\partial^2 X^\mu(\tau,\sigma)}{\partial\tau^2} - \frac{\partial^2 X^\mu(\tau,\sigma)}{\partial\sigma^2} = 0. \tag{2.4}$$

This is the two–dimensional wave equation. Depending on the kind of strings, we can impose different boundary conditions. In the case of closed strings the worldsheet is a tube and we have to impose periodic boundary conditions

$$X^\mu(\tau,0) = X^\mu(\tau,l), \quad \partial_\sigma X^\mu(\tau,0) = \partial_\sigma X^\mu(\tau,l), \tag{2.5}$$

in coordinates where $-\infty \leq \tau \leq \infty$, $0 \leq \sigma \leq l$.

For open strings the worldsheet is a strip and there are two kinds of boundary conditions. Neumann boundary conditions

$$\frac{\partial}{\partial\sigma} X^\mu(\tau,0) = 0, \quad \frac{\partial}{\partial\sigma} X^\mu(\tau,l) = 0 \tag{2.6}$$

and Dirichlet boundary conditions:

$$\frac{\partial}{\partial\tau} X^\mu(\tau,0) = 0, \quad \frac{\partial}{\partial\tau} X^\mu(\tau,l) = 0. \tag{2.7}$$

Neumann conditions imply that no momentum flows off the end of the string. The Dirichlet condition implies that the end points of the string are fixed in spacetime. They will be relevant when we discuss D–branes.[3]

After quantisation we can find the states in the string spectrum. For the closed string, we have a scalar field Φ, the dilaton, the graviton $g_{\mu\nu}$ and an antisymmetric tensor field $B_{\mu\nu}$ also called the Kalb–Ramond field. The graviton is the background spacetime metric. The dilaton sets the dimensionless string coupling through $g_s = e^{<\Phi>}$. These are the massless states. There is also a tachyon field and an infinite tower of massive states.

For the open string the spectrum is slightly different. There is a massless state which is a $U(1)$ gauge boson A_μ. Again there is a tachyonic state and an infinite tower of massive states.

[3]The open string Neumann boundary conditions (2.6) and the closed string periodic boundary conditions (2.5) are the only possibilities consistent with D–dimensional Poincarè invariance. Relaxing this condition admits the occurrence of Dirichlet boundary conditions which are important when discussing D–branes.

The bosonic theory has a few problems. First it can only live in twenty six dimensions. Second and most important it has a tachyonic state, which may render the theory unstable. Third it contains no spacetime fermions.

2.1.2 Superstrings

One solution to this problem is to add worldsheet fermions in (2.2) as supersymmetric partners of the worldsheet bosons. Supersymmetry constrains a lot the way we can formulate theories. There are actually only five consistent superstring theories: type I, type IIA, type IIB and two heterotic with $SO(32)$ and $E_8 \times E_8$ gauge groups. These theories live in ten dimensions, have no tachyon in their spectrum and they contain spacetime fermions [160, 161].

We are mainly interested in type IIA string theory. This is a theory of closed strings and has $\mathcal{N} = 2$ supersymmetry in ten spacetime dimensions. The states of this theory come from two sectors, the Neveu-Schwarz–Neveu-Schwarz (NS–NS) and the Ramond–Ramond (R–R). In the NS–NS sector the massless bosonic states are the same as in the bosonic string, the dilaton, the graviton and the Kalb–Ramond field. In the R–R sector the massless bosonic fields are p–form gauge fields: $C_{(1)}$, $C_{(3)}$ and their magnetic duals $C_{(7)}$ and $C_{(5)}$. Type IIB string theory is similar with the difference that it contains chiral spacetime fermions. The massless bosonic states are the same in the NS–NS spectrum, while in the R–R sector the gauge fields are now $C_{(0)}$, $C_{(2)}$, $C_{(4)}$, $C_{(6)}$, $C_{(8)}$ and the self dual $C_{(4)}$.

2.2 D–branes

Now let us turn to the Dirichlet boundary conditions (2.7). We mentioned earlier that when these boundary conditions are satisfied, the endpoints of the string are fixed. Imagine that we impose Neumann boundary conditions on time and p spatial directions, and Dirichlet boundary conditions on the rest $D-p-1$ spatial directions. The ends of the string are fixed in the $D-p-1$ directions and can move freely to the rest p directions and time. When one imposes Dirichlet boundary conditions the momentum is not conserved in these directions. This leads us to the conclusion that the hypersurface to which the strings are attached is a dynamical object. This dimensional object has a $p+1$ worldvolume and it is called Dp–brane [12, 162][4].

Open strings can end on a D–brane and we can use them to determine its dynamics. We can get the most important contribution from the massless states of the strings attached to the branes. These are for a Dp–brane, a p–dimensional $U(1)$ gauge field A^{α}, $a = 0 \ldots, p$ and $D-p-1$ scalar fields Φ^i. These scalars correspond to the transverse oscillations of the brane. Their vacuum expectation values correspond to the position of the brane in the transverse space.

An important and relatively easy generalisation is to have N parallel D–branes. Then there are additional open strings that stretch between different branes. The spectrum of these strings is massive and the mass is proportional to the separation of the D–branes they connect. As the branes approach each other, these states become lighter. When the D–branes coincide they become massless. These extra massless states enhance the symmetry from the initial $U(1)^N$, when all the branes are apart, to $U(N)$ in the adjoint representation, when all of them coincide [171]. This is just like the Higgs mechanism of symmetry breaking. The distances between the branes correspond to the Higgs expectation values and the masses come from the stretched strings.

Especially in the case of superstrings, D–branes have a very natural interpretation. Perturbative string states can not carry charges with respect to the R–R potentials. Dp–branes are actually the sources for these potentials. They should be included along with the corresponding open string sectors in type II theories, with p even for IIA and odd for IIB.

Again the dynamics of a Dp–brane are determined by the open strings attached to it. The leading contribution comes from the massless states. These correspond to the dimensional reduction of pure $\mathcal{N}=1$ ten–dimensional Super Yang–Mills to p–dimensions. In the case of N coinciding Dp–branes, the massless states have the spectrum of the dimensionally reduced $U(N)$ Super Yang–Mills.

Before we continue we should stress a property of D–branes that is very useful.

[4]Further references on D–branes can be found in [163–170].

D–branes interact with each other through closed strings (gravity and scalar attractive forces) and open strings (gauge repulsive forces). The sum of these forces is zero between parallel Dp–branes. In supersymmetric models, D–branes preserve half the supersymmetries of the initial background. This is a sign that D–branes are BPS objects.

2.3 D–brane action

One can write down an action that describes the dynamics of the D–branes. For slowly varying field strengths[5] and for arbitrary supergravity background this is [173–175]

$$S = S_{DBI} + S_{WZ}, \tag{2.8}$$

where

$$S_{DBI} = -\tau_p \int d^{p+1}x e^{-\phi}\sqrt{-det(G_{ab} + B_{ab} + 2\pi\alpha' F_{ab})}\mathcal{G}_{DBI}, \tag{2.9}$$

is the Dirac–Born–Infeld action and

$$S_{WZ} = -\mu_p \int_{M_{p+1}} \sum_p C_{(p+1)} \wedge e^{2\pi\alpha' F_{ab} + B_{ab}} \wedge \mathcal{G}_{WZ}, \tag{2.10}$$

is a Wess–Zumino type action. The x^a are independent coordinates on the worldvolume of the brane. τ_p is the tension of the brane and μ_p its charge[6]. G_{ab} is the induced metric on the brane and and B_{ab} is the induced Kalb–Ramond field on the brane

$$\begin{aligned} G_{ab} &= \frac{\partial X^M \partial X^N}{\partial \xi^a \partial \xi^b} G_{MN}, \\ B_{ab} &= \frac{\partial X^M \partial X^N}{\partial \xi^a \partial \xi^b} B_{MN}. \end{aligned} \tag{2.11}$$

F_{ab} is the field strength of the brane worldvolume gauge field. $C_{(p+1)}$ is the $(p+1)$–form R–R potential which is sourced by the D–brane.

[5] There are corrections from derivatives of F_{ab} which can be suppressed for slowly varying fields [172].

[6] One can calculate the tension and charge of the Dp–brane from the amplitude of an exchanged closed string and comparison of this result with a background field computation [163].

The DBI action describes the Dp-brane coupling to the massless NS-NS fields of the bulk closed string theory. This is a generalisation of the action of a moving massive particle.

D-brane interactions with the massless Ramond-Ramond fields are incorporated in the generalised Wess-Zumino-like term. This is again a more general form of the coupling of the charge of the particle to a gauge field. From (2.10) we can see that a Dp–brane can couple with lower rank potentials apart from the bulk $C_{(p+1)}$.

Before we continue, we should note something about the DBI action (2.9). Earlier we claimed that the dynamics of the D–branes can be deduced from the open string leaving on the brane. The effective action of this string in lower order is the dimensional reduction of ten dimensional $\mathcal{N} = 1$ super Yang–Mills. This is the leading order if we expand the DBI action in a flat background. The DBI action is true to all orders in α' with the limitation we mentioned above. The effective gauge theory action is just the leading order term.

2.3.1 Anomalous couplings

For a dynamical object such as a D–brane, which couples to the background spacetime and to gauge fields, it is expected that in order to describe its dynamics we should be able to incorporate the influence of these couplings to its action.

Both DBI and WZ terms receive corrections from background curvature. The DBI action gets several corrections [176,177] but the set of curvature–squared terms that we are interested are given by

$$\mathcal{G}_{DBI} = 1 - \frac{(4\pi^2\alpha')^2}{768\pi^2}\left(R^{abcd}R_{abcd} - R^{\alpha\beta ab}R_{\alpha\beta ab} - 2\hat{R}^{ab}\hat{R}_{ab} + 2\hat{R}^{\alpha\beta}\hat{R}_{\alpha\beta}\right) + O(\alpha'^4). \tag{2.12}$$

where $a, \ldots, d$ are the tangent space indices running along the brane world-volume, while α, β are normal indices, running transverse to the world-volume. Also $\hat{R}_{ab}$, $\hat{R}_{\alpha\beta}$ are obtained by contraction of the pulled-back Riemann tensor.

We are mainly interested in the corrections imposed by wrapping branes on a special manifold called $K3$[7]. For the case of $K3$, which is Ricci–flat, everything with

[7] A few technical details about this manifold can be found in Appendix A.1.

normal indices vanishes and we have only $R^{abcd}R_{abcd}$ appearing, which is computed in (A.1.1). After integrating over the $K3$ the action becomes

$$S_{DBI} = -\int d^{p-3}xe^{-\phi}\left(\tau_p V_{K3} - \tau_{p-4}\right)\sqrt{-det(G_{ab} + B_{ab} + 2\pi\alpha' F_{ab})}. \qquad (2.13)$$

Notice that the tension of this composite object has changed. It involves the correction imposed by the curvature of the $K3$. As for the WZ part [178, 179], the geometric term reads

$$\mathcal{G}_{WZ} = \sqrt{\frac{\hat{\mathcal{A}}(4\pi^2\alpha' R_T)}{\hat{\mathcal{A}}(4\pi^2\alpha' R_N)}} = 1 - \frac{(4\pi^2\alpha')^2}{48}(p_1(R_T) - p_1(R_N)) + O(\alpha'^4) \qquad (2.14)$$

where $\hat{\mathcal{A}}$ is the 'A–roof' or Dirac genus, R_T, R_N are the curvature two forms of the tangent and normal bundles and p_1 is the first Pontryagin class. For the case of $K3$ we take the normal bundle to be trivial and the first Pontryagin class is

$$p_1(K_3) = -\frac{1}{8\pi^8}\mathrm{Tr}R \wedge R = 48. \qquad (2.15)$$

The additional term can be written as

$$-\frac{\mu_p}{48}\int C_{(p-3)} \wedge p_1(\mathcal{R}) \qquad (2.16)$$

and since $\mu_p = (2\pi)^{-p}\alpha'^{-(p+1)/2}$, $\mathcal{R} = 4\pi^2\alpha' R$ it is equal to

$$-\mu_{p-4}\int C_{p-3} \qquad (2.17)$$

on the unwrapped part of the worldvolume of the Dp–brane.

There is an important lesson from this setup. When a Dp–brane wraps a manifold with non–trivial curvature, its tension may change and most importantly it may seem as carrying an effective charge under a R–R field of different rank. These facts are going to be used to describe the enhançon mechanism later.

2.4 Supergravity and p–brane solutions

2.4.1 Ten dimensional supergravity

In the low energy limit $\alpha' \to 0$ one can focus on the massless sector of string theory and describe the physics using a low energy effective action. It turns out that these effective actions are ten dimensional supergravities [55][8].

Since we are interested in Type IIA/B string theory, their effective low energy limits are Type IIA/B supergravity respectively. The bosonic part of the Type IIA supergravity action in string frame is

$$\begin{aligned} S_{IIA} &= \frac{1}{2\kappa^2}\int d^{10}x(-G)^{1/2}e^{-2\Phi}\Big(R + d\Phi\wedge *d\Phi - H_3\wedge *H_3\Big) && (2.18)\\ &-\frac{1}{4\kappa^2}\int\Big(F_2\wedge *F_2 + \tilde{F}_4\wedge *\tilde{F}_4 + B_2\wedge F_4\wedge F_4\Big), && (2.19)\end{aligned}$$

where

$$\tilde{F}_4 = F_4 - C_1\wedge H_3 \quad , \quad F_4 = dC_3 \quad , \quad F_2 = dC_1. \tag{2.20}$$

Similarly the bosonic part of type IIB supergravity[9] can be written as

$$\begin{aligned} S_{IIB} &= \frac{1}{2\kappa^2}\int d^{10}x(-G)^{1/2}e^{-2\Phi}\Big(R + d\Phi\wedge *d\Phi - H_{(3)}\wedge *H_{(3)}\Big)\\ &-\frac{1}{4\kappa^2}\int\Big(F_{(1)}\wedge *F_{(1)} + \tilde{F}_{(3)}\wedge *\tilde{F}_{(3)} + \frac{1}{2}\tilde{F}_{(5)}\wedge\tilde{F}_{(5)}\\ &+C_{(4)}\wedge H_{(3)}\wedge F_{(3)}\Big), \end{aligned} \tag{2.21}$$

where

$$\begin{aligned} &\tilde{F}_{(5)} = F_{(5)} - \frac{1}{2}C_{(2)}\wedge H_{(3)} + \frac{1}{2}B_{(2)}\wedge F_{(3)}\\ &\tilde{F}_{(3)} = F_{(3)} - C_{(0)}\wedge H_{(3)},\\ &F_{(1)} = dC_{(0)}, \quad F_{(3)} = dC_{(2)}, \quad F_{(5)} = dC_{(4)}. \end{aligned} \tag{2.22}$$

$G_{\mu\nu}$, Φ and $H_3 = dB_{(2)}$ are the fields from the massless bosonic sector of Type II string theory. The $F_{(p+1)}$ fields are the field strengths of the respective R–R potentials $C_{(p)}$ for each theory. The gravitational coupling κ is set by

$$2\kappa^2 = (2\pi)^7\alpha'^4 g_s^2, \tag{2.23}$$

and g_s is set by the asymptotic value of the dilaton at infinity $g_s = e^{<\Phi_\infty>}$.

[8]For more details the reviews on string theory mentioned earlier can be consulted.

[9]Type IIB supergravity has a problem due to the self dual field strength $F_{(5)} = *F_{(5)}$. There is no covariant action for such a field, so we have to impose this constraint by hand in the equations of motion.

2.4.2 p-brane solutions

There is a family of ten dimensional solutions which are charged under R–R fields and have p translational isometries. These are the black p–branes [85][10] and they can be described by the metric

$$ds^2 = Z_p^{-1/2}(r)\left(-K(r)dt^2 + \sum_{i=1}^{p} dx_i^2\right) + Z_p^{1/2}(r)\left(\frac{dr^2}{K(r)} + r^2 d\Omega_{8-p}^2\right), \tag{2.24}$$

where $d\Omega_{8-p}^2$is the metric on a unit S^{8-p} sphere, dilaton

$$e^{2\Phi} = Z_p(r)^{\frac{3-p}{2}} \tag{2.25}$$

and R–R gauge potential

$$C_{(p+1)} = g_s^{-1}(Z_p(r)^{-1} - 1)dx^0 \wedge \cdots \wedge dx^p. \tag{2.26}$$

The functions

$$Z_p(r) = 1 + \alpha_p \left(\frac{r_p}{r}\right)^{7-p}, \tag{2.27}$$

$$K(r) = 1 - \left(\frac{r_0}{r}\right)^{7-p}, \tag{2.28}$$

are harmonic in transverse space and

$$\alpha_p = -\left(\frac{r_0}{2r_p}\right)^{7-p} + \sqrt{1 + \left(\frac{r_0}{2r_p}\right)^{2(7-p)}}, \tag{2.29}$$

$$r_p^{7-p} = d_p(2\pi)^{p-2} g_s N \alpha'^{\frac{7-p}{2}}, \quad d_p = 2^{7-2p}\pi^{\frac{9-3p}{2}}\Gamma\left(\frac{7-p}{2}\right). \tag{2.30}$$

These solutions represent the non–extremal p–brane solutions. They are resembling black hole solutions (if we compactify them accordingly) and have a horizon at $r = r_0$. These solutions do not conserve any supercharges. The important thing is that they describe objects that carry N units of the basic Dp–brane R–R charge.

Extremal limit and D–branes

We can take the extremal limit of the above p–brane solutions. This is $r_0 = 0$. The extremal p–branes are BPS solutions of the ten dimensional supergravity and

[10] [180, 181] for more details.

conserve half supercharges. In this case the above p–brane solution simplifies considerably. Again it carries N units of a Dp–brane R–R charge

$$\mu_p = (2\pi)^{-p}(\alpha')^{-\frac{p+1}{2}} \tag{2.31}$$

The tension of this solution consists of N units of a Dp–brane tension

$$\tau_p = g_s^{-1}\mu_p. \tag{2.32}$$

This is not a surprising result. These solutions have the right charge and tension so as to say that they are made of N coincident Dp–branes sitting at the origin. Thus, these p–branes solutions provide a description of the D–branes in the supergravity regime.

There is a systematic way [182–184] for construction of supergravity solutions corresponding to intersections of BPS branes called the 'harmonic function rule'. One simply superimposes the harmonic functions of the various branes. This ansatz works for both parallel and perpendicular intersections. There is one restriction, that the harmonic functions depend only on the overall transverse directions.

2.5 Summary

String theory apart from its ordinary perturbative states, it has other objects in its spectrum which are charged under the Ramond–Ramond fields. These objects are like p–brane solutions and they have the property that open strings can end on them. They are dynamical objects and interact with spacetime (using closed strings) and with each other (open and closed strings). Their name is D–branes.

We described their dynamics using the action (2.8-2.10) and we studied the way this action gets corrected from anomalous curvature and gauge couplings if we wrap a D–brane on a compact manifold of non–trivial curvature. These we will use later.

We also wrote down the supergravity black p–brane solutions. These have a horizon at $r = r_0$. We studied briefly their extremal limit and saw that we could think of them as being N parallel Dp–branes sitting at the origin.

We can use this technology in order to construct supergravity solutions by combining numbers of D–branes in various ways. As we will see this is not always the case even when supersymmetry is preserved. There are geometries like the repulson geometry which has R–R charges but we can not really say that it is made naively of D–branes, since it has a naked singularity. This situation will be considered in detail in the rest of the thesis.

Chapter 3

The enhançon mechanism

In this chapter we will review the enhançon mechanism. Many facts needed later in this thesis, such as the details of the supergravity solutions, extremal and non–extremal, the junction conditions on the shell and the cases with extra, unwrapped D2–branes will be discussed here.

There is a class of supergravity solutions with eight supercharges which have an unwanted feature. These solutions have a naked curvature singularity which is repulsive. This means that a particle feels a repulsive force as it moves near it. This kind of singularity is called 'repulson' in the literature.

There are brane configurations in string theory which appear to give rise to such a singularity. The example we consider in the first section of this chapter is wrapped D6–branes on a $K3$ manifold. The curvature of this manifold induces a negative D2–brane charge. The naive supergravity solution has a naked singularity of the repulson type. Using a constituent brane as a probe for this geometry reveals a different situation. The branes expand into a sphere forming a shell around the would–be naked singularity, leaving a flat geometry inside. The constituent branes are delocalised in the transverse directions and form a shell, the enhançon shell, as they approach a special value of the radius. We will review the probe calculation and see that there are extra degrees of freedom which come from the full string theory and cannot be grasped from supergravity.

It is not very difficult to extend the problem by adding extra D2–branes. Their tension is constant and they can move freely past the enhançon shell, in the interior.

Some of the wrapped D6–branes can be attached to them and be removed from the shell to the interior. The interior is not flat anymore because it can have D2 and D6–branes which curve space.

We then proceed to study the enhançon at finite temperature. In this case supersymmetry is broken and it is very difficult to study them using string theory. There are two branches of non-extremal solutions, arising from an ambiguity of a choice of sign in the solution of the supergravity equations. One branch joins on to the extremal enhançon solution, and always has a shell of branes outside the horizon. The other branch appears at a finite value of the non-extremality parameter and has a horizon. Again we can generalise by adding extra D2–branes. The discussion is similar to the extreme case. These D2–branes can fall in the interior and help some or the wrapped D6–branes to fall inside. A similar two branch structure is observed.

As we will review in Section 3.4 supergravity is not so ignorant about the configuration. We carry out the procedure of removing the interior space and replace it with flat space. The surface where the exterior and the interior spaces meet is the enhançon shell. There is a discontinuity on the exterior curvature of this surface. This discontinuity can be interpreted as a δ–function source of stress–energy located at the surface. Calculating this stress–energy tensor shows that it correctly catches the content of the shell. We are able to exactly match this stress–energy tensor, with a stress–energy tensor for wrapped D6–branes distributed uniformly over a two–sphere. A very similar discussion can be made for the case of extra D2–branes present.

We also calculate the stress–energy tensor of the shell in the shell branch of the non–extremal enhançon using Israel's junction conditions. Unfortunately here we do not have a model that can describe the physics of the shell, as we have in the extremal case.

Finally we briefly discuss some of the features of the non–extremal enhançons. There are some differences to the two branches of solutions and some concerns about the shell branch solution.

There is no original material in this chapter. The original paper on the enhançon mechanism is [127]. A non–extremal extension also appeared in the same article. The discussion of the consistency of the enhançon in supergravity, the addition of extra D2–branes and the more general non–extremal solutions appeared in [129].

3.1 The repulson geometry

3.1.1 Wrapping branes on $K3$

We would like to describe a supergravity solution consisting of D–branes which preserves eight supercharges. Brane configurations with this amount of supersymmetry can be constructed with an amount of Dp and D$(p+4)$ branes with p spatial directions parallel. Another way is by wrapping a D–brane on a manifold which breaks half of the supersymmetry. Such a manifold is the four dimensional $K3$ manifold.

Wrapping a brane on a compact manifold means that part of the worldvolume of the brane resides on this manifold. If we wrap a D6–brane, which has a seven–dimensional worldvolume, on a four–dimensional $K3$, we have four of its spatial worldvolume directions wrapped on the $K3$, while the other three remain unwrapped.

$K3$ is not a flat space, so wrapping a D6–brane on it will alter its dynamics as we saw in the previous chapter. This can be seen from the Wess–Zumino part of the D–brane action which gets an additional term.

$$-\frac{\mu_6}{48}\int C_{(3)}\wedge p_1(\mathcal{R}) \tag{3.1}$$

on the D6–worldvolume. Since $\mu_6 = (2\pi)^{-6}\alpha'^{-7/2}$, $\mu_2 = (2\pi)^{-2}\alpha'^{-3/2}$, $\mathcal{R} = 4\pi^2\alpha' R$ and for the $K3$ manifold

$$p_1(R) = \frac{1}{8\pi^2} R\wedge R = 48, \tag{3.2}$$

This is equal to

$$-\mu_2\int C_3, \tag{3.3}$$

on the unwrapped part of the worldvolume of the D6–brane. N D6–branes wrapped on $K3$ induce N units of negative D2 charge.

We will try to give a description of this object. A D6–brane carries a Ramond–Ramond charge which couples to a $C_{(7)}$ seven–form R–R potential. The wrapped brane also couples to this potential. The wrapped brane also induces a D2–charge which couples to a $C_{(3)}$ R–R potential. This wrong sign D2–branes conserves the same amount of supercharges as a correct sign D2–brane with the same orientation. For this reason it is not an anti–D2–brane. We can think of it as an effective bound state of a D2–brane within the unwrapped part of the D6–brane worldvolume and delocalised in the $K3$ directions.

The effective tension of the composite object is also affected from the curvature couplings. As we saw in Section 2.3.1 the effective tension is for the case of D6–branes wrapping $K3$

$$\tau = \tau_6 V_{\mathrm{K3}} - \tau_2. \tag{3.4}$$

3.1.2 The geometry

We can write down a supergravity solution if we consider a large number of wrapped branes. The form is determined by the harmonic function rule for p–brane solutions. The string–frame metric is

$$\begin{aligned}
ds^2 &= Z_2^{-1/2} Z_6^{-1/2} \eta_{\mu\nu} dx^\mu dx^\nu + Z_2^{1/2} Z_6^{1/2} dx^i dx^i + V^{1/2} Z_2^{1/2} Z_6^{-1/2} ds^2_{\mathrm{K3}} \ , \\
e^{2\Phi} &= g_s^2 Z_2{}^{1/2} Z_6{}^{-3/2} \ , \\
C_{(3)} &= (Z_2 g_s)^{-1} dx^0 \wedge dx^1 \wedge dx^2 \ , \\
C_{(7)} &= (Z_6 g_s)^{-1} dx^0 \wedge dx^1 \wedge dx^2 \wedge V\, \varepsilon_{\mathrm{K3}} \ ,
\end{aligned} \tag{3.5}$$

where the harmonic functions are

$$Z_6 = 1 + \frac{r_6}{r} \ , \quad Z_2 = 1 + \frac{r_2}{r} \ , \tag{3.6}$$

the parameters are related by

$$r_6 = \frac{g_s N \alpha'^{1/2}}{2} \ , \quad r_2 = -\frac{V_*}{V} r_6 \ . \tag{3.7}$$

μ, ν run over the directions $0, 1, 2$ tangent to all branes and i over the directions $3, 4, 5$ transverse to all branes. ds^2_{K3} is the metric of the unit volume $K3$. $V_* = (2\pi\sqrt{\alpha'})^4$ is a special value of the volume of $K3$. It is significant for the physics of this configuration as it will be revealed later. V is the volume of $K3$ as it is measured at infinity and the solution adjusts itself in such a way that

$$V(r) = V\frac{Z_2(r)}{Z_6(r)} . \tag{3.8}$$

is the volume of $K3$ in radius r.

We can see from the above solution of the wrapped D6–branes on the $K3$, that there is something wrong. There is a naked singularity at $r = -r_2$. This singularity is known as the repulson, because for small enough r it represents a repulsive gravitational field. The curvature diverges at this radius and, as it can be seen from (3.8), the volume of the $K3$ goes to zero.

3.2 The extremal enhançon

It is very important to see if the above solution can be trusted. Just the fact that it has a naked repulsive singularity gives us a hint that it cannot. In order to check the solution we will try to construct it from its constituent wrapped D–branes. The fundamental building blocks of this construction is the wrapped D6–brane which we have described earlier. These objects are still BPS, the net force on them is zero, and we can move them slowly around without spending energy. We would like to see if by bringing them one by one from infinity, we can make a geometry described by (3.5)[1].

3.2.1 Brane-probes

In order to understand the physics of the repulson, we will probe[2] the geometry (3.5) with a single D6–brane wrapped on $K3$. The effective action of such a probe in string frame is

$$S = -\int_{\mathcal{M}_2} d^3\xi e^{-\Phi}(\tau_6 V(r) - \tau_2)(-\det G_{\mu\nu})^{1/2} + \mu_6 \int_{\mathcal{M}_2\times K3} C_{(7)} - \mu_2 \int_{\mathcal{M}_2} C_{(3)}, \tag{3.9}$$

[1]We must stress here that in order to remain BPS the branes must be moved very slowly.

[2]Using a D–brane as a probe is a very helpful technique [185–189]. For a description of the method we refer to [163].

where $G_{\mu\nu}$ is the induced string-frame metric and $\mathcal{M}_2$ is the unwrapped part of the worldvolume. The first term is the DBI action with the position–dependent tension taken into account (3.8). The second and third terms are the Wess–Zumino terms and are the couplings of the brane charges to the background R–R fields. Remember that the composite object we use as our probe, carries D6–brane charge and D2–brane charge which is induced from the wrapping of the D6–brane on the $K3$.

We choose a static gauge, where we align the worldvolume coordinates ξ^μ with the first three spacetime coordinates (t, x^1, x^2) and then allow the transverse location of the brane–probe to depend only on time. Next we substitute the background (3.5) in the action (3.9), expand it in terms of velocity in x^i and keep only terms of quadratic order. This gives the effective Lagrangian density for the problem of moving slowly the brane–probe in the background produced by all the other branes:

$$\begin{aligned}\mathcal{L} &= -\frac{\mu_6 V Z_2 - \mu_2 Z_6}{g_s Z_2 Z_6} + \frac{1}{2g_2}(\mu_6 V Z_2 - \mu_2 Z_6)v^2 - \frac{mu_2}{g_s Z_2} + \frac{\mu_6 V}{g_s Z_6} \\ &= \frac{1}{2g_s}(\mu_6 V Z_2 - \mu_2 Z_6)v^2. \end{aligned} \tag{3.10}$$

So we see that in the effective Lagrangian density the term which plays the role of potential energy vanishes and only the kinetic term remains. This is expected from supersymmetry since our objects are BPS. From the kinetic part we can read the effective tension of the probe which can be written as

$$\tau_{eff} = \frac{1}{g_s}(\mu_6 V Z_2 - \mu_2 Z_6) = \frac{\mu_6 Z_6}{g_s}\left(\frac{Z_2}{Z_6} - \frac{V_*}{V}\right), \tag{3.11}$$

where we have used $\mu_2/\mu_6 = V_*$. The tension is changing as the probe is moving in the transverse space. We want the tension at spatial infinity to be positive and to suppress higher order corrections so we assume that the asymptotic volume $V \gg V_*$. As the probe moves towards the origin its effective tension is decreasing. It can be seen from (3.11) that it becomes zero when

$$r_e = \frac{2V}{V - V_*}|r_2| = \frac{2V_*}{V - V_*}r_6. \tag{3.12}$$

This is exactly the radius where the geometry becomes repulsive [129]. Furthermore, for radii smaller than that the effective tension of the probe becomes negative. At this radius the running $K3$ volume takes the special value $V(r_e) = V_*$.

From (3.12) it can be seen that the radius where the effective tension becomes zero is strictly larger than the radius of the singularity. Below r_e the brane tension is negative, which is something quite exotic yet unphysical. The interpretation of the process is that as the brane–probe moves towards the origin, its tension decreases up until it reaches zero. At that point the brane–probe ceases to be pointlike in the transverse directions and smears around over a two–sphere with radius r_e.

3.2.2 Enhanced symmetry

The wrapped D6–branes are BPS objects. From the six–dimensional point of view, they are higher dimensional realisations of magnetic monopoles. They carry a magnetic charge under a $U(1)$ form potential. Compactification of type IIA string theory on $K3$ produces twenty four one-form fields in six dimensions. Among others, the direct descendant of the ten–dimensional $C_{(1)}$ R–R potential and one coming from the $C_{(5)}$ potential wrapped on a four–cycle of the $K3$. In ten dimensions the D6–brane charge couples magnetically to $C_{(1)}$, while the D2–brane couples similarly to $C_{(5)}$. From the six–dimensional point of view, the BPS monopole is charged under a diagonal combination of these two form fields.

Apart from magnetic monopoles we have W–bosons and Higgs fields. The former are D4 and anti–D4–branes wrapped on the $K3$. From the six–dimensional point of view they are pointlike objects. The Higgs field is related to the running volume of the $K3$. This is a setup of $SU(2)$ monopoles.

When the tension of the wrapped D6–brane is zero, the wrapped D4–brane is massless, because $\mu_2/\mu_6 = \mu_0/\mu_4 = V_*$. This happens exactly at the same radius $r = r_e$, or equivalently when $V(r) = V_*$, for both objects. Since wrapped D4–branes are non–abelian bosons in this setup, when they become massless the broken $SU(2)$ symmetry is restored. The D4–brane combines with an anti-D4-brane along with the $U(1)$ R-R field into an $SU(2)$ gauge field. Due to this enhancement of symmetry from broken $U(1)$ to unbroken $SU(2)$ we name the resulting geometry the enhançon.

The mass of the $SU(2)$ monopole is proportional to the mass of the corresponding W-boson. Its characteristic size is inversely proportional to the mass. When W-bosons are massless and $SU(2)$ is restored, the monopole becomes massless and grows in size. Thus it ceases to be localised. This means that the probe that we use, cannot be localised within the enhançon radius. As it approaches the enhançon radius it starts to expand and it smears out reaching that radius, where it forms a shell.

It is interesting to try and construct the repulson geometry by bringing slowly wrapped D6–branes one by one from infinity. As they approach the enhançon radius, each of them behaves as the probe mentioned earlier. They grow and they smoothly smear into the shell already at the enhançon locus. The shell grows in size as it depends from the number of the D6–branes.

Since we cannot move the branes inside the enhançon radius, there are no brane sources in the interior. This means that the interior must be flat to a first approximation. The geometry inside is modified and the repulson singularity excised and replaced by a smooth geometry. Although supergravity tells us that the geometry is singular, the full string theory does not see any singularity; it is impossible to be formed.

Repulson geometry (3.5) represents the naive supergravity description of a solution with the correct asymptotic charges. In this solution the volume of the $K3$ is decreasing as it approaches the core of the configuration and becomes zero when it reaches the origin. This is the cause of the singularity. However at finite distance from the singularity, at the enhançon radius, something interesting happens. The running volume of the $K3$ takes the value $V = V_*$. At this volume there is an enhancement of symmetry from $U(1)$ to $SU(2)$, which is a stringy phenomenon. This cannot be described by the supergravity. There are extra light degrees of freedom which the supergravity misses. However, the supergravity seems to understand more about the solution than this statement suggests as we will see in Section 3.4.

3.2.3 Worldvolume gauge theory

One can study the system of N wrapped D6–branes from the point of view of the gauge theory that lives on the worldvolume[3]. There is an $SU(N)$ gauge theory with eight supercharges on the $(2+1)$–dimensional unwrapped world-volume of the N D6-branes. The gauge multiplet consists of a gauge field A_μ and three scalars Φ^i $(i = 3, 4, 5)$, transforming in the adjoint representation of $SU(N)$. These scalars encode information about the positions of the D6–branes in the transverse directions x^i. The gauge theory has a scalar potential of the form $\mathrm{Tr}[\Phi^i, \Phi^j]^2$, and the moduli space of supersymmetric vacua is parameterised by the vacuum expectation values of the scalars. To make the potential vanish, the vacuum expectation values live in the Cartan subalgebra of $SU(N)$, breaking the gauge symmetry from $SU(N)$ to $U(1)^N$. This is known as the "Coulomb branch" of the moduli space since there are generically U(1)'s unbroken.

The moduli space parameterised by the three scalars Φ^i is $3(N-1)$ dimensional, but in $2+1$ dimensions we can dualise the abelian gauge fields A_μ to give $N-1$ more scalars. Therefore the classical moduli space of the theory is $4(N-1)$-dimensional

$$\mathcal{M}_{cl}^N = \frac{(R^3 \times S^1)^N}{S_{N-1}} \tag{3.13}$$

where the S^1 factors represent the periodic scalars resulting from dualising the gauge fields, and S_{N-1} is the Weyl group of $SU(N)$ permuting the $N-1$ eigenvalues of the Φ^i. The $U(1)^{N-1}$ is the gauge symmetry of N wrapped D6–branes at arbitrary positions in the transverse dimensions. The extra $U(1)$ corresponds to the overall centre of mass of the system.

Now we take all the wrapped D6–branes to be coincident (meaning all the vacuum expectation values of adjoint scalars are given the same value in the gauge theory), except for a single brane, which has a complete multiplet of four scalars giving its location in the background of all the others. We can use this single wrapped D6–brane to probe the resulting subspace of the moduli space. In fact, we have already

[3] A detailed study goes beyond the scope of this thesis. More details can be found at [127, 130, 138, 163].

done the probing. Because probing the moduli space in gauge theory corresponds to probing the geometry in the supergravity picture.

Looking our previous probe calculation results (3.10) there seems to be one important bit of data missing. Our supergravity probe was moving in three transverse directions r, θ, ϕ, but as we have established just before, the gauge theory relative moduli space (i.e. the moduli space corresponding to the motion of a single brane in the background of others) must be four dimensional.

In general a $(2+1)$–dimensional theory with eight supercharges has a moduli space which is hyper-Kähler [190], requiring a dimension multiple of four. There is an extra modulus which is missing from our probe calculation which is related to the $2+1$–dimensional gauge field on the worldvolume of the branes. This can be dualised to a periodical scalar. This feature is specific to the $p=2$ case.

To get the coupling for this extra modulus right we should augment the previous probe calculation to include A_μ. The DBI part of the action is modified by an extra term in the determinant

$$-detG_{\mu\nu} \rightarrow -det(G_{\mu\nu} + 2\pi\alpha' F_{\mu\nu}), \tag{3.14}$$

where $F_{\mu\nu}$ is the field strength of A_μ. In the presence of the worldvolume gauge field there is a coupling to the WZ part of the probe action

$$-2\pi\alpha' \int_M C_1 \wedge F, \tag{3.15}$$

where $C_1 = C_\phi d\phi$ is the magnetic potential produced by the D6–brane

$$C_\phi = -\frac{r_6}{g_s} cos\theta. \tag{3.16}$$

Instead of operating with a A_μ we would like to exchange it with a scalar s, Hodge dual to a vector potential in three dimensions. The trick [191, 192] is to introduce an auxiliary vector field v_μ and replace $2\pi\alpha' F_{\mu\nu}$ by $e^{2\phi}(\mu_6 V(r) - \mu_2)^{-2} v_\mu v_\nu$ in the DBI part and add the term $2\pi\alpha' \int_M F \wedge v$ overall.

Integrating out v will give an action involving F as the one we started with. Treating $F_{\mu\nu}$ as a Lagrange multiplier enforces

$$\epsilon^{\mu\nu\lambda} \partial_\nu (\mu_2 \hat{C}_\lambda + v_\lambda) = 0. \tag{3.17}$$

$\hat{C}_\lambda$ are the components of the pullback of C_1 to the probe's worldvolume. The solution to the above constrain is

$$\mu_2 \hat{C}_\mu + v_\mu = \partial_\mu s, \tag{3.18}$$

where the scalar s is the fourth modulus. We can now replace v_μ by $\partial_\mu s - \mu_2 \hat{C}_\mu$ in the action. Using a static gauge we can calculate the effective lagrangian of the probe

$$\mathcal{L} = F(r)\left(\dot{r} + r^2 \dot{\Omega}^2\right) + F(r)^{-1}\left(\frac{\dot{s}}{2} - \mu_2 C_\phi \frac{\dot{\phi}}{2}\right)^2, \tag{3.19}$$

where

$$F(r) = \frac{Z_6}{2g_s}(\mu_6 V(r) - \mu_2) \tag{3.20}$$

and $\dot{\Omega}^2 = \dot{\theta}^2 + sin^2\theta\dot{\phi}^2$. Notice that this effective lagrangian still vanishes at $r = r_e$.

One can separate the gauge theory data from the rest of the bulk physics by taking the decoupling limit [93] $\alpha' \to 0$, while holding the gauge theory coupling $g^2_{YM} = g^2_{YM,6} V^{-1} = (2\pi)^4 g_s \alpha'^{3/2} V^{-1}$ and the energy scale $U = r/\alpha'$ fixed.

In this limit we can extract from the kinetic lagrangian (3.19) the following metric for the moduli space of the gauge theory:

$$ds^2 = f(u)\left(\dot{U}^2 + U^2 d\Omega^2\right) + f(U)^{-1}\left(d\sigma - \frac{N}{4\pi^2} A_{phi} d\phi\right)^2, \tag{3.21}$$

where

$$f(U) = \frac{1}{4\pi^2 g^2_{YM}}\left(1 - \frac{g^2_{YM} N}{U}\right). \tag{3.22}$$

The $U(1)$ monopole potential is $A_\phi = \pm 1 - cos\theta$ and $\sigma = \alpha' s$. This metric is meaningful only for $U > U_e$ which corresponds to the enhançon radius.

This metric is the hyper–Kähler Taub–NUT metric and it is singular. It has the interpretation of tree plus one–loop result [127]. The singularity warns that the moduli space metric is still incomplete. However, it does not receive any more perturbative corrections from higher loops, but gets fixed non-perturbatively by instanton corrections. This proof goes beyond the scope of the thesis and the references mentioned earlier can be consulted.

3.2.4 Extra D2–branes

Adding M extra real D2–branes in the extremal solution of (3.5) has the effect that it increases the D2–brane charge from $-N$ to $M - N$. In the exterior solution this shift is accomplished by modifying accordingly the harmonic function Z_2. r_2 in (3.7) is now

$$r_2 = -\frac{V_*}{V} r_6 \left(1 - \frac{M}{N}\right) \tag{3.23}$$

with r_6 remaining as it is in (3.7). The enhançon radius is also modified and it is now given by the expression

$$r_\mathrm{e} = \frac{2V_* r_6}{V - V_*} \left(1 - \frac{M}{2N}\right) . \tag{3.24}$$

The exterior solution (3.5) with the modified scale (3.23) applies for $r > r_\mathrm{e}$. It can be seen from (3.24) that for increasing number M of extra D2–branes the enhançon radius is decreasing. Actually for $M \geq 2N$, there is no enhançon shell at all and the D6–branes and D2–branes can coalesce on the origin.

We will briefly discuss the physics of the above configuration. We will assume that $M < 2N$ so that there is an enhançon shell. A single D2–brane encounters no obstacle to moving past the enhançon radius and finally to the origin, because its tension is constant. We would expect that in a system with M extra D2–branes, they could all be at the origin, while all N wrapped D6–branes remain at the shell. In this case, the six–brane harmonic function in the interior is simply a constant $H_6 = Z_6(r_\mathrm{e})$. From (3.30)

$$H_2 = \gamma + \frac{r_2'}{r} \tag{3.25}$$

with γ a constant and r_2' positive for $N' = 0$. This grows as r decreases. The volume of $K3$ is given by

$$V(r) = V\frac{H_2}{H_6} = V\frac{\gamma + r_2'/r}{Z_6(r_\mathrm{e})} , \tag{3.26}$$

where the constants are fixed by the condition $V(r_\mathrm{e}) = V_*$. The volume increases as the r increases. This means that there is no obstruction for some wrapped D6–branes from the shell to move to the origin. It is easy to check if there is a limit to how many D6–branes can we move this way. We require that the maximum number N' of D6–branes we can move to the origin, is achieved when the running volume of the $K3$ at the origin is equal to the special volume V_*

$$V(r=0) = V\frac{H_2(0)}{H_6(0)} = V\frac{r_2'}{r_6'} = V_* \ . \tag{3.27}$$

This is satisfied when $N' = M/2$. What this means is that, having $N' = M/2$ D6–branes in the origin along with the M D2–branes, a wrapped D6–brane probe cannot move past the enhançon radius and has to stop there.

There is a mechanism that can allow for even more wrapped D6–branes to move in the interior. This can be achieved by carrying some of the D2–branes back out to the enhançon shell and binding them to an equal number of wrapped D6–branes. This composite unit can move past the enhançon radius since the negative tension induced from the $K3$ is cancelled by the tension of the instantonic D2–branes, smeared over the worldvolume of the D6–branes. The threshold bound state becomes a BPS state for $r < r_e$ and can move in the interior. Using this mechanism we can form configurations with up to $N' = M$ wrapped D6–branes in the origin. This is the maximum we can have since for $N' > M$, $r_2' < 0$ so there is a repulson singularity in the interior.

In this limiting solution it can be seen that the interior solution has zero net D2–charge. One also finds that the $K3$ volume shrinks below the stringy scale V_*. One should notice that the enhançon radius (3.24) does not change by the migration of D6–branes from the shell to the origin.

The interior will be described by the metric of M D2–branes and N' D6–branes placed at the origin. The interior geometry is given by

$$g_s^{1/2} = H_2^{-5/8}H_6^{-1/8}\eta_{\mu\nu}dx^\mu dx^\nu + H_2^{3/8}H_6^{7/8}\left(dr^2 + r^2 d\Omega\right) + V^{1/2}H_2^{3/8}H_6^{-1/8}ds^2_{K3} \tag{3.28}$$

in Einstein frame. The non–trivial fields are

$$\begin{aligned} e^{2\Phi} &= g_s^2 H_2^{1/2} H_6^{-3/2} \ , \\ C_{(3)} &= (g_s H_2)^{-1} dt \wedge dx^1 \wedge dx^2 \ , \\ C_{(7)} &= (g_s H_6)^{-1} dt \wedge dx^1 \wedge dx^2 \wedge V\,\varepsilon_{\mathrm{K3}} \ , \end{aligned} \tag{3.29}$$

where

$$H_2 = 1 + \frac{r_2 - r_2'}{r_{\rm e}} + \frac{r_2'}{r}, \qquad r_2' = -r_6 \frac{V_*}{V} \frac{N' - M}{N} , \tag{3.30}$$

$$H_6 = 1 + \frac{r_6 - r_6'}{r_{\rm e}} + \frac{r_6'}{r}, \qquad r_6' = r_6 \frac{N'}{N} = \frac{g_s N' \alpha'^{1/2}}{2} . \tag{3.31}$$

The constant terms in the harmonic functions are chosen in such a way that it ensures continuity with the exterior solution at the incision radius.

3.3 The non–extremal enhançon

A non-extremal solution can be written using again the harmonic function rule for non–extremal p–brane solutions. Such a solution was first written down in [127]. In [129], it was found that there are two branches of non-extremal solutions, arising from an ambiguity of a choice of sign in the solution of the supergravity equations for the usual ansatz. A non-extremal generalisation[4] of the exterior geometry in the Einstein frame is

$$\begin{aligned} g_s^{1/2}\, ds^2 &= Z_2^{-5/8} Z_6^{-1/8} (-K dt^2 + dx_1^2 + dx_2^2) + Z_2^{3/8} Z_6^{7/8} (K^{-1} dr^2 + r^2 d\Omega_2^2) \\ &\qquad + V^{1/2} Z_2^{3/8} Z_6^{-1/8} ds_{\rm K3}^2 , \end{aligned} \tag{3.32}$$

the dilaton and R–R fields are

$$\begin{aligned} e^{2\Phi} &= g_s^2 Z_2^{1/2} Z_6^{-3/2} , \\ C_{(3)} &= (g_s \alpha_2 Z_2)^{-1} dt \wedge dx^1 \wedge dx^2 , \\ C_{(7)} &= (g_s \alpha_6 Z_6)^{-1} dt \wedge dx^1 \wedge dx^2 \wedge V\, \varepsilon_{\rm K3} , \end{aligned} \tag{3.33}$$

and the various harmonic functions are given by

$$\begin{aligned} K &= 1 - \frac{r_0}{r} , \\ Z_2 &= 1 + \frac{\hat{r}_2}{r} \qquad Z_6 = 1 + \frac{\hat{r}_6}{r} . \end{aligned} \tag{3.34}$$

[4]This comes from a general rule of writing non–extremal solutions as we saw in the previous chapter. We solve the equations in more generality in Chapter 7.

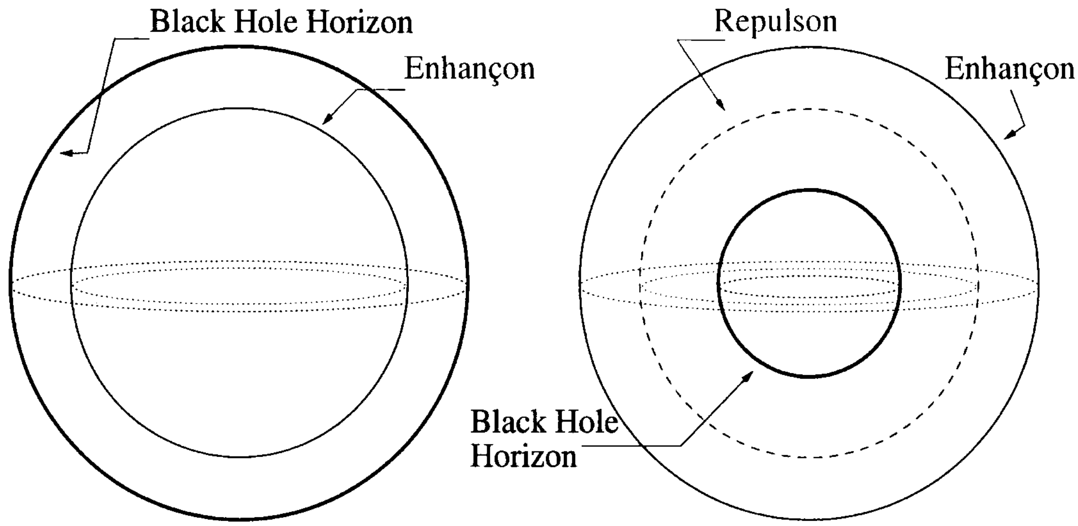

Figure 3.1: *The two branches of the non–extremal enhançon solution as they look in the transverse space. On the left the horizon branch, which looks like a black hole, and on the right the shell branch with the enhançon shell outside the black hole horizon.*

Here

$$\hat{r}_6 = -\frac{r_0}{2} + \sqrt{r_6^2 + \left(\frac{r_0}{2}\right)^2}\,, \tag{3.35}$$

and $\alpha_6 = \hat{r}_6/r_6$. There are two choices for $\hat{r}_2$ consistent with the equations of motion:

$$\hat{r}_2 = -\frac{r_0}{2} \pm \sqrt{r_2^2 + \left(\frac{r_0}{2}\right)^2}\,, \tag{3.36}$$

and $\alpha_2 = \hat{r}_2/r_2$. Here, r_2 and r_6 are still given by (3.7). The repulson singularity, if there is one, is at $r = -\hat{r}_2$.

There are two branches of solutions. In Figure 3.1 one can see these two branches as they would look in the transverse space.

Horizon branch

For the upper sign in (3.36), $\hat{r}_2 > 0$, so there is no repulson singularity[5]. The solution has a regular horizon at $r = r_0$. It looks like a black hole with R–R charges. For large values of the non–extremality parameter r_0, the R–R charges are negligible so the solution looks like an uncharged black hole. Actually it approaches a four dimensional Schwarzschild metric smeared over the $K3$ and longitudinal x^1, x^2 directions. We refer to this as the horizon branch.

Shell branch

For the lower choice of sign, however, the repulson singularity always lies outside the would-be horizon, $|\hat{r}_2| > r_0$, and the geometry will be corrected by an enhançon shell. We refer to this as the shell branch of solutions.

The shell branch exterior solution is cut off by an enhançon shell at

$$r_{\rm e} = \frac{V_* \hat{r}_6 - V \hat{r}_2}{V - V_*} \ . \tag{3.37}$$

As in the extremal case, this shell will contain N D6-branes, while the interior solution is

$$\begin{aligned} g_s^{1/2}\, ds^2 &= H_2^{-5/8} H_6^{-1/8} \left(-\frac{K(r_{\rm e})}{L(r_{\rm e})} L dt^2 + dx_1^2 + dx_2^2 \right) + H_2^{3/8} H_6^{7/8} (L^{-1} dr^2 + r^2 d\Omega) \\ &\qquad + V^{1/2} H_2^{3/8} H_6^{-1/8} ds_{K3}^2 \ , \end{aligned} \tag{3.38}$$

with accompanying fields

$$\begin{aligned} e^{2\Phi} &= g_s^2 H_2^{1/2} H_6^{-3/2} \ , \\ C_{(3)} &= \left(\frac{K(r_{\rm e})}{L(r_{\rm e})} \right)^{1/2} (g_s \alpha_2' H_2)^{-1} dt \wedge dx^1 \wedge dx^2 \ , \\ C_{(7)} &= \left(\frac{K(r_{\rm e})}{L(r_{\rm e})} \right)^{1/2} (g_s \alpha_6' H_6)^{-1} dt \wedge dx^1 \wedge dx^2 \wedge V\, \varepsilon_{\rm K3} \ , \end{aligned} \tag{3.39}$$

[5]The volume of the $K3$ is still running and there is an enhançon radius when it reaches V_*. This means that there can be an enhançon shell inside the horizon. In the case when M extra D2–branes are present, there can be a shell outside the horizon for an appropriate value of r_0. For $M > 2N$ there is no enhançon shell at all. More details can be found at [129].

where

$$
\begin{aligned}
L &= 1 - \frac{r_0'}{r} , \\
H_2 &= 1 + \frac{\hat{r}_2}{r_e} , \\
H_6 &= 1 + \frac{\hat{r}_6}{r_e} .
\end{aligned} \tag{3.40}
$$

Note that we have introduced an independent non-extremality scale r_0' for the interior solution. Implicitly $r_0' < r_e$ in order that the interior black hole actually fits inside the shell. We have taken the horizon branch for the interior solution.

This parameter r_0', is not determined by the asymptotic charges of the solution. We expect that it will be fixed by the physics of the enhançon. Currently we lack such an understanding so we will keep it as an undetermined parameter.

3.3.1 Extra D2–branes

As in the extremal case, the addition of extra D2–branes in the non–extremal case causes an increase in the D2–charge. This increase is the same as in the extreme case (3.23). The presence of the D2–branes causes the enhançon radius to shrink and so for a large number of D2–branes there will be no enhançon shell at all.

The addition of the extra D2–branes does not change the two branch structure of the initial solution. Again there is a horizon branch solution and a shell branch solution.

In the case of the shell branch, the extra D2–branes can move past the enhançon radius, as in the extremal case, and fall into the black hole in the interior. They can also help some of the wrapped D6–branes from the shell to fall into the black hole.

3.4 Junction Conditions

3.4.1 Extremal case

We saw that the repulson geometry is replaced by a space with a shell of D–branes at a radius larger than the repulson radius. We also conjectured that the spacetime inside the shell is flat. We would like to check if this is consistent from the point of view of supergravity. This can be done by using standard General Relativistic techniques [193]. We can calculate the stress–energy and charges of the shell matching the exterior repulson solution and the interior flat space. This calculation first appeared in [129].

The standard procedure is as follows. We would like to join two solutions of Einstein's equations on a surface Σ. There may be a discontinuity in the extrinsic curvature at the surface. We can interpret this discontinuity as a δ–function source of stress-energy located at the surface Σ. In the following we will describe how to derive the stress–energy of the shell of branes. In the next section we will show that it is consistent with the model of the shell constructed from wrapped D6-branes.

First of all we must stress that in order to be able to interpret the discontinuity in the extrinsic curvature as a stress–energy tensor, we must perform the computation in Einstein frame. In ten dimensions one gets the Einstein frame metric from the string frame metric by the conformal rescaling

$$ds_E^2 = e^{-\Phi/2} ds_s^2, \tag{3.41}$$

so in the Einstein frame the repulson metric is

$$g_s^{1/2} ds^2 = Z_2^{-5/8} Z_6^{-1/8} \eta_{\mu\nu} dx^\mu dx^\nu + Z_2^{3/8} Z_6^{7/8} (dr^2 + r^2 d\Omega_2^2) + V^{1/2} Z_2^{3/8} Z_6^{-1/8} ds_{\mathrm{K3}}^2 \, . \tag{3.42}$$

where Z_2 and Z_6 are given by (3.6). The dilaton and the RR gauge fields remain as in (3.5). We will denote the components of the metric tensor as G_{AB}.

We perform an incision at arbitrary radius $r = r_\mathrm{i}$ and replace the solution for $r < r_\mathrm{i}$ by a flat spacetime. Since we make a radial slice, we can define unit normal vectors

$$\eta_\pm = \mp \frac{1}{\sqrt{G_{rr}}} \frac{\partial}{\partial r}, \tag{3.43}$$

where η_+ (η_-) is the outward pointing normal for the spacetime region $r > r_\mathrm{i}$ ($r < r_\mathrm{i}$). Now we can write the extrinsic curvature of the junction surface Σ as

$$K^\pm_{AB} = \frac{1}{2} \eta^C_\pm \partial_C G_A B = \mp \frac{1}{2\sqrt{G_{rr}}} \frac{\partial G_{AB}}{\partial r} \tag{3.44}$$

We define the discontinuity in the extrinsic curvature across the junction as

$$\gamma_{AB} = K^+_{AB} + K^-_{AB}. \tag{3.45}$$

We can write now the stress–energy supported at the junction as

$$S_{AB} = \frac{1}{\kappa^2}\left(\gamma_{AB} - G_{AB}\gamma^C{}_C\right), \tag{3.46}$$

where κ is the ten–dimensional gravitational coupling. In our conventions it is $2\kappa^2 = 16\pi G_N = (2\pi)^7(\alpha')^4 g_s^2$.

We want to match the exterior metric (3.42) with the RR and dilaton fields (3.5), with a flat geometry

$$\begin{aligned}
g_s^{1/2}\,ds^2 &= H_2^{-5/8}(r_{\rm i})H_6^{-1/8}(r_{\rm i})\eta_{\mu\nu}dx^\mu dx^\nu + H_2^{3/8}(r_{\rm i})H_6^{7/8}(r_{\rm i})(dr^2 + r^2 d\Omega_2^2)\\
&\qquad V^{1/2}H_2^{3/8}(r_{\rm i})H_6^{-1/8}(r_{\rm i})ds^2_{\rm K3}\\
e^{2\Phi} &= g_s^2 H_2{}^{1/2}(r_{\rm i})H_6{}^{-3/2}(r_{\rm i})\ ,\\
C_{(3)} &= (H_2(r_{\rm i})g_s)^{-1}dx^0\wedge dx^1\wedge dx^2\ ,\\
C_{(7)} &= (H_6(r_{\rm i})g_s)^{-1}dx^0\wedge dx^1\wedge dx^2\wedge V\,\varepsilon_{\rm K3}\ .
\end{aligned} \tag{3.47}$$

The interior solution (3.47) is written in such coordinates, so that all fields are continuous through the incision.

We can now compute the discontinuity tensor γ_{AB}

$$\begin{aligned}
\gamma_{\mu\nu} &= \frac{1}{16}\frac{1}{\sqrt{G_{rr}}}\left(5\frac{Z_2'}{Z_2} + \frac{Z_6'}{Z_6}\right)G_{\mu\nu},\\
\gamma_{ij} &= -\frac{1}{16}\frac{1}{\sqrt{G_{rr}}}\left(3\frac{Z_2'}{Z_2} + 7\frac{Z_6'}{Z_6}\right)G_{\mu\nu},\\
\gamma_{ab} &= -\frac{1}{16}\frac{1}{\sqrt{G_{rr}}}\left(3\frac{Z_2'}{Z_2} - \frac{Z_6'}{Z_6}\right)G_{\mu\nu},
\end{aligned} \tag{3.48}$$

where a prime denotes differentiation with respect to r, and all quantities are evaluated at the incision radius $r_{\rm i}$. μ,ν are for the directions along the brane, i,j the two angular directions transverse to the brane and a,b the four $K3$ directions. The trace is

$$\gamma^C{}_C = -\frac{1}{16}\frac{1}{\sqrt{G_{rr}}}\left(3\frac{Z_2'}{Z_2} + 7\frac{Z_6'}{Z_6}\right) \tag{3.49}$$

Now we can put everything together and compute the stress energy tensor at the discontinuity

$$\begin{aligned}
S_{\mu\nu} &= \frac{1}{2\kappa^2\sqrt{G_{rr}}}\left(\frac{Z_2'}{Z_2} + \frac{Z_6'}{Z_6}\right)G_{\mu\nu},\\
S_{ij} &= 0,\\
S_{ab} &= \frac{1}{2\kappa^2\sqrt{G_{rr}}}\left(\frac{Z_6'}{Z_6}\right)G_{ab}.
\end{aligned} \tag{3.50}$$

The result is quite interesting. The last line, which gives the components of the stress–energy tensor along the $K3$ directions involves only the harmonic function of the D6–brane. This is consistent with the fact that there are only D6–branes wrapped there. The middle line shows that there is no pressures in the direction transverse to the branes. There are no forces between the branes to support the shell in the transverse space and this is consistent with the fact that the branes are BPS.

Another result from (3.50) is that the stress–energy of unwrapped part is proportional to $\frac{Z_2'}{Z_2} + \frac{Z_6'}{Z_6}$ which vanishes at $r = r_{\rm e}$. This is the radius where the probe has zero tension and the supergravity starts becoming repulsive. So the probe calculation and the above calculation which was done using only supergravity come to the same result; at the enhançon radius there is a shell of zero tension branes.

For values for $r_{\rm i} < r_{\rm e}$ we would get a negative tension from the stress–energy tensor. This is a situation that can not be allowed, since in supergravity the Weak Energy Condition should be satisfied for physical solutions. On the other hand, the computation shows that there is no obstacle to choose any other radius for the incision, larger than the enhançon radius, and place a shell of branes of positive tension. This is due to the fact that the constituent objects are BPS and experience no potential, so we can place them at any position outside the enhançon radius. The enhançon radius works as a limit as to where we can place the branes. This is obvious both from the probe and junction conditions calculations.

When extra D2–branes are present the discussion does not change much. The difference is now that the extra D2–branes can move in the interior and some of the wrapped D6–branes can migrate with them. The internal geometry is no longer flat since H_2 and H_6 are not constants but they are given by (3.30,3.31). We can again compute the stress–energy tensor using the Israel junction conditions as we did earlier. In this case it is

$$\begin{aligned} S_{\mu\nu} &= \frac{1}{2\kappa^2\sqrt{G_{rr}}}\left(\frac{Z_2'}{Z_2} + \frac{Z_6'}{Z_6} - \frac{H_2'}{H_2} - \frac{H_6'}{H_6}\right) G_{\mu\nu}, \\ S_{ij} &= 0, \\ S_{ab} &= \frac{1}{2\kappa^2\sqrt{G_{rr}}}\left(\frac{Z_6'}{Z_6} - \frac{H_6'}{H_6}\right) G_{ab}. \end{aligned} \tag{3.51}$$

Again the pressure in the shell directions vanishes in agreement with the fact that the system is still BPS. It is trivial to check that this stress–energy tensor is exactly the same as the stress–energy of $N - N'$ wrapped D6–branes distributed uniformly on the sphere.

A model for the shell

We saw earlier that there is some agreement between the supergravity calculation (3.50) and the notion that the shell consists of wrapped D6–branes. We will now see that the stress–energy of the shell is exactly the same as the stress–energy of N wrapped D6–branes distributed uniformly on the sphere.

The stress–energy should be given by

$$S_{AB} = \int \sqrt{G_{rr}} dr \left(-\frac{2}{\sqrt{-G}} \sum_{shell} \frac{\delta S_{brane}}{\delta G_{AB}} \right) \delta(r - r_{\rm i}), \tag{3.52}$$

where G is the determinant of G_{AB} and the sum means that we include the contributions from all the constituent branes in the shell. The term in the parentheses is the standard definition of the stress–energy tensor. The source coming from the shell of branes is a distribution so the integral is included to eliminate the radial δ function.

S_{brane} is the action which describes the dynamics of the brane. The metric appears only in the DBI part of the D–brane action (3.9). The action for N wrapped D6–branes in Einstein frame is

$$S_{DBI} = -N \int_{\mathcal{M}_\in} d^3\xi e^{-\Phi/4} (\mu_6 e^{\Phi} V_E(r) - \mu_2)(-\det G_{\mu\nu})^{1/2} \tag{3.53}$$

where

$$V_E(r) = \int_{K3} d^4x \sqrt{-G_{ab}}$$

is the volume of the $K3$ in the Einstein frame and $G_{\mu\nu}$ is the pull back of the Einstein frame metric to the effective membrane worldvolume. Now using (3.52), (3.53) and the fact that the N D6–branes are distributed over a two–sphere S^2, the stress–energy of the source branes can be written as

$$\begin{aligned} S_{\mu\nu} &= \frac{Ne^{-\Phi/4}}{V_E Vol(S^2)}\left(\mu_2 - \mu_6 e^{\Phi} V_E\right) G_{\mu\nu}, \\ S_{ij} &= 0, \\ S_{ab} &= \frac{Ne^{3\Phi/4}}{Vol(S^2)}\mu_6 G_{ab}. \end{aligned} \tag{3.54}$$

Using the identities $N\mu_6 = \frac{4\pi}{2\kappa^2}\tau_6$ and $N\mu_2 = -\frac{4\pi}{2\kappa^2}V\tau_2$ we can see that the above stress–energy is identical to (3.50).

We can follow the same procedure in order to calculate the discontinuity to the rest of the fields. Regarding the Ramond-Ramond fields, the argument is easy since the interior is just flat space. The exterior geometry contains N units of $C_{(7)}$ flux and $-N$ units of $C_{(3)}$ flux, while the interior has none. Thus the shell carries the charges of N wrapped D6–branes. Regarding the dilaton things are a bit more complicated but similar to the calculation of of the stress–energy tensor. The dilaton discontinuity is given by

$$S_\Phi = \frac{1}{2\kappa^2 G_{rr}}\left(\Phi'|_{r=r_i+\epsilon} - \Phi'|_{r=r_i-\epsilon}\right) = \frac{1}{2\kappa^2 G_{rr}}\left(-\frac{3}{4}\frac{Z_6'}{Z_6} + \frac{1}{4}\frac{Z_2'}{Z_2}\right)\delta(r - R_i), \tag{3.55}$$

where ϵ is a small number. We can compute from (3.53) the source term for the dilaton

$$S_\Phi = \int \sqrt{G_{rr}}dr\left(-\frac{2}{\sqrt{-G}}\sum_{shell}\frac{\delta S_{brane}}{\delta\Phi}\right), \tag{3.56}$$

which is equal to

$$S_\Phi = \frac{N}{4\pi g_s Vol(S^2)}\left(\frac{3}{4}e^{3\Phi/4}\mu_6 + \frac{1}{4}\frac{e^{-\Phi/4}}{V_E(r)}\mu_2\right). \tag{3.57}$$

It can be shown again quite easily that this is exactly equal to (3.55).

As another check of this interpretation, we can expand the results in (3.50) for large r_i. Up to an overall sign, the coefficient of the metric components in the stress–energy tensor, gives the effective tension in the various directions. The leading contributions are

$$\begin{aligned} \tau_{mem}(r_i) &= \frac{1}{\kappa^2}\frac{r_6}{r_i^2}\left(1 - \frac{V_*}{V}\right) \\ &= \frac{N}{(2\pi)^6(\alpha')^{7/2}g_s}(V - V_*)\frac{1}{4\pi r_i^2 V} = N(\tau_6 V - \tau_2)\frac{1}{4\pi r_i^2 V} \end{aligned} \tag{3.58}$$

$$\tau_{K3}(r_i) = \frac{1}{\kappa^2}\frac{r_6}{r_i^2} = \frac{N}{(2\pi)^6(\alpha')^{7/2}g_s}\frac{1}{4\pi r_i^2} = N\tau_6\frac{1}{4\pi r_i^2} \tag{3.59}$$

which is in agreement with what we expect. In the $K3$ directions, the effective tension matches that of N fundamental D6–branes. The additional averaging factor $1/(4\pi r_{\rm i}^2)$ indicates that the branes are smeared over the shell in the transverse space. In the unwrapped $x^{0,1,2}$ directions we have an effective membrane tension which matches that of N D6–branes and includes the $-N$ units of D2–brane tension, which is a result of the wrapping on the $K3$.

The above discussion can easily be extended to the case of extra D2–branes present. Using the same arguments we can see that the shell can be modelled by the remaining wrapped D6–branes smeared over a two–sphere at the enhançon radius.

All the above results provide a verification of the argument that the matching of the exterior 'repulson' geometry with a flat interior geometry at any radius has the interpretation of introducing a shell of wrapped D6–branes as the source. This is just a small indication that even supergravity which cannot describe the 'repulson' geometry correctly, understands that it is not correct and grasps some of the physics that string theory was used to unveil. Unfortunately when discussing the non–extremal case, supergravity alone can not help us in understanding the shell. We find that physics beyond supergravity is essential in order to write down a physically acceptable solution.

3.4.2 Non–extremal case

As we did in the extremal case we can calculate the stress energy of the shell from the Israel junction conditions. We will perform this only for the shell branch since only then we have a shell. The techniques are the same as in the extremal case. We will use (3.32) as the exterior metric and (3.38) as the interior and insert a shell at a radius $r_{\rm i}$. The stress tensor becomes:

$$
\begin{aligned}
2\kappa^2 S_{tt} &= \frac{1}{\sqrt{G_{rr}}}\left(\frac{\hat{Z}_2'}{\hat{Z}_2}+\frac{\hat{Z}_6'}{\hat{Z}_6}+\frac{4}{r_{\rm i}}\left(1-\sqrt{\frac{L}{K}}\right)\right)G_{tt}\ ,\\
2\kappa^2 S_{\mu\nu} &= \frac{1}{\sqrt{G_{rr}}}\left(\frac{\hat{Z}_2'}{\hat{Z}_2}+\frac{\hat{Z}_6'}{\hat{Z}_6}+\frac{K'}{K}-\frac{L'}{L}\sqrt{\frac{L}{K}}+\frac{4}{r_{\rm i}}\left(1-\sqrt{\frac{L}{K}}\right)\right)G_{\mu\nu}\ ,\\
2\kappa^2 S_{ij} &= \frac{1}{\sqrt{G_{rr}}}\left(\frac{K'}{K}-\frac{L'}{L}\sqrt{\frac{L}{K}}+\frac{4}{r_{\rm i}}\left(1-\sqrt{\frac{L}{K}}\right)\right)G_{ij}\ ,\\
2\kappa^2 S_{ab} &= \frac{1}{\sqrt{G_{rr}}}\left(\frac{\hat{Z}_6'}{\hat{Z}_6}+\frac{K'}{K}-\frac{L'}{L}\sqrt{\frac{L}{K}}+\frac{4}{r_{\rm i}}\left(1-\sqrt{\frac{L}{K}}\right)\right)G_{ab}\ ,
\end{aligned}
\tag{3.60}
$$

where μ, ν run over the x^1 and x^2 directions, and G_{rr} is the radial component of the exterior metric (3.32). With respect to the extremal stress-energy tensor (3.50), there is a difference. Now there are stresses in the transverse directions, since S_{ij} is non-zero.

Note that the stress–energy tensor depends on the extra parameter r_0' through the function $L(r)$. We can try and constrain this parameter by examining the transverse part of the stress–energy tensor. The sign of S_{ij} is completely determined by r_0 and r_0'. For $r_0' > r_0$, the sign is negative, so there is a positive tension in these directions. The shell wants to expand in these directions but there is an internal tension which holds it in place. For $r_0' < r_0$, the sign is positive so there is a positive pressure in these directions. The shell wants to collapse but there is an internal pressure which prevents that. Since the gravitational attraction of the black hole in the interior causes this imbalance of the forces, we restrict our attention to the later case $r_0' < r_0$. This also means that r_0' is always smaller than the enhançon radius so that the interior black hole fits inside the enhançon radius.

A rather exceptional case is $r_0' = r_0$. For this choice the stress–energy tensor simplifies and $S_{ij} = 0$. Its form is very similar to the BPS configuration (3.50). As in the BPS case we can calculate the effective tension of the branes in the various directions. The leading contributions are:

$$
\begin{aligned}
\tau_{mem}(r_{\rm i}) &= \frac{N-N'}{4\pi r_{\rm i}^2 V}(\hat{\tau}_6 V - \hat{\tau}_2)\\
\tau_{K3}(r_{\rm i}) &= \frac{N-N'}{4\pi r_{\rm i}^2}\hat{\tau}_6\ ,
\end{aligned}
\tag{3.61}
$$

where $\hat{\tau}_6 = \sqrt{L(r_{\rm i})}\alpha_6\tau_6$ and $\hat{\tau}_2 = \sqrt{L(r_{\rm i})}\alpha_2\tau_2$. The results are essentially the same as in (3.58) with modified fundamental tensions. One could follow the procedure of Sections 3.4 and 3.4.1 and model the source, as a shell of wrapped six–branes distributed over a two–sphere, with an appropriate action, as in (3.53) but with modified tensions. It can be verified that these tensions do not correspond to those of a wrapped D6–brane for any value of $r_{\rm i}$. There is no object which looks like a six brane, and has such a tension in string theory. Supergravity configurations with $r_0' = r_0$ are unlikely to be physically relevant.

By using some physical arguments, we managed to constrain the r_0' parameter. It is quite difficult to fix it completely. This is an unphysical degree of freedom and it requires a better understanding of the physics of the non–extremal enhançon. It could then be determined uniquely in terms of the asymptotic mass and charges of the configuration. Since supergravity provides a very crude description of the shell and string theory is not very illuminating in non–extremal scenarios, we will have to keep it as a free parameter.

An almost identical discussion can be made when we have additional D2–branes and the enhançon shell is present. We can calculate the stress–energy tensor of the shell using the Israel junction conditions, which is a more general form of (3.60). As in the original case we do not know how to model the shell using a shell made of D–branes and this leads to the same problems as with the original.

3.5 Some concerns on non–extremal enhançons

There are two branches of non-extremal solutions, arising from an ambiguity of a choice of sign in the solution of the supergravity equations. One branch joins on to the extremal enhançon solution studied previously, and always has a shell of branes outside the horizon. The other branch appears at a finite value of the non-extremality parameter. Above this critical value of the non-extremality, both types of solution are possible. At large energies, the effects of the D-brane charges should be negligible, so the solution with a horizon, which for large mass is approximately the usual uncharged black hole solution, has the right physical behaviour. On the other hand, if we begin slowly adding energy to the extremal enhançon, we will obtain a solution on the branch with a shell.

Notice that the solution does not make a smooth transition between the two branches. Consider the limit $r_2 \to 0$. From (3.7), we see that this is equivalent to $V \to \infty$. From (3.36) we see that for the horizon branch (upper sign) it gives $\hat{Z}_2 = 1$, while for the shell branch (lower sign) it gives the non–trivial $\hat{Z}_2 = 1 - r_0/r$. (This discontinuity vanishes for the extremal limit.) The latter behaviour is puzzling. $V \to \infty$ means that the volume of the compactification space $K3$ goes to infinity so in this limit we effectively have an unwrapped non–extremal D6–brane. The effective D2–charges are infinitely diluted over the D6–brane worldvolume. In the first case (horizon branch) we get the result that we expect: unwrapped non–extremal D6–branes. In the shell branch we get something different. The three–form R–R potential vanishes in this limit but the harmonic function $\hat{Z}_2$ does not. This harmonic function has a non–trivial contribution to the metric components of the solution and the dilaton. Hence instead of having the expected result, we have a non–extremal D6–brane with additional dilaton hair.

The shell branch of solutions has these two puzzling features. The first is that the exterior solution never contains an event horizon, no matter how large the non–extremality parameter r_0 became, in contradiction to our expectation that the system would eventually collapse to form a black hole. The second puzzle is that in the limit of large K3 volumes, these solutions do not reproduce the expected non-extremal $D6$–brane.

Physically, one expects that adding a small charge to a large black hole should not drastically change the physics; therefore, it seems that the horizon branch is the physically relevant solution for masses much greater than the extremal value. However, there are no horizon branch solutions for small enough mass difference. At least sufficiently close to extremality, the same 'smearing out' of the branes seen in the extremal case would prevent us from assembling branes to form a simple black hole solution. Instead, smeared branes would remain outside the horizon, giving rise to a solution with an enhançon shell. Thus, the shell branch solution with the shell at the enhançon radius is the physically relevant solution close to extremality.

Perhaps another solution is needed to describe the physics near extremality. Actually the shell–branch solution is unphysical because it violates the Weak Energy Condition, as we will see in Chapter 6. We find more general solutions in Chapter 7, which bypass this problem, but we are unable to find the exact solution, because information from supergravity is not sufficient to describe the physics of the shell.

We are interested in understanding the physics of such solutions in more detail in supergravity. Taken together, the two statements above imply an interesting phase structure, with different solution families providing the physical description in different regimes of parameters. There might be a classical instability which could provide the mechanism for transitions between them[6]. This could provide a useful example of the kind of non-trivial phase structure we expect to see in similar constructions we discussed in Section 1.8. Since we have the explicit solutions, it should be possible to understand the phase structure in detail. As we will see later on we do not succeed in this goal. We cannot find a unique solution which describes the shell–branch and the degrees of freedom of the shell.

3.6 Summary

In this chapter we have provided an overview of the enhançon mechanism. Apart from explaining the mechanism of the resolution, we also explained some of the techniques that we use in the rest of the thesis.

We used a configuration which conserves eight supercharges; N D6–branes wrapped over a $K3$ manifold. Because $K3$ space has non–trivial curvature, there are corrections in the brane worldvolume action which induce a negative D2–bane charge on the unwrapped part of their worldvolume. We wrote a corresponding supergravity solution which has a naked singularity at $r = |r_2|$.

[6]Since the enhançon is like a monopole solution, we expect the physics to be similar to that of the Einstein-Yang Mills Higgs system (see [194] and references therein). For any given value of the asymptotic charges, only one of the two solutions should be stable. However, to see this physics, it may be necessary to include the effects of the non-Abelian gauge fields, as in [147], which we do not do.

Next we used a single constituent brane as a probe of the geometry generated by the rest of the branes. We found that the effective tension varies with the radius in the transverse directions and it is zero at a radius $r_e > r_2$. At that point the brane–probe ceases to be pointlike in the transverse directions and smears around over a two–sphere with radius r_e. We made a connection with $SU(2)$ monopoles and regarding the probe as a magnetic monopole, and the enhançon radius $r = r_e$ corresponds to the locus where the gauge symmetry is restored from $U(1)$ to the full $SU(2)$.

New degrees of freedom become massless at this locus which are not described by the supergravity. Since there are no brane sources in the interior of this locus, the spacetime must be flat to a first approximation. Therefore, the repulson singularity gets excised as it was a remnant of the inability of the supergravity to describe the new light degrees of freedom. These are described by string theory and are needed in order to determine the correct geometry.

Actually this excision is consistent in supergravity. We replaced the interior geometry with flat space and using standard junction conditions techniques we calculated the stress–energy tensor at the junction surface. This stress–energy tensor corresponds precisely to that of a thin shell of wrapped D6–branes. Furthermore the shell provides sources for the dilaton and R–R fields, which again match precisely to those of wrapped D6–branes. It is interesting that although supergravity can not grasp the string physics needed to describe the enhançon mechanism properly, it displays some awareness of the behaviour of the branes that source this geometry. This construction is easily extended to adding extra D2–branes in the setup.

The supergravity argument can be extended to non-extremal generalisations of the enhançon solution, which are difficult to study from the string theory point of view. It was found that there are two branches of non-extremal solutions, arising from an ambiguity of a choice of sign in the solution of the supergravity equations. One branch joins on to the extremal enhançon solution, and always has a shell of branes outside the horizon, while the other branch appears at a finite value of the non-extremality parameter and there is no repulson singularity. The solution has a regular horizon at $r = r_0$. It looks like a black hole with R–R charges. For large values of the non–extremality parameter r_0, the R–R charges are negligible so the solution looks like an uncharged black hole.

In the former case, the repulson singularity always lies outside the would-be horizon, and the geometry will be corrected by an enhançon shell. We also computed the stress–energy of the shell using standard junction condition techniques. We introduced a free parameter r_0', which is not determined by the asymptotic charges of the solution. We expect this free parameter to be fixed by the physics of the enhançon. Although we could not fully determine it we were able to constrain it using physical arguments to $r_0' < r_0$.

Finally we discuss some peculiarities of the non–extremal solution. The shell branch has two puzzling features, namely the exterior never contains an event horizon and in the large $K3$ volume limit it does not reproduce the expected non–extremal D6–branes.

We will study the physics of the enhançon further, using supergravity. We will confirm that the extremal and the horizon branch of the non–extremal solutions are physical and we will also see that the shell branch solutions require a modification.

Chapter 4

Perturbations of the enhançon

In the previous chapter we saw that the enhançon mechanism is consistent in supergravity, although supergravity can not grasp the whole physics behind the resolution of the singularity. It is interesting that supergravity sees some of the results of the string theory physics. Maybe we can use it in order to have some insight in situations where it is difficult to use string theory.

Such is the case of the non–extremal enhançon. We saw earlier that there are two branches of solutions for finite–temperature enhançons. The shell branch and the horizon branch. We argued that these two solutions provide physical descriptions in two different regimes of parameters. There might be a classical instability providing the physical mechanism for transitions between them. A nice test of the validity of the supergravity solution would also be the stability of the supersymmetric extremal enhançon.

We would like to check the stability of the various enhançon solutions against small linearised perturbations. The object of this chapter is to introduce the methods and the techniques we used in order to investigate this matter.

Initially we introduce a perturbation ansatz for the problem at hand. We use the more general non–extremal exterior solution as the background we would like to perturb. We choose a perturbation ansatz which is more general than one used earlier in the literature [195] but still one which describes a very restricted class of perturbations. Finally we produce the differential equations that the modes in the perturbation ansatz must satisfy.

This system is overdetermined since there are more equations than unknown functions. In the third section we use a very beautiful argument in order to simplify our system of differential equations to a set of coupled differential equations. Our ansatz does not fix diffeomorphism invariance completely. By exploiting this invariance we are able to write down a reduced system which is not overdetermined and can be used for our later studies.

Before we try to solve the complicated system of differential equations we will discuss the stability of the system under the perturbation mode $\delta\psi_3$ which does not couple with any other perturbation mode. This mode also does not couple with the shell, so it is relatively easy to deduce the outcome of the stability under this mode, using analytical methods from standard gravitational stability literature [196, 197].

4.1 Perturbation ansatz

Perturbations of stars and black holes have been one of the main topics of relativistic astrophysics for the last four decades. They are of importance in gravitational wave astronomy, stellar structure and stability analysis of stars and black holes[1]. The study of black hole perturbations was initiated by the work of Regge and Wheeler [199], and continued by Zerilli [200]. Their motivation was to study black hole stability. Later Thorne and collaborators [201, 202] extended this methods to relativistic stars, calculating frequencies and energies of gravitational waves originating from oscillating bodies. The theory of perturbations of gravitational systems is reviewed and explained in the classic monograph by Chandrasekhar [196]. Recently, there was some work on non–linear perturbations of black holes (see [203] for a review). We will not use such methods in this thesis as we expect that a potential instability will show in the linear case.

Our main objective is the consideration of the stability of the enhançon solutions, extremal and non–extremal. We are interested in studying the enhançon using supergravity. One nice test of the setup would be to study the stability of the

[1] For a recent review and more detailed references with more astrophysical orientation the reader can consult [198].

extremal and non–extremal cases. In the extremal case proof of stability would give support to the supergravity description of the shell as being made of wrapped D6–branes. A transition between the two branches of the non–extremal enhançon, would signal a phase transition in the gauge theory dual.

We wish to consider the simplest set of linearised perturbations of the enhançon solutions which could provoke such a transition. We consider only perturbations which are spherically symmetric in the transverse space and translationally invariant along the branes, as we are looking for a transition between two solutions which preserve these symmetries.

We will therefore assume that the perturbations preserve many of the symmetries of the background (3.32). Specifically, we assume the spherical symmetry in the θ, ϕ directions, translational invariance in x_1 and x_2, and the discrete symmetries under $x_1 \to -x_1$, $x_2 \to -x_2$, $\phi \to -\phi$ are preserved. By a suitable choice of coordinates, the most general perturbation consistent with these symmetries can be written as the metric

$$\begin{aligned} g_s^{1/2}\, ds^2 \;=\; & e^{-\psi_1/2}\Big[\bar{Z}_2^{-1/2}\bar{Z}_6^{-1/2}(-\bar{K}e^{\delta\psi_2}dt^2 + e^{-\frac{1}{2}\delta\psi_2+\delta\psi_3}dx_1^2 + e^{-\frac{1}{2}\delta\psi_2-\delta\psi_3}dx_2^2) \\ & +\bar{Z}_2^{1/2}\bar{Z}_6^{1/2}(\bar{K}^{-1}dr^2 + r^2 d\Omega_2^2) + V^{1/2}\bar{Z}_2^{1/2}\bar{Z}_6^{-1/2}ds_{\mathrm{K3}}^2\Big]\,, \end{aligned} \tag{4.1}$$

dilaton

$$\bar{\phi} = \phi + \delta\phi, \tag{4.2}$$

and R–R fields

$$\bar{C}_{(3)} = C_{(3)} + \delta C_{(3)}, \quad \bar{C}_{(7)} = C_{(7)} + \delta C_{(7)}. \tag{4.3}$$

Here

$$\psi_1 = \phi + \delta\psi_1,\ \bar{Z}_2 = Z_2(1+\delta Z_2),\ \bar{Z}_6 = Z_6(1+\delta Z_6),\ \bar{K} = K(1+\delta K), \tag{4.4}$$

the harmonic functions Z_2, Z_6, K are as in (3.34), the unperturbed dilaton ϕ is as in (3.33), and the R–R potentials are as in (3.33). The first-order perturbations are all functions of (r,t) only, while the background quantities are functions only of r. We look for perturbations of the form $f(r)e^{i\omega t}$.

Our ansatz is slightly more general than the ansatz adopted in the study of perturbations of the extremal enhançon geometry in [195]. We have introduced three new perturbation functions, $\delta\psi_2$, $\delta\psi_3$, and δK. As we will see shortly, we can choose to set $\delta K = 0$ by a gauge transformation. The first-order function $\delta\psi_3$ is the only thing that breaks the rotational symmetry between x_1 and x_2. As a consequence, it decouples from the other perturbations. We could set it to zero without affecting the other modes; instead, we retain it, and study it independently of the others. This provides us with a single simple (but non-trivial) perturbation equation, which we study in section 4.4. One might think that $\delta\psi_2$ would also decouple, as it breaks the boost symmetry between t and x_1, x_2 which (3.32) respects. However, the assumption that the perturbations depend on t and not on x_1, x_2 also breaks this symmetry, so we will find that $\delta\psi_2$ couples to the time derivatives of the other perturbations, and it is not possible to set it to zero. That is, it is necessary to consider the more general ansatz containing $\delta\psi_2$ to satisfy all the field equations, even in the extreme case.

We must stress here that this ansatz describes only a restricted class of perturbations. It is not the most general ansatz that we can write, because it respects the symmetries of the background. In the non–extremal case we have two branches of solutions with the same symmetries. We expect an instability in both branches for different values of the parameters. We do not expect that a perturbation mode which breaks the symmetry becomes unstable[2], because we expect a symmetry–preserving transition.

We will now consider the full set of linearised equations for the perturbations. The R–R gauge field equations give

$$\partial_r \delta C_{(3)} = -\frac{1}{2}(4\delta Z_2 + \delta\phi - \delta\psi_1)\partial_r C_{(3)} \tag{4.5}$$

and

$$\partial_r \delta C_{(7)} = -\frac{1}{2}(4\delta Z_6 - 3\delta\phi + 3\delta\psi_1)\partial_r C_{(7)}. \tag{4.6}$$

The R-R fields' perturbations are expressed by the perturbations of other fields and obtained just by integrating these equations after we determine the other fields.

[2]There are unstable perturbations which break the symmetry resulting the Gregory–Laflamme instability [204, 205]. This is not the instability that we are interested in considering; as it seems unlikely to mediate a transition between the two branches of non–extremal solution.

The linear part of the stress tensor only involves $\partial_r \delta C_{(3)}$ and $\partial_r \delta C_{(7)}$, so we can substitute (4.5,4.6) directly into the stress tensor.

There are seven distinct equations coming from the linearised Einstein's equations: six different diagonal components, and an off-diagonal $[tr]$ component. With the dilaton equation, this gives us eight equations; but with the gauge field perturbations fixed by (4.5,4.6), there are only seven undetermined functions in our ansatz. The problem seems overdetermined, so it is important to ask whether there will be any non-trivial solutions of the full set of equations. We have written down the most general perturbation consistent with the symmetries we have assumed, so we expect there is sufficient redundancy in the equations to admit non-trivial solutions.

4.2 Particular Integral

Actually we can use a procedure described in detail in [196] and explained partly in [206][3]. In the context that we use it, it has to do with diffeomorphism freedom left, which we can exploit in a way that we can simplify our problem.

We can reduce the system of eight differential equations to four differential equations. This is achieved by defining two non–trivial radius–dependent linear combinations of the perturbation modes, that can reduce the initial system. Xanthopoulos [207], [208], gives an algorithm which determines this particular integral and which was further utilised in [206]. Since the linear combinations which reduce the equations are known, we can construct the general solution.

As in [206], we will argue that the particular integral is a manifestation of the fact that the gauge is not completely set by (4.1). We will exploit this fact in order to find the particular integral in this section and we will use it in the next section in order to reduce the order of the equations.

Coordinate transformations change the form of the metric but they have no physical effect. So a perturbation which can be undone by (or be 'equal' to) a

[3]Chandrasekhar in his book [196] claims that this procedure has to do with the deeper nature of differential equations. This is something that Xanthopoulos showed more generally in [207], without any relation to gravity or general relativity.

coordinate transformation, automatically satisfies the equations of motion. In fact, we can use this insight to see directly that there are non-trivial solutions to the linearised equations of motion. We observe that the ansatz (4.1) does not completely fix the gauge, as there are infinitesimal diffeomorphisms which preserve its form. The infinitesimal coordinate transformation

$$t \to t' = t + e^{i\omega t}\delta t(r), \quad r \to r' = r + e^{i\omega t}\delta r(r), \tag{4.7}$$

changes the unperturbed metric. We must demand that the off–diagonal components vanish to preserve the form of the perturbation ansatz. This means that

$$\partial_r \delta t = i\omega \frac{Z_2 Z_6}{K^2}\delta r. \tag{4.8}$$

If we apply this diffeomorphism to the non-extremal enhançon geometry (3.32), we obtain a metric of the form (4.1) with

$$\begin{aligned}
\delta\psi_1^d &= \left(\phi' - \frac{4}{3r}\right)\delta r - \frac{2}{3}\partial_r\delta r - \frac{2}{3}i\omega\delta t, \\
\delta\psi_2^d &= -\frac{4}{3r}\delta r + \frac{4}{3}\partial_r\delta r + \frac{4}{3}i\omega\delta t, \\
\delta Z_6^d &= \left(\frac{Z_6'}{Z_6} + \frac{2}{r}\right)\delta r, \\
\delta Z_2^d &= \left(\frac{Z_2'}{Z_2} + \frac{2}{3r}\right)\delta r - \frac{2}{3}\partial_r\delta r - \frac{2}{3}i\omega\delta t, \\
\delta K^d &= \left(\frac{K'}{K} + \frac{2}{r}\right)\delta r - 2\partial_r\delta r, \\
\delta\phi^d &= \phi'\delta r.
\end{aligned} \tag{4.9}$$

Since this particular perturbation comes from a coordinate transformation, it must solve the equations of motion. Thus, there are non-trivial solutions of these equations. Of course, we are not interested in solutions which are pure gauge, but this serves to demonstrate that there is some redundancy in the equations.

This diffeomorphism contains an arbitrary function; since we are not interested in pure gauge perturbations, we should fix this additional gauge symmetry. We can do so by setting one of the perturbations to zero. It is convenient to choose $\delta K = 0$. There remain diffeomorphisms which will preserve $\delta K = 0$: these have

$$\delta r = a r K^{1/2} \tag{4.10}$$

and

$$\delta t = i\omega a\left[-\frac{2(r_0+\hat{r}_2)(r_0+\hat{r}_6)}{\sqrt{K(r)}}+\left(\frac{r}{2}+\frac{7r_0}{4}+\hat{r}_2+\hat{r}_6\right)r\sqrt{K(r)}+\right. \tag{4.11}$$
$$\left.+\left(\frac{15r_0^2}{8}+\frac{3r_0(\hat{r}_2+\hat{r}_6)}{2}+\hat{r}_2\hat{r}_6\right)\ln\frac{1+\sqrt{K(r)}}{1-\sqrt{K(r)}}\right]+i\omega b$$

where a and b are arbitrary constants. The perturbations (4.9) with this δt, δr then give a two-parameter family of solutions of the linearised equations with $\delta K = 0$. We will exploit this remaining coordinate freedom to simplify the equations later.

Having set $\delta K = 0$, the contributions to the Ricci tensor linear in the perturbations are

$$\begin{aligned}\delta R_{tt} &= \frac{1}{4}(2\delta\ddot{\psi}_2+9\delta\ddot{\psi}_1-5\delta\ddot{Z}_2+3\delta\ddot{Z}_6) \\ &+\frac{K^2}{32Z_2Z_6}\left[16\left(\delta\psi_2''+\frac{2}{r}\delta\psi_2'\right)-8\left(\delta\psi_1''+\frac{2}{r}\delta\psi_1'\right)-8\left(\delta Z_2''+\frac{2}{r}\delta Z_2'\right)\right. \\ &-8\left(\delta Z_6''+\frac{2}{r}\delta Z_6'\right)+16\delta\psi_2'\frac{K'}{K}+4\delta\psi_1'\left(-10\frac{K'}{K}+5\frac{Z_2'}{Z_2}+\frac{Z_6'}{Z_6}\right) \\ &-\delta Z_2'\left(5\frac{Z_2'}{Z_2}+\frac{Z_6'}{Z_6}\right)+\delta Z_6'\left(-32\frac{K'}{K}+15\frac{Z_2'}{Z_2}+3\frac{Z_6'}{Z_6}\right) \\ &\left.+(\delta\psi_2-\delta Z_2-\delta Z_6)\left(10\frac{Z_2'^2}{Z_2^2}-10\frac{K'}{K}\frac{Z_2'}{Z_2}+2\frac{Z_6'^2}{Z_6^2}-2\frac{K'}{K}\frac{Z_6'}{Z_6}\right)\right],\end{aligned} \tag{4.12}$$

$$\begin{aligned}\delta_+ &= \delta R_{tt}+\frac{1}{2}K\left(\delta R_{11}+\delta R_{22}\right)=\frac{1}{4}\left(\delta\ddot{\psi}_2+8\delta\ddot{\psi}_1-6\delta\ddot{Z}_2+2\delta\ddot{Z}_6\right) \\ &+\frac{K^2}{32Z_2Z_6}\left[24\left(\delta\psi_2''+\frac{2}{r}\delta\psi_2'\right)+\frac{K'}{K}(24\delta\psi_2'-32\delta\psi_1'-24\delta Z_6'+8\delta Z_2')\right. \\ &\left.+\delta\psi_2\left(15\frac{Z_2'^2}{Z_2^2}-15\frac{K'}{K}\frac{Z_2'}{Z_2}+3\frac{Z_6'^2}{Z_6^2}-3\frac{K'}{K}\frac{Z_6'}{Z_6}\right)\right],\end{aligned} \tag{4.13}$$

$$\begin{aligned}\delta_- &= K\left(\delta R_{11}-\delta R_{22}\right)=\delta\ddot{\psi}_3+\frac{K^2}{8Z_2Z_6}\left[-8\left(\delta\psi_3''+\frac{2}{r}\delta\psi_3'\right)\right. \\ &\left.-8\delta\psi_3'\frac{K'}{K}+\delta\psi_3\left(-5\frac{Z_2'^2}{Z_2^2}+5\frac{K'}{K}\frac{Z_2'}{Z_2}-\frac{Z_6'^2}{Z_6^2}+\frac{K'}{K}\frac{Z_6'}{Z_6}\right)\right],\end{aligned} \tag{4.14}$$

$$\begin{aligned}\delta R_{tr} &= \frac{1}{8}\left[4\delta\dot{\psi}_2'+16\delta\dot{\psi}_1'-8\delta\dot{Z}_2'+8\delta\dot{Z}_6'-2\delta\dot{\psi}_2\frac{K'}{K}+\delta\dot{\psi}_1\left(-8\frac{K'}{K}+5\frac{Z_2'}{Z_2}+\frac{Z_6'}{Z_6}\right)\right. \\ &\left.+\delta\dot{Z}_2\left(4\frac{K'}{K}-5\frac{Z_2'}{Z_2}-\frac{Z_6'}{Z_6}\right)+\delta\dot{Z}_6\left(-4\frac{K'}{K}+3\frac{Z_2'}{Z_2}-\frac{Z_6'}{Z_6}\right)\right],\end{aligned} \tag{4.15}$$

$$\begin{aligned}
\delta R_{rr} &= \frac{Z_2 Z_6}{4K^2}\left(-\delta\ddot{\psi}_1 + \delta\ddot{Z}_2 + \delta\ddot{Z}_6\right) \\
&+\frac{1}{32}\left[72\delta\psi_1'' - 24\delta Z_2'' + 40\delta Z_6'' - 16\delta\psi_2'\frac{K'}{K} + \delta\psi_1'\left(\frac{16}{r} + 40\frac{K'}{K} - 12\frac{Z_2'}{Z_2} - 28\frac{Z_6'}{Z_6}\right)\right. \\
&\left.+\, \delta Z_2'\left(-\frac{16}{r} - 27\frac{Z_2'}{Z_2} + \frac{Z_6'}{Z_6}\right) + \delta Z_6'\left(-\frac{16}{r} + 32\frac{K'}{K} - 15\frac{Z_2'}{Z_2} - 35\frac{Z_6'}{Z_6}\right)\right],
\end{aligned} \tag{4.16}$$

$$\begin{aligned}
\delta R_{\theta\theta} &= \frac{r^2 Z_2 Z_6}{4K}\left(-\delta\ddot{\psi}_1 + \delta\ddot{Z}_2 + \delta\ddot{Z}_6\right) \\
&+\frac{r^2 K}{32}\left[8\delta\psi_1'' - 8\delta Z_2'' - 8\delta Z_6'' + \delta\psi_1'\left(\frac{80}{r} + 8\frac{K'}{K} + 12\frac{Z_2'}{Z_2} + 28\frac{Z_6'}{Z_6}\right)\right. \\
&\left.+\, \delta Z_2'\left(-\frac{32}{r} - 8\frac{K'}{K} - 3\frac{Z_2'}{Z_2} - 7\frac{Z_6'}{Z_6}\right) + \delta Z_6'\left(\frac{32}{r} - 8\frac{K'}{K} + 9\frac{Z_2'}{Z_2} + 21\frac{Z_6'}{Z_6}\right)\right],
\end{aligned} \tag{4.17}$$

and

$$\begin{aligned}
\delta R_{mn}[K3] &= \frac{\sqrt{V}Z_2}{4K}\left(-\delta\ddot{\psi}_1 + \delta\ddot{Z}_2 - \delta\ddot{Z}_6\right) \\
&+\frac{\sqrt{V}K}{32Z_6}\left[8\left(\delta\psi_1'' + \frac{2}{r}\delta\psi_1'\right) - 8\left(\delta Z_2'' + \frac{2}{r}\delta Z_2'\right) + 8\left(\delta Z_6'' + \frac{2}{r}\delta Z_6'\right)\right. \\
&+\delta\psi_1'\left(8\frac{K'}{K} + 12\frac{Z_2'}{Z_2} - 4\frac{Z_6'}{Z_6}\right) + \delta Z_2'\left(-8\frac{K'}{K} - 3\frac{Z_2'}{Z_2} + \frac{Z_6'}{Z_6}\right) \\
&+\delta Z_6'\left(8\frac{K'}{K} + 9\frac{Z_2'}{Z_2} - 3\frac{Z_6'}{Z_6}\right) \\
&\left.+\, \delta Z_6\left(-6\frac{Z_2'^2}{Z_2^2} + 6\frac{K'}{K}\frac{Z_2'}{Z_2} + 2\frac{Z_6'^2}{Z_6^2} - 2\frac{K'}{K}\frac{Z_6'}{Z_6}\right)\right],
\end{aligned} \tag{4.18}$$

where we have introduced certain combinations which simplify the resulting equations, $\dot{}$ signifies ∂_t, and $'$ signifies ∂_r.

The linearised Einstein's equations give seven equations. First, there are the simple equations from δ_- and δ_+, which are respectively

$$\frac{Z_2 Z_6}{K^2}\delta\ddot{\psi}_3 - \delta\psi_3'' - \delta\psi_3'\left(\frac{2}{r} + \frac{K'}{K}\right) = 0 \tag{4.19}$$

and

$$\frac{Z_2 Z_6}{K^2}(\delta\ddot{\psi}_2 + 8\delta\ddot{\psi}_1 - 6\delta\ddot{Z}_2 + 2\delta\ddot{Z}_6) + 3\delta\psi_2'' + 3\delta\psi_2'\left(\frac{2}{r} + \frac{K'}{K}\right) + (-4\delta\psi_1' - 3\delta Z_6' + \delta Z_2')\frac{K'}{K} = 0. \tag{4.20}$$

There are three more independent second-order equations,

$$\begin{aligned} -2\frac{Z_2Z_6}{K^2}\delta\ddot{Z}_6 + 2\delta Z_6'' + \delta Z_6'\left(-\frac{2}{r} + 2\frac{K'}{K} - 3\frac{Z_6'}{Z_6}\right) & \\ +\delta\psi_1'\left(-\frac{8}{r} - 4\frac{Z_6'}{Z_6}\right) + \delta Z_2'\left(\frac{2}{r} + \frac{K'}{K} + \frac{Z_6'}{Z_6}\right) & \\ +\delta Z_6\frac{3}{4}\left(\frac{Z_6'^2}{Z_6^2} - \frac{K'}{K}\frac{Z_6'}{Z_6}\right) + (3\delta\phi + \delta\psi_1 - \delta Z_2)\left(\frac{Z_6'^2}{Z_6^2} - \frac{K'}{K}\frac{Z_6'}{Z_6}\right) & = 0, \end{aligned} \tag{4.21}$$

$$\begin{aligned} -2\frac{Z_2Z_6}{K^2}(4\delta\ddot{\psi}_1 + 2\delta\ddot{\psi}_2 + \delta\ddot{Z}_6) + 6(\delta Z_2'' + \frac{2}{r}\delta Z_2') + & \\ \delta\psi_1'\left(4\frac{K'}{K} - 12\frac{Z_2'}{Z_2}\right) + \delta Z_2'\left(5\frac{K'}{K} + 3\frac{Z_2'}{Z_2}\right) + \delta Z_6'\left(3\frac{K'}{K} - 9\frac{Z_2'}{Z_2}\right) & \\ -3(\delta\phi - 5\delta\psi_1 + 5\delta Z_2 - 3\delta Z_6)\left(\frac{Z_2'^2}{Z_2^2} - \frac{K'}{K}\frac{Z_2'}{Z_2}\right) & = 0, \end{aligned} \tag{4.22}$$

and

$$\begin{aligned} -8\frac{Z_2Z_6}{K^2}(7\delta\ddot{\psi}_1 + 2\delta\ddot{\psi}_2 - 3\delta\ddot{Z}_2 + \delta\ddot{Z}_6) + 24\delta\psi_1'' & \\ +\delta\psi_1'\left(\frac{144}{r} + 40\frac{K'}{K} - 12\frac{Z_2'}{Z_2} + 36\frac{Z_6'}{Z_6}\right) & \\ +\delta Z_2'\left(-\frac{24}{r} - 4\frac{K'}{K} + 3\frac{Z_2'}{Z_2} - 9\frac{Z_6'}{Z_6}\right) + \delta Z_6'\left(\frac{72}{r} + 12\frac{K'}{K} - 9\frac{Z_2'}{Z_2} + 27\frac{Z_6'}{Z_6}\right) & \\ +3(-\delta\phi + 5\delta\psi_1 - 5\delta Z_2 + 3\delta Z_6)\left(\frac{Z_2'^2}{Z_2^2} - \frac{K'}{K}\frac{Z_2'}{Z_2}\right) & \\ +9(-3\delta\phi - \delta\psi_1 + \delta Z_2 + \delta Z_6)\left(\frac{Z_6'^2}{Z_6^2} - \frac{K'}{K}\frac{Z_6'}{Z_6}\right) & = 0. \end{aligned} \tag{4.23}$$

The remaining Einstein's equations give us two equations which are first-order in ∂_r. Integrating the tr equation in t gives

$$\begin{aligned} 4\delta\psi_2' + 16\delta\psi_1' - 8\delta Z_2' + 8\delta Z_6' - 2\delta\psi_2\frac{K'}{K} + \delta\psi_1\left(-8\frac{K'}{K} + 5\frac{Z_2'}{Z_2} + \frac{Z_6'}{Z_6}\right) & \\ +\delta Z_2\left(4\frac{K'}{K} - 5\frac{Z_2'}{Z_2} - \frac{Z_6'}{Z_6}\right) + \delta Z_6\left(-4\frac{K'}{K} + 3\frac{Z_2'}{Z_2} - \frac{Z_6'}{Z_6}\right) + \delta\phi\left(-\frac{Z_2'}{Z_2} + 3\frac{Z_6'}{Z_6}\right) & = f(r), \end{aligned} \tag{4.24}$$

and a suitable combination gives the equation

$$
\begin{aligned}
& 16\frac{Z_2 Z_6}{K^2}\left(4\delta\ddot{\psi}_1 + \delta\ddot{\psi}_2 - 2\delta\ddot{Z}_2 + 2\delta\ddot{Z}_6\right) \\
& -8\delta\psi_2'\frac{K'}{K} + \delta\psi_1'\left(-\frac{128}{r} - 32\frac{K'}{K} - 12\frac{Z_2'}{Z_2} - 28\frac{Z_6'}{Z_6}\right) \\
& +\delta Z_2'\left(\frac{32}{r} + 16\frac{K'}{K} - 12\frac{Z_2'}{Z_2} + 4\frac{Z_6'}{Z_6}\right) + \delta Z_6'\left(-\frac{96}{r} - 16\frac{K'}{K} - 12\frac{Z_2'}{Z_2} - 28\frac{Z_6'}{Z_6}\right) \\
& +\delta\phi'\left(-4\frac{Z_2'}{Z_2} + 12\frac{Z_6'}{Z_6}\right) + (\delta\psi_1 - \delta Z_2)\left(20\frac{Z_2'^2}{Z_2^2} - 20\frac{K'}{K}\frac{Z_2'}{Z_2} + 4\frac{Z_6'^2}{Z_6^2} - 4\frac{K'}{K}\frac{Z_6'}{Z_6}\right) \\
& +\delta Z_6\left(-3\frac{Z_2'^2}{Z_2^2} + 3\frac{K'}{K}\frac{Z_2'}{Z_2} - 4\frac{Z_6'^2}{Z_6^2} + 4\frac{K'}{K}\frac{Z_6'}{Z_6}\right) \\
& +\delta\phi\left(-4\frac{Z_2'^2}{Z_2^2} + 4\frac{K'}{K}\frac{Z_2'}{Z_2} + 24\frac{Z_6'^2}{Z_6^2} - 24\frac{K'}{K}\frac{Z_6'}{Z_6}\right) = 0.
\end{aligned}
\tag{4.25}
$$

Finally, there is the dilaton equation

$$
\begin{aligned}
-8\frac{Z_2 Z_6}{K^2}\delta\ddot{\phi} \;+\; & \frac{8}{r^2}\partial_r(Kr^2\partial_r\delta\phi) = \\
& (4\delta\psi_1' - \delta Z_2' + 3\delta Z_6')\left(\frac{Z_2'}{Z_2} - 3\frac{Z_6'}{Z_6}\right) \\
& +3(3\delta\phi + \delta\psi_1 - \delta Z_6 - \delta Z_2)\left(\frac{Z_6'^2}{Z_6^2} - \frac{K'}{K}\frac{Z_6'}{Z_6}\right) \\
& +(\delta\phi - 5\delta\psi_1 + 5\delta Z_2 - 3\delta Z_6)\left(\frac{Z_2'^2}{Z_2^2} - \frac{K'}{K}\frac{Z_2'}{Z_2}\right).
\end{aligned}
\tag{4.26}
$$

These equations are coupled in a complicated fashion, but we see that as mentioned earlier, there is one simple equation, (4.19). In fact, this is the free wave equation.

4.3 The reduction of the perturbation equations

To simplify the other equations, we exploit the remaining two-parameter family of diffeomorphisms (4.10,4.11). These can be used to construct a change of variables which will simplify the equations: we replace a and b by functions $a(r)$ and $b(r)$, and set

$$\begin{aligned}
\delta\psi_1 &= \delta\psi_1^d(a(r), b(r)), \\
\delta\psi_2 &= \delta\psi_2^d(a(r), b(r)) + \Psi_2, \\
\delta Z_6 &= \delta Z_6^d(a(r), b(r)) + \mathcal{Z}_6, \\
\delta Z_2 &= \delta Z_2^d(a(r), b(r)), \\
\delta\phi &= \delta\phi^d(a(r), b(r)) + \Phi,
\end{aligned} \tag{4.27}$$

with $\delta K = 0$. The first term on the right-hand sides is the diffeomorphism-induced perturbation (4.9) for the diffeomorphism (4.10,4.11), but with a and b now functions. Since the diffeomorphism satisfies the equations of motion for arbitrary constants a and b, the linearised equations will only involve derivatives of $a(r)$ and $b(r)$. The two first-order equations (4.24,4.25) can then be solved for $\partial_r a(r)$ and $\partial_r b(r)$. Inserting these values into the other four second-order equations (4.20-4.23) and the dilaton equation (4.26) gives two equations which are trivially satisfied, and a coupled set of three second-order equations for Ψ_2, $\mathcal{Z}_6$ and Φ.

It is convenient to write the coupled equations so that each one only involves second derivatives of one of the functions. Then the equation which involves Φ'' is (where $'$ again denotes ∂_r, and we assume that all the perturbations behave as $e^{i\omega t}$)

$$D(\Phi'' + \frac{2r - r_0}{r^2 K}\Phi' + \frac{Z_2 Z_6}{K^2}\omega^2\Phi) + P_2^1(\Psi_2' + 2\mathcal{Z}_6') + Q_1^1\Phi + Q_2^1\Psi_2 + Q_3^1\mathcal{Z}_6 = 0, \tag{4.28}$$

with the polynomial coefficients

$$D = r^2 K(8r^2 + 5r\hat{r}_2 + 5r\hat{r}_6 + 2\hat{r}_2\hat{r}_6)(4r^2 + 3r\hat{r}_2 + 3r\hat{r}_6 + 2\hat{r}_2\hat{r}_6), \tag{4.29}$$

$$P_2^1 = -2r^2 K(-2r^2\hat{r}_2 + 6r^2\hat{r}_6 + 8r\hat{r}_2\hat{r}_6 + 3\hat{r}_2^2\hat{r}_6 + \hat{r}_2\hat{r}_6^2), \tag{4.30}$$

$$\begin{aligned}
Q_1^1 &= -r^2(4r_0\hat{r}_2 + 36r_0\hat{r}_6 + 3\hat{r}_2^2 + 6\hat{r}_2\hat{r}_6 + 27\hat{r}_6^2) \\
&\quad -r(40r_0\hat{r}_2\hat{r}_6 + 2\hat{r}_2^2\hat{r}_6 + 30\hat{r}_2\hat{r}_6^2) - 12r_0\hat{r}_2^2\hat{r}_6 - 8\hat{r}_2^2\hat{r}_6^2,
\end{aligned} \tag{4.31}$$

$$Q_2^1 = r_0(-2r^2\hat{r}_2 + 6r^2\hat{r}_6 + 8r\hat{r}_2\hat{r}_6 + 3\hat{r}_2^2\hat{r}_6 + \hat{r}_2\hat{r}_6^2), \tag{4.32}$$

$$\begin{aligned}
Q_3^1 &= r^2(8r_0\hat{r}_2 + 24r_0\hat{r}_6 + 9\hat{r}_2^2 + 10\hat{r}_2\hat{r}_6 + 9\hat{r}_6^2) \\
&\quad +r(24r_0\hat{r}_2\hat{r}_6 + 6\hat{r}_2^2\hat{r}_6 + 10\hat{r}_2\hat{r}_6^2) + 6r_0\hat{r}_2^2\hat{r}_6 - 2r_0\hat{r}_2\hat{r}_6^2.
\end{aligned} \tag{4.33}$$

The equation involving Ψ_2'' is

$$D(\Psi_2'' + \frac{Z_2 Z_6}{K^2}\omega^2\Psi_2) + P_2^2\Psi_2' + P_3^2\mathcal{Z}_6' + Q_1^2\Phi + Q_2^2\Psi_2 + Q_3^2\mathcal{Z}_6 = 0, \tag{4.34}$$

where D is as before, and the other polynomial coefficients are

$$\begin{aligned} P_2^2 &= 64r^5 + r^4(-32r_0 + 120\hat{r}_2 + 88\hat{r}_6) \\ &\quad + r^3(-76r_0\hat{r}_2 - 44r_0\hat{r}_6 + 30\hat{r}_2^2 + 172\hat{r}_2\hat{r}_6 + 30\hat{r}_6^2) \\ &\quad + r^2(-15r_0\hat{r}_2^2 - 118r_0\hat{r}_2\hat{r}_6 - 15r_0\hat{r}_6^2 + 44\hat{r}_2^2\hat{r}_6 + 52\hat{r}_2\hat{r}_6^2) \\ &\quad + r(-28r_0\hat{r}_2^2\hat{r}_6 - 36r_0\hat{r}_2\hat{r}_6^2 + 8\hat{r}_2^2\hat{r}_6^2) - 4r_0\hat{r}_2^2\hat{r}_6^2, \end{aligned} \tag{4.35}$$

$$P_3^2 = -8r^2\hat{r}_2K(8r^2 + 16r\hat{r}_6 + 3\hat{r}_2\hat{r}_6 + 5\hat{r}_6^2), \tag{4.36}$$

$$Q_1^2 = 4\hat{r}_2(r^2(-8r_0 - 6\hat{r}_2 - 6\hat{r}_6) + r(4r_0\hat{r}_6 - 7\hat{r}_2\hat{r}_6 + 3\hat{r}_6^2) + 6r_0\hat{r}_2\hat{r}_6 + 2\hat{r}_2\hat{r}_6^2), \tag{4.37}$$

$$Q_2^2 = -2r_0\hat{r}_2(8r^2 + 16r\hat{r}_6 + 3\hat{r}_2\hat{r}_6 + 5\hat{r}_6^2), \tag{4.38}$$

$$Q_3^2 = 4\hat{r}_2(r^2(16r_0 + 18\hat{r}_2 + 2\hat{r}_6) + r(12r_0\hat{r}_6 + 21\hat{r}_2\hat{r}_6 - \hat{r}_6^2) - 3r_0\hat{r}_2\hat{r}_6 + 5r_0\hat{r}_6^2 + 6\hat{r}_2\hat{r}_6^2). \tag{4.39}$$

The equation involving $\mathcal{Z}_6''$ is

$$D(\mathcal{Z}_6'' + \frac{Z_2 Z_6}{K^2}\omega^2\mathcal{Z}_6) + P_2^3\Psi_2' + P_3^3\mathcal{Z}_6' + Q_1^3\Phi + Q_2^3\Psi_2 + Q_3^3\mathcal{Z}_6 = 0, \tag{4.40}$$

where D is as before, and the other polynomial coefficients are

$$P_2^3 = -2r^2K(6r^2\hat{r}_2 - 2r^2\hat{r}_6 + 8r\hat{r}_2\hat{r}_6 + \hat{r}_2^2\hat{r}_6 + 3\hat{r}_2\hat{r}_6^2), \tag{4.41}$$

$$\begin{aligned} P_3^3 &= 64r^5 + r^4(-32r_0 + 64\hat{r}_2 + 96\hat{r}_6) \\ &\quad + r^3(-20r_0\hat{r}_2 - 52r_0\hat{r}_6 + 30\hat{r}_2^2 + 76\hat{r}_2\hat{r}_6 + 30\hat{r}_6^2) \\ &\quad + r^2(-15r_0\hat{r}_2^2 - 22r_0\hat{r}_2\hat{r}_6 - 15r_0\hat{r}_6^2 + 28\hat{r}_2^2\hat{r}_6 + 20\hat{r}_2\hat{r}_6^2) \\ &\quad + r(-12r_0\hat{r}_2^2\hat{r}_6 - 4r_0\hat{r}_2\hat{r}_6^2 + 8\hat{r}_2^2\hat{r}_6^2) - 4r_0\hat{r}_2^2\hat{r}_6^2, \end{aligned} \tag{4.42}$$

$$Q_1^3 = r^2(12r_0\hat{r}_2 + 12r_0\hat{r}_6 + 9\hat{r}_2^2 + 10\hat{r}_2\hat{r}_6 + 9\hat{r}_6^2) + r(8r_0\hat{r}_2\hat{r}_6 + 10\hat{r}_2^2\hat{r}_6 + 6\hat{r}_2\hat{r}_6^2) - 4r_0\hat{r}_2^2\hat{r}_6, \tag{4.43}$$

$$Q_2^3 = r_0(6r^2\hat{r}_2 - 2r^2\hat{r}_6 + 8r\hat{r}_2\hat{r}_6 + \hat{r}_2^2\hat{r}_6 + 3\hat{r}_2\hat{r}_6^2), \tag{4.44}$$

$$\begin{aligned} Q_3^3 &= -r^2(24r_0\hat{r}_2 + 8r_0\hat{r}_6 + 27\hat{r}_2^2 + 6\hat{r}_2\hat{r}_6 + 3\hat{r}_6^2) \\ &\quad - r(24r_0\hat{r}_2\hat{r}_6 + 30\hat{r}_2^2\hat{r}_6 + 2\hat{r}_2\hat{r}_6^2) + 2r_0\hat{r}_2^2\hat{r}_6 - 6r_0\hat{r}_2\hat{r}_6^2 - 8\hat{r}_2^2\hat{r}_6^2). \end{aligned} \tag{4.45}$$

We have now reduced the perturbation problem to these three second-order equations plus the equation for the uncoupled mode (4.19). We will use these equations in the remainder to study the stability of the enhançon solutions.

4.4 Perturbations of gravitational systems and their stability

Before we discuss the boundary conditions at the shell for the coupled mode, we will very briefly discuss the standard lore concerning perturbations of gravitational systems[4] and use the uncoupled perturbation mode of the non–extremal enhançon solution as an example. We would like to investigate the non–extremal enhançon stability under small perturbations of the metric and the rest of the fields. What we are looking for is the following: given any initial perturbation confined to a finite interval of the radial coordinate, will it remain bounded at all times (which is a sign of stability) as it evolves or not?

For the case at hand we will use the differential equation (4.19) of the uncoupled mode. The most general form of these differential equations can be written as

$$\frac{K^2}{Z_2 Z_6}\left[\partial_r^2\Psi_3 + \left(\frac{K'}{K}+\frac{2}{r}\right)\partial_r\Psi_3\right] + \omega^2\Psi_3 = 0. \tag{4.46}$$

for the exterior and

$$\frac{L^2}{H_2 H_6}\left[\partial_r^2\Psi_3 + \left(\frac{L'}{L}+\frac{2}{r}\right)\partial_r\Psi_3\right] + \frac{L(r_e)}{K(r_e)}\omega^2\Psi_3 = 0 \tag{4.47}$$

for the interior. The standard method for investigating stability is to translate the problem to a one–dimensional bound state problem. This can be done by introducing the tortoise coordinate

$$r_* = \begin{cases} \sqrt{\frac{L(r_e)}{K(r_e)}}\int_{r_e}^{r}\frac{\sqrt{H_2H_6}}{L}d\bar{r} & r < r_e, \\ \int_{r_e}^{r}\frac{\sqrt{Z_2Z_6}}{K}d\bar{r} & r > r_e. \end{cases} \tag{4.48}$$

[4]The standard source for the following is Chandrasekhar's book [196]. Further references about the original contributors can be found in there. The method we describe is not original but the example we use in order to show it is. Another nice article reviewing the methods one can use in order to find instabilities is [197].

This coordinate runs from $-\infty$ at $r = r_0$, to $+\infty$ at $r = \infty$. We make a change of variable

$$\Psi_3 = \begin{cases} \frac{1}{(Z_2 Z_6)^{1/4} r}\psi & r < r_{\rm e}, \\ \frac{1}{(H_2 H_6)^{1/4} r}\psi & r > r_{\rm e}. \end{cases} \tag{4.49}$$

Then (4.47) becomes

$$\partial^2_{r_*}\psi + \omega^2\psi + W\psi = 0, \tag{4.50}$$

where for $r > r_{\rm e}$,

$$\begin{aligned} W(r) = W_> \equiv\ & \frac{K^2}{Z_2 Z_6}\left[\frac{1}{4}\frac{Z_2''}{Z_2} + \frac{1}{4}\frac{Z_6''}{Z_6} - \frac{5}{16}\left(\frac{Z_2'}{Z_2}\right)^2 - \frac{5}{16}\left(\frac{Z_6'}{Z_6}\right)^2 - \frac{1}{8}\frac{Z_2'}{Z_2}\frac{Z_6'}{Z_6}\right. \\ & \left. + \frac{1}{4}\left(\frac{Z_2'}{Z_2} + \frac{Z_6'}{Z_6}\right)\frac{K'}{K} + \frac{1}{r}\frac{K'}{K}\right], \end{aligned} \tag{4.51}$$

while for $r < r_{\rm e}$,

$$\begin{aligned} W(r) = W_< \equiv\ & \frac{K(r_{\rm e})}{L(r_{\rm e})}\frac{L^2}{H_2 H_6}\left[\frac{1}{4}\frac{H_2''}{H_2} + \frac{1}{4}\frac{H_6''}{H_6} - \frac{5}{16}\left(\frac{H_2'}{H_2}\right)^2 - \frac{5}{16}\left(\frac{H_6'}{H_6}\right)^2 - \frac{1}{8}\frac{H_2'}{H_2}\frac{H_6'}{H_6}\right. \\ & \left. + \frac{1}{4}\left(\frac{H_2'}{H_2} + \frac{H_6'}{H_6}\right)\frac{L'}{L} + \frac{1}{r}\frac{L'}{L}\right]. \end{aligned} \tag{4.52}$$

The criterion for stability is that there are no solutions to equation (4.50) which grow exponentially with time. From the form of the time–dependent ansatz that we used, $\delta\psi_3(t, r) = \Psi_3(r)e^{i\omega t}$, we can deduce that solutions that grow exponentially with time are the ones with imaginary frequencies ω or stated differently with negative eigenvalues of ω^2.

Since we have written the problem as an one–dimensional bound state problem, we can use the well known techniques of quantum mechanics. The problem of finding perturbations with negative eigenvalues of ω^2 is equivalent to the problem of finding negative energy bound states as solutions of the Schrödinger–like equation in the potential W. The existence of a number of bound states with negative energy is enough to prove that the system is unstable. Of course the value of the negative energy is important if we would like to investigate a bit further the properties of the system.

From the form of the potential W we can have a hint about stability. If W were positive throughout the range of r, then the problem could not support bound states with negative energy and it is stable. If the potential W had the form of a well, there could be bound state solutions of the differential equations. If the bound state energy is negative (which means that ω is imaginary) then this is a sign of instability.

Plugging in the functions from (3.34), we have

$$\begin{aligned} W_{>} &= \frac{K}{16Z_2^3Z_6^3}\{[8(\hat{r}_2+\hat{r}_6)+16r_0]r^{-3}+[3\hat{r}_2^2+3\hat{r}_6^2+30\hat{r}_2\hat{r}_6+20r_0(\hat{r}_2+\hat{r}_6)]r^{-4} \\ &\quad +[12\hat{r}_2\hat{r}_6(\hat{r}_2+\hat{r}_6)+9r_0(\hat{r}_2+\hat{r}_6)^2]r^{-5}+[4\hat{r}_2^2\hat{r}_6^2+8r_0\hat{r}_2\hat{r}_6(\hat{r}_2\hat{r}_6)]r^{-6} \\ &\quad +4r_0\hat{r}_2^2\hat{r}_6^2r^{-7}\}. \end{aligned} \tag{4.53}$$

The general form of $W_<$ is complicated, but in the case of no extra D2–branes, where we have simply an uncharged black hole inside the shell,

$$W_< = \frac{K(r_e)}{Z_2(r_e)Z_6(r_e)}\frac{L}{L(r_e)}\frac{r_0'}{r^3}\,. \tag{4.54}$$

On the horizon branch, where $\hat{r}_2 > 0$, $W > 0$ everywhere, and there can be no instability associated with this mode. This is as we would expect; the horizon branch looks like a normal charged black hole solution, and the free wave equation has no non-constant solutions regular both on the horizon and at infinity. However, on the shell branch, there may be a region with $W_> < 0$. (Since we take the horizon branch for the solution inside the shell, $W_<$ is always positive.) The leading term is always positive, as

$$\hat{r}_2+\hat{r}_6+r_0 = \frac{1}{2}\sqrt{4r_6^2+r_0^2}\pm\frac{1}{2}\sqrt{4r_2^2+r_0^2} > 0, \tag{4.55}$$

since $|r_2| < r_6$. On the other hand, $W_>$ is always negative near $r = -\hat{r}_2$. As $r \to -\hat{r}_2$,

$$W_> \approx -\frac{5}{16}\frac{\hat{r}_2^2K^2}{r^4Z_2^3Z_6} < 0. \tag{4.56}$$

If we considered just the pure repulson solution, this divergence would lead us to suspect the solution is unstable to a perturbation by $\delta\psi_3$. Although one would need to consider the issue of boundary conditions at the singularity, $W_>$ diverges sufficiently quickly that there could be bound states supported away from $r = -\hat{r}_2$. The question, then, is whether the enhançon excises this instability, along with the various other undesirable features of the geometry.

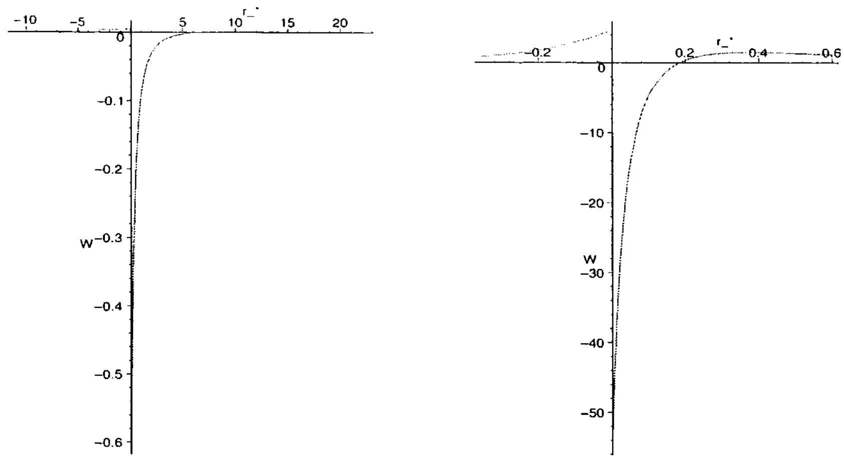

Figure 4.1: *$r_6^2 W$ plotted against r_*/r_6 for (left) $r_0 = 10r_6$, $V = 1000V_*$, $M = 0$, (right) $r_0 = r_6/10$, $V = 1000V_*$, $M = 0$.*

In figure 4.1, we plot the potential for some representative values of the parameters. We see that there is a substantial region outside the shell where the potential is negative, and might suspect that this signals an instability.

However, there is a general argument which says that there can never be an instability in this case [209]. First, we note that as (4.46) is simply the free wave equation in this background, it always has $\delta\psi_3 =$ constant as a solution. In terms of the bound state problem (4.50), this translates into the statement that there is a zero energy ($\omega = 0$) eigenmode ψ_0 of (4.50), which is of the same sign and is bounded everywhere; we can take it to be always positive. This zero mode ψ_0 does not vanish at the boundaries, so it is not a physical perturbation but it is still an acceptable mathematical solution of this equation.

Now assume there is a discrete spectrum of bound states ψ_ω with negative energy. These are our hypothetical unstable modes with $\omega^2 < 0$. We can see from the form of (4.50) that they go to zero as $r_* \to \pm\infty$. This means that they are bounded solutions and physical perturbations of our problem. The standard 'node rule' for the number of nodes of the eigenfunctions of the discrete bound states says that in order of increasing energy, the nth eigenmode has $n-1$ nodes (without including the boundary ones). Thus, the lowest negative mode $\psi_{\omega_{max}}$ must have no nodes in the sense of the above rule: we can take it to be everywhere positive.

Both ψ_0 and $\psi_{\omega_{max}}$ are solutions of the wave equation (4.50). By multiplying the equation for each mode by the other and taking the difference, and integrating over r_*, we can obtain the equation

$$(\psi_{\omega_{max}}\partial_{r_*}\psi_0 - \psi_0\partial_{r_*}\psi_{\omega_{max}})|_{r_*=\pm\infty} = -\omega_{max}^2 \int_{-\infty}^{\infty} \psi_{\omega_{max}}\psi_0 dr_* \tag{4.57}$$

The left-hand side is the difference of the Wronskians calculated at the boundaries. Since the eigenmode ψ_0 approaches a positive constant at the boundaries $r_* = \pm\infty$, while the eigenmode $\psi_{\omega_{max}}$ goes to zero, the Wronskian vanishes at each boundary. Hence, the left-hand side is zero. On the other hand, since both $\psi_{\omega_{max}}$ and ψ_0 are supposed to be everywhere positive, the right-hand side cannot be zero unless $\omega_{max} = 0$. Thus, assuming the existence of eigenmodes ψ_ω with $\omega^2 < 0$ produces a contradiction. Hence there can be no such modes, implying that the geometry is stable to perturbation by $\delta\psi_3$.

4.5 Summary

In this chapter we derived the equations that we we will use in the study of the stability of the enhançon solutions. Initially we introduced the perturbation ansatz for the problem at hand. We used the most general ansatz that preserves the symmetries of the background. This ansatz is still very restricted but since we expect to find an instability signalling a transition from the shell branch to the horizon branch, we do not expect that such an instability will break the symmetries of the background solutions. Finally we produce the differential equations that the modes in the perturbation ansatz must satisfy.

This system is overdetermined since there are more equations than unknown functions. In the third section we used a very beautiful argument in order to simplify our system of differential equations to a set of coupled differential equations. Our ansatz does not fix diffeomorphism invariance completely. By exploiting this invariance we are able to write down a reduced system (4.19, 4.28, 4.34, 4.40).

Before we embark to the more difficult problem of solving numerically these equations we study the stability of the shell under the uncoupled mode ψ_3. We also use this as an example of the techniques used in studying stability. We find that the shell is stable under this particular mode.

For the horizon branch of solutions, we will need to solve the full equations with appropriate boundary conditions on the horizon, since there is no shell. For the extremal case and the shell branch we will need to formulate appropriate matching conditions at the shell. The determination of these conditions and the numerical investigation of their properties will be the subject of Chapter 5 and Section 6.2.

Chapter 5

Stability of extremal enhançon shell

In this chapter we will discuss the stability of the extremal enhançon. In the first section we introduce the perturbation ansätze for the exterior and the interior to the shell regions. Following the general technique explained in the previous chapter, we give a few details regarding the diffeomorphism invariance of our ansätze and how this can be used to reduce to the system of the differential equations which govern the dynamics of the small linearised perturbations. For the exterior geometry these have a rather complicated form and must be solved numerically, while for the interior, which is flat space, they can be solved analytically.

Next we discuss the boundary conditions at the shell. Since we can solve the equations in the interior analytically we are interested in the boundary conditions for the exterior perturbations at the shell. To obtain these we work out the stress–energy tensor of the perturbed shell from the Israel junction conditions and keep terms in linear order in the perturbed modes. We can model this shell by a collection of BPS wrapped D6–branes and calculate the stress–energy tensor of the perturbed shell. The matching conditions for the perturbation modes are obtained by setting this brane stress–energy tensor equal to the stress–energy tensor calculated from supergravity. The same can be done with the dilaton discontinuity. Using these equations relating interior and exterior functions at the shell, the boundary conditions of the interior functions at the shell and exploiting the extra diffeomorphism freedom we find the initial boundary conditions for the exterior functions at the shell. It is remarkable that although the location of the shell is also perturbed, we can use some of the diffeomorphism freedom to fix the coordinate position of the shell at the enhançon radius.

Now we have everything we need in order to study the problem numerically. Before we start, we describe briefly the numerical method ("Relaxation Method") we use in order to solve the system of differential equations. Using this method we can see that our system of differential equations has no solution respecting the set of boundary conditions appropriate to it. This means that the extremal enhançon is stable under this limited set of small radial perturbations.

Finally we close this chapter with a survey of the situation when there are extra unwrapped D2–branes included. We again describe briefly the perturbation ansatz for the interior. The exterior is roughly the same as the exterior for the case with no extra D2–branes; the only difference is the value of r_2 which now includes the extra contribution from the unwrapped branes. The most important result comes from a discussion of the Israel junction conditions of the shell. There is some extra structure in the shell which is not obvious from the initial no–extra–D2–branes setup. It seems that in the shell there is a certain number of D2–anti–D2–branes pairs which also contribute to the shell stress–energy tensor of the shell.

5.1 Perturbation equations

In this section we will describe briefly how we find the system of differential equations which we need in order to study the stability of the extremal enhançon. Since the procedure was explained in detail in the previous chapter we will just point the differences with the more general case.

5.1.1 Exterior

We use again the ansatz (4.1) but with the background fields taking their extremal values (3.5-3.7). We can analyse the perturbations and use diffeomorphism freedom to reduce to a system of three coupled differential equations plus one which is not coupled to the others. The diffeomorphisms preserving the form of our ansatz in the extremal case are

$$\delta r = ar, \tag{5.1}$$

$$\delta t = \sigma a\left(\frac{1}{2}r^2 + (r_2 + r_6)r + r_2 r_6 \ln r\right) + \sigma b, \tag{5.2}$$

where $\sigma = i\omega$.

We can now reduce the system following exactly the same procedure as in the previous chapter. There is an equation involving Φ'',

$$D(\Phi'' + \frac{2}{r}\Phi' - Z_2 Z_6 \sigma^2 \Phi) + P_2^1(\Psi_2' + 2\mathcal{Z}_6') + Q_1^1\Phi + Q_3^1\mathcal{Z}_6 = 0, \tag{5.3}$$

with the polynomial coefficients

$$D = r^2(8r^2 + 5rr_2 + 5rr_6 + 2r_2r_6)(4r^2 + 3rr_2 + 3rr_6 + 2r_2r_6), \tag{5.4}$$

$$P_2^1 = -2r^2(-2r^2r_2 + 6r^2r_6 + 8rr_2r_6 + 3r_2^2r_6 + r_2r_6^2), \tag{5.5}$$

$$Q_1^1 = -r^2(3r_2^2 + 6r_2r_6 + 27r_6^2) - r(2r_2^2r_6 + 30r_2r_6^2) - 8r_2^2r_6^2, \tag{5.6}$$

$$Q_3^1 = r^2(9r_2^2 + 10r_2r_6 + 9r_6^2) + r(6r_2^2r_6 + 10r_2r_6^2). \tag{5.7}$$

The equation involving Ψ_2'' is

$$D(\Psi_2'' - Z_2Z_6\sigma^2\Psi_2) + P_2^2\Psi_2' + P_3^2\mathcal{Z}_6' + Q_1^2\Phi + Q_3^2\mathcal{Z}_6 = 0, \tag{5.8}$$

where D is as before, and the other polynomial coefficients are

$$\begin{aligned} P_2^2 &= 64r^5 + r^4(120r_2 + 88r_6) + r^3(+30r_2^2 + 172r_2r_6 + 30r_6^2) \\ &\quad + r^2(44r_2^2r_6 + 52r_2r_6^2) + 8rr_2^2r_6^2, \end{aligned} \tag{5.9}$$

$$P_3^2 = -8r^2\hat{r}_2(8r^2 + 16rr_6 + 3r_2r_6 + 5r_6^2), \tag{5.10}$$

$$Q_1^2 = 4r_2(r^2(-6r_2 - 6r_6) + r(-7r_2r_6 + 3r_6^2) + 2r_2r_6^2), \tag{5.11}$$

$$Q_3^2 = 4r_2(r^2(18r_2 + 2r_6) + r(21r_2r_6 - r_6^2) + 6r_2r_6^2). \tag{5.12}$$

The equation involving $\mathcal{Z}_6''$ is

$$D(\mathcal{Z}_6'' - Z_2Z_6\sigma^2\mathcal{Z}_6) + P_2^3\Psi_2' + P_3^3\mathcal{Z}_6' + Q_1^3\Phi + +Q_3^3\mathcal{Z}_6 = 0, \tag{5.13}$$

where D is as before, and the other polynomial coefficients are

$$P_2^3 = -2r^2(6r^2r_2 - 2r^2r_6 + 8rr_2r_6 + r_2^2r_6 + 3r_2r_6^2), \tag{5.14}$$

$$\begin{aligned} P_3^3 &= 64r^5 + r^4(64r_2 + 96r_6) + r^3(30r_2^2 + 76r_2r_6 + 30r_6^2) \\ &\quad + r^2(28r_2^2r_6 + 20r_2r_6^2) + 8rr_2^2r_6^2, \end{aligned} \tag{5.15}$$

$$Q_1^3 = r^2(9r_2^2 + 10r_2r_6 + 9r_6^2) + r(10r_2^2r_6 + 6r_2r_6^2), \tag{5.16}$$

$$Q_3^3 = -r^2(27r_2^2 + 6r_2r_6 + 3r_6^2) - r(30r_2^2r_6 + 2r_2r_6^2) - 8r_2^2r_6^2. \tag{5.17}$$

These are the final system of differential equations of motion of the perturbations in the exterior. We are going to use them together with the boundary conditions on the shell, in order to investigate the stability of the extremal enhançon shell.

5.1.2 Interior

Perturbation ansatz

In the interior space we use an ansatz similar to the one for the exterior (4.1). We can write for the metric

$$\begin{aligned} g_s^{1/2}\,ds^2 &= e^{-\gamma_1/2}\Big[\bar{H}_2^{-1/2}\bar{H}_6^{-1/2}(-e^{\delta\gamma_2}dt^2 + e^{-\frac{1}{2}\delta\gamma_2}(dx_1^2 + dx_2^2)) \\ &\quad + \bar{H}_2^{1/2}\bar{H}_6^{1/2}(dr^2 + r^2d\Omega_2^2) + V^{1/2}\bar{H}_2^{1/2}\bar{H}_6^{-1/2}ds_{\mathrm{K3}}^2\Big], \end{aligned} \tag{5.18}$$

dilaton

$$\bar{\phi} = \phi + \delta\xi, \tag{5.19}$$

and R–R fields

$$\bar{C}_{(3)} = C_{(3)} + \delta C_{(3)}, \quad \bar{C}_{(7)} = C_{(7)} + \delta C_{(7)}. \tag{5.20}$$

Here

$$\gamma_1 = \phi + \delta\gamma_1, \ \bar{H}_2 = H_2(1 + \delta H_2), \ \bar{H}_6 = H_6(1 + \delta H_6), \tag{5.21}$$

and H_2, H_6 as well as the unperturbed dilaton ϕ and R–R fields are constants.

Particular Integral and equations of motion

We can analyse the perturbations of the interior geometry following the same route used above for the exterior geometry. The diffeomorphisms preserving the form of our ansatz are now

$$\delta r = cr, \qquad \delta t = \sigma H_2 H_6 c r^2/2 + \sigma d. \tag{5.22}$$

We can write

$$\begin{aligned}
\delta\gamma_1 &= \delta\gamma_1^d(c(r), d(r)), \\
\delta\gamma_2 &= \delta\gamma_2^d(c(r), d(r)) + \Gamma_2, \\
\delta H_6 &= \delta H_6^d(c(r), d(r)) + \mathcal{H}_6, \\
\delta H_2 &= \delta H_2^d(c(r), d(r)), \\
\delta\xi &= \delta\xi^d(c(r), d(r)) + \Xi,
\end{aligned} \tag{5.23}$$

and then we find that the equations for the free perturbation functions are all

$$\partial_r^2 f + \frac{2}{r}\partial_r f - H_2 H_6 \sigma^2 f = 0, \tag{5.24}$$

where $f = \Xi, \Gamma_2, \mathcal{H}_6$. The solution regular at $r = 0$ is

$$f = f_0 \frac{\sinh \bar{\sigma} r}{r}, \tag{5.25}$$

where $\bar{\sigma} = \sqrt{H_2 H_6}\sigma$.

The above system is very simple, since it is a system of three decoupled equations. This is expected since the interior space is nothing but flat space and we expect the modes to decouple.

5.2 Boundary conditions

Now we have the differential equations describing the dynamics of the perturbation modes in the interior and exterior to the shell regions. Since the perturbation modes couple to the shell, we must find how the interior and exterior functions are related. In order to do that we have to see how exactly the shell is affected by the perturbation modes. We need a model describing the degrees of freedom of the shell.

At the enhançon shell $r = r_e$, the interior perturbations studied above will satisfy the boundary conditions

$$r_e f'(r_e) + (1 - \bar{\sigma} r_e \coth \bar{\sigma} r_e) f(r_e) = 0. \tag{5.26}$$

What we really want is boundary conditions for the exterior perturbations $\Phi, \Psi_2, \mathcal{Z}_6$ at the shell. To obtain these from the above conditions on $\Xi, \Gamma_2, \mathcal{H}_6$, we need to work out the junction conditions at the shell for the perturbations, and solve for $\Xi, \Gamma_2, \mathcal{H}_6$ and their first derivatives in terms of $\Phi, \Psi_2, \mathcal{Z}_6$ and their derivatives.

In general, the location of the shell separating the interior and and exterior is also perturbed. Its equation of motion can be determined from the action of the wrapped branes

$$S = -N \int_{\mathcal{M}_2} d^3\xi e^{-\bar{\phi}} (\mu_6 V(r) - \mu_2)(-\det G_{\mu\nu})^{1/2} + \mu_6 \int_{\mathcal{M}_2 \times K3} \bar{C}_{(7)} - \mu_2 \int_{\mathcal{M}_2} \bar{C}_{(3)}, \tag{5.27}$$

where $G_{\mu\nu}$ is the induced string-frame metric, and the string-frame volume $V(r) = V e^{\bar{\phi} - \psi_1} \bar{Z}_2 \bar{Z}_6^{-1}$. In static gauge $t = \xi^0$, $x^{1,2} = \xi^{1,2}$, the position of the shell is parametrised by $r = \bar{r}_i = r_e + \delta r_i(\xi^0)$. The effective action of the shell up to second order in $\delta r(\xi^0)$ is in Einstein frame

$$\begin{aligned} S &= -N \int d^3\xi e^{\frac{3}{4}(\bar{\phi} - \psi_1)} \bar{Z}_2^{1/4} \bar{Z}_6^{-3/4} \left(\frac{\mu_6 V e^{-\psi_1}}{\bar{Z}_6} - \frac{\mu_2 e^{-\bar{\phi}}}{\bar{Z}_2} \right) \left(1 - \frac{1}{2} (\delta \dot{r}_i)^2 \bar{Z}_2 \bar{Z}_6 e^{-\psi_2} \right) \\ &\quad + \int d^3\xi (\mu_6 \bar{C}_{(7)} - \mu_2 \bar{C}_{(3)}), \end{aligned} \tag{5.28}$$

where $\dot{}$ denotes differentiation with respect to ξ^0. From this effective action we can deduce the equation of motion for the position of the shell.

We can use some of the remaining diffeomorphism freedom in the ansatz to fix the coordinate position of the shell to be $r_i = r_e$, the enhançon radius of the unperturbed metric. We can substitute (4.9) in the differential equation which minimises (5.28). We see that it depends on the undetermined constants a, b in (4.10),(4.11). The dynamics of the shell will then find its expression through the variation of the perturbed metric at the shell location. This choice greatly simplifies the problem of matching the perturbations at the shell.

Continuity of the metric and fields at the shell implies

$$\delta\phi(r_e) = \delta\xi(r_e), \quad \delta\psi_1(r_e) = \delta\gamma_1(r_e), \quad \delta\psi_2(r_e) = \delta\gamma_2(r_e), \tag{5.29}$$
$$\delta Z_2(r_e) = \delta H_2(r_e), \quad \delta Z_6(r_e) = \delta H_6(r_e).$$

To relate the first derivatives, we compute the discontinuity in the extrinsic curvature at the surface $r = r_e$ when we patch the two geometries together. This allows us to infer the stress tensor of the perturbed shell from the supergravity point of view, with the result

$$S_{tt} = \frac{1}{2\kappa^2\sqrt{g_{rr}}}\left[2\frac{\bar{Z}_2'}{\bar{Z}_2} - 2\frac{\bar{Z}_6'}{\bar{Z}_6} - 4\psi_1' - \delta\psi_2' - 2\frac{\bar{H}_2'}{\bar{H}_2} + 2\frac{\bar{H}_6'}{\bar{H}_6} + 4\gamma_1' + \delta\gamma_2'\right] g_{tt}, \tag{5.30}$$

$$S_{\rho\sigma} = \frac{1}{2\kappa^2\sqrt{g_{rr}}}\left[2\frac{\bar{Z}_2'}{\bar{Z}_2} - 2\frac{\bar{Z}_6'}{\bar{Z}_6} - 4\psi_1' + \frac{1}{2}\delta\psi_2' - 2\frac{\bar{H}_2'}{\bar{H}_2} + 2\frac{\bar{H}_6'}{\bar{H}_6} + 4\gamma_1' - \frac{1}{2}\delta\gamma_2'\right] g_{\rho\sigma}, \tag{5.31}$$

$$S_{ij} = \frac{1}{2\kappa^2\sqrt{g_{rr}}}\left[\frac{\bar{Z}_2'}{\bar{Z}_2} - 3\frac{\bar{Z}_6'}{\bar{Z}_6} - 4\psi_1 - \frac{\bar{H}_2'}{\bar{H}_2} + 3\frac{\bar{H}_6'}{\bar{H}_6} + 4\gamma_1'\right] g_{ij}, \tag{5.32}$$

$$S_{ab} = \frac{1}{2\kappa^2\sqrt{g_{rr}}}\left[\frac{\bar{Z}_2'}{\bar{Z}_2} - 2\frac{\bar{Z}_6'}{\bar{Z}_6} - 4\psi_1' - \frac{\bar{H}_2'}{\bar{H}_2} + 2\frac{\bar{H}_6'}{\bar{H}_6} + 4\gamma_1'\right] g_{ab} \tag{5.33}$$

(coordinates ρ, σ run over $1, 2$, i, j over θ, ϕ, and a, b over the K3). We will assume that this shell stress tensor is still sourced by a collection of BPS branes. Using the worldvolume action for a wrapped D6-brane 5.27, one easily obtains the Einstein-frame stress-energy for a single brane in the exterior geometry,

$$S_{\mu\nu}^{brane} = -e^{3\bar{\phi}/4}(\mu_6 - \mu_2 V(r)^{-1})g_{\mu\nu}, \tag{5.34}$$

$$S_{ab}^{brane} = -e^{3\bar{\phi}/4}\mu_6 g_{ab} \tag{5.35}$$

(where μ, ν run over $t, 1, 2$). If we use this to calculate the stress-energy of the shell, we find that the value the stress tensor should take can be written as

$$S_{\mu\nu}^{shell} = \frac{1}{2\kappa^2\sqrt{g_{rr}}}\frac{e^{3\bar{\phi}/4+\psi_1/4}}{\bar{Z}_2^{1/4}\bar{Z}_6^{-3/4}}\left[\frac{\bar{Z}_2'}{\bar{Z}_2}e^{-\bar{\phi}+\psi_1} + \frac{\bar{Z}_6'}{\bar{Z}_6}\right] g_{\mu\nu}, \tag{5.36}$$

$$S_{ij}^{shell} = 0, \tag{5.37}$$

$$S_{ab}^{shell} = \frac{1}{2\kappa^2\sqrt{g_{rr}}}\frac{e^{3\bar{\phi}/4+\psi_1/4}}{\bar{Z}_2^{1/4}\bar{Z}_6^{-3/4}}\frac{\bar{Z}_6'}{\bar{Z}_6}g_{ab}. \tag{5.38}$$

The matching conditions for first derivatives of the metric are then obtained by setting this brane stress tensor equal to the stress tensor calculated from the supergravity point of view above. Similarly, matching the discontinuity in the dilaton to the brane source gives

$$\phi'_{out} - \phi'_{in} = \frac{e^{3\bar{\phi}/4+\psi_1/4}}{4\bar{Z}_2^{1/4}\bar{Z}_6^{-3/4}}\left[e^{\psi_1-\bar{\phi}}\frac{Z'_2}{\bar{Z}_2} - 3\frac{Z'_6}{\bar{Z}_6}\right]. \tag{5.39}$$

Taking the first-order part of all these equations gives us five equations relating the derivatives of $\delta\phi, \delta\psi_1, \delta\psi_2, \delta Z_2, \delta Z_6$ to the corresponding interior quantities.

We then have ten matching equations at the shell. However, we only have nine quantities to specify: we want to solve for the three free interior functions $\Xi, \Gamma_2, \mathcal{H}_6$ and their first derivatives at the shell in terms of Φ, Ψ_2, $\mathcal{Z}_6$ and their first derivatives, and we also have three undetermined constants in the diffeomorphisms to fix (since we already fixed one to satisfy $r_i = r_e$).[1] Remarkably, this over-determined system has a solution, and substituting into the boundary condition (5.26) gives us, after considerable algebra, the relatively simple expressions

$$\begin{aligned} 0 &= -2\hat{r}_6(v^2+1)\Phi'(r_e) - \hat{r}_6(v^2+4v-1)\Psi'_2(r_e) + 4\hat{r}_6(v+1)\mathcal{Z}'_6(r_e) \\ &\quad +v(v-1)^2\Phi(r_e) + (v-1)^2\mathcal{Z}_6(r_e), \end{aligned} \tag{5.40}$$

$$\begin{aligned} 0 &= -8\hat{r}_6(v+1)\Phi'(r_e) + 4\hat{r}_6(v+1)\Psi'_2(r_e) \\ &\quad +[4\bar{\sigma}r_e\coth(\bar{\sigma}r_e)(v^2-1) - v^2 - 6v + 7]\Phi(r_e) \\ &\quad +[-2\bar{\sigma}r_e\coth(\bar{\sigma}r_e)(v^2-1) + 2v^2 - 2]\Psi_2(r_e) - 3(v-1)^2\mathcal{Z}_6(r_e), \end{aligned} \tag{5.41}$$

$$\begin{aligned} 0 &= 4\hat{r}_6(v+1)\Phi'(r_e) + 4\hat{r}_6(v+1)\mathcal{Z}'_6(r_e) \\ &\quad +[-2\bar{\sigma}r_e\coth(\bar{\sigma}r_e)(v^2-1) + v^2 + 2v - 3]\Phi(r_e) \\ &\quad +[-2\bar{\sigma}r_e\coth(\bar{\sigma}r_e)(v^2-1) + 3v^2 - 2v - 1]\mathcal{Z}_6(r_e), \end{aligned} \tag{5.42}$$

where $v = V/V_*$ and $\bar{\sigma} = \sqrt{H_2H_6}\sigma$.

[1] We have also checked explicitly that we get the same boundary conditions at the shell for the physical degrees of freedom even if we work in a coordinate system where the coordinate location of the shell is not fixed.

Before we continue to the numerical investigation we should stress an assumption regarding the perturbation of the shell. We assume that the perturbations are small enough so that the branes constituting the shell are not excited and remain BPS. If the system remains BPS, we can use the machinery developed in this section without any problems. We can model the shell by wrapped BPS D6–branes smeared over a 2–sphere, as we did. In case the branes would go non–BPS we would have to complicate things by introducing another model for the shell. That would be dangerous since we could not be really sure that this model could describe the physics of the shell correctly.

5.3 Numerical investigation

5.3.1 Relaxation Method

We will very briefly describe the 'Relaxation Method'[2] [210] for solving boundary value problems.

In relaxation methods we replace the ODEs by approximate finite–difference equations on a grid of points that spans the domain of interest. A trial solution consists of values for the dependent functions at every grid point, not satisfying the finite–difference equations. It is not necessary for the trial solution to satisfy the required boundary conditions. The procedure is to iteratively adjust the values of the dependent functions on the grid so as to successively bring them into closer agreement with the finite–difference equations and at the same time with the boundary conditions.

A good initial guess is essential for the method to be efficient. The biggest advantage of this method comes when you want to solve the problem many times with slightly different values of the parameters. Most of the time the previous solution is a very good choice for an initial guess solution. For a slight change of

[2]This is a standard method for solving two point boundary value problems and can be found on most books on Numerical Analysis. A more detailed description of the method can be found at the Appendix.

the parameters the new solution usually does not differ a lot from the old one so the method converges quite fast.

5.3.2 Results

The problem of finding instabilities of the extremal enhançon solution reduces to looking for solutions of the equations of motion for $\Phi, \Psi_2, \mathcal{Z}_6$ for some σ which satisfy the boundary conditions (5.40), (5.41) and (5.42) at the shell and fall off at large distance. We have searched for such solutions using relaxation techniques as described briefly in Section 5.3.1. The iteration procedure does not converge at all. This means that there are no eigenvalues σ which satisfy the desired boundary conditions. Since the form of the ansatz for the perturbations was such that it described unstable modes, the non–existence of solutions of this form implies that there are no instabilities. We studied these equations numerically for a wide range of the parameters r_2 and r_6, and failed to find a solution which rendered the shell unstable. We could claim that at least for radial perturbations, the extremal enhançon shell is stable.

This result is, of course, what one would expect on the basis of supersymmetry. A solution which satisfies the BPS bound may have flat directions—it may be marginally stable to some perturbation—but one would not expect that it will have any truly unstable perturbations.

This result strengthens the argument of [129] for the consistency of the excision procedure [127]. This excision is accomplished by the introduction of a shell of wrapped $D6$–branes at the enhançon radius. The fact that this solution is stable is another argument in favour of the excision and of the idea that the solution is a sensible construction from the point of view of supergravity.

5.4 Additional D2–branes

If we add extra D2–branes in the extremal solution the situation does not change much. We saw in Chapter 3 that the extra D2–branes can move in the interior and they can help some of the wrapped D6–branes to migrate inside the shell. Although the solution in the interior is no longer flat, in principle we can solve the problem since we can model the shell using the remaining wrapped D6–branes. We can then calculate the boundary conditions for the perturbation modes on the shell.

It would be interesting to examine another extremal solution. We start with the 'horizon' branch of solutions and we add extra D2–branes. Then we take the non–extremality parameter $r_0 = 0$. This solution is not exactly the extremal solution with additional D2–branes. It would be helpful to study this solution, since it will help us understand the difference of the two branches of the non–extremal solution. We will not complete the stability analysis in this case. Instead, we will focus on explaining how the model for the shell changes and exploring the influence of this on the matching conditions for the perturbations.

The difference with the case of the extremal enhançon with extra D2–branes , reviewed in Section 3.2.4, is that now r_2 is

$$r_2 = r_6 \frac{V}{V_*} \left(1 - \frac{M}{N}\right) , \tag{5.43}$$

for the case $M < N$. The exterior solution of the extremal limit of the above can be described by (3.5) and (3.6) with r_2 described by (5.43). The interior will be described by (3.28), (3.29), (3.30) and (3.31).

The enhançon radius is at

$$r_e = \frac{2V_* r_6}{V - V_*} \frac{2N - M}{2N} \tag{5.44}$$

As we remember from Chapter 3, for $M \geq 2N$ there is no enhançon radius. So we consider that $M < 2N$. Another thing is that an unwrapped D2–brane can move past the enhançon radius to the origin without an obstacle. $N' = M$ in total D6–branes can move in the interior of the shell. Since we want to have some D6–branes on the shell we will assume that $M < N$.

The stress tensor of the shell from the Israel junction conditions is:

$$\begin{aligned}
2\kappa^2 S_{\mu\nu} &= \frac{1}{\sqrt{G_{rr}}} \left(\frac{Z_2'}{Z_2} + \frac{Z_6'}{Z_6} - \frac{H_2'}{H_2} - \frac{H_6'}{H_6} \right) G_{\mu\nu} , \\
S_{ij} &= 0 , \\
2\kappa^2 S_{ab} &= \frac{1}{\sqrt{G_{rr}}} \left(\frac{Z_6'}{Z_6} - \frac{H_6'}{H_6} \right) G_{ab} .
\end{aligned} \tag{5.45}$$

Plugging in (5.45) the equivalents from (3.6), (3.30) and (3.31) we can rewrite it as:

$$\begin{aligned} 2\kappa^2 S_{\mu\nu} &= \frac{1}{\sqrt{G_{rr}}}\frac{r_6}{r^2}\left[\frac{N'-N}{N}\left(-\frac{V_*}{V}\frac{1}{Z_2}+\frac{1}{Z_6}\right)+\frac{2(M-N)}{N}\frac{V_*}{V}\frac{1}{Z_2}\right]G_{\mu\nu}\,, \\ S_{ij} &= 0\,, \\ 2\kappa^2 S_{ab} &= \frac{1}{\sqrt{G_{rr}}}\frac{r_6}{r^2}\frac{N'-N}{N}\frac{1}{Z_6}G_{ab}. \end{aligned} \tag{5.46}$$

Its is obvious from the above than something is quite different from what it is expected. At the enhançon radius, $S_{\mu\nu}$ is not zero as it is in the ordinary BPS case without extra D2–branes. There is an extra term which depends on M. This term is only in the directions associated with the D2–branes. Since we assumed that all the D2–branes are in the interior and not on the shell it is strange to have such a term in the stress tensor. If we try to model the shell by $N-N'$ D6–branes then from the DBI action one can take only the first term in $S_{\mu\nu}$ and of course the other two equations. Another hint could be given from the source of the dilaton:

$$\begin{aligned} 2\kappa^2 S_\Phi &= \frac{1}{\sqrt{G_{rr}}}(\Phi'_+ - \Phi'_-) = \frac{1}{4\sqrt{G_{rr}}}\left(\frac{Z_2'}{Z_2}-\frac{H_2'}{H_2}-3\left(\frac{Z_6'}{Z_6}-\frac{H_6'}{H_6}\right)\right) \\ &= \frac{1}{4\sqrt{G_{rr}}}\frac{r_6}{r^2}\left[\frac{N'-N}{N}\left(-\frac{V_*}{V}\frac{1}{Z_2}-\frac{3}{Z_6}\right)+\frac{2(M-N)}{N}\frac{V_*}{V}\frac{1}{Z_2}\right] \end{aligned} \tag{5.47}$$

Again we have an extra term which can not be modelled by the DBI action. We expect the shell to consist of $N-N'$ wrapped D6–branes and no extra D2–branes at all. The evidence from above leads us to the conjecture that we have some number $2(N-M)$ of unwrapped extra D2–branes, as it can be seen from their contribution as dilaton source and from the stress–energy tensor, which do not couple with any Ramond–Ramond field. This indicates that this behaviour might be caused from a number of D2 branes with an equal number of anti–D2–branes. This is a plausible setup which partly explains the above result. It is by no means a hypothesis based on a concise physical argument. We cannot really say how and why these pairs of branes and anti–branes show up. We just have an expression in (5.46) and (5.47) which could be a result of such a configuration[3]. We will use this hypothesis later

[3] In fact, in [211] it was proposed that above a finite temperature, pairs of branes and anti–D–branes can form from the vacuum. It was also shown that it is not favourable to annihilate to give a closed string vacuum [212–219]. This system was used to calculate the entropy of p–branes at finite temperature. A similar approach was also used earlier in [220].

in order to calculate the boundary conditions satisfied by the perturbations of the fields on the shell.

5.4.1 Perturbation equations in the interior

Inside the shell, we will have a perturbed space,

$$\begin{aligned} g_s^{1/2}\, ds^2 &= e^{-\gamma_1/2}\Big[\bar{H}_2^{-1/2}\bar{H}_6^{-1/2}(-e^{\delta\gamma_2}dt^2 + e^{-\frac{1}{2}\delta\gamma_2}(dx_1^2+dx_2^2)) \\ &\quad +\bar{H}_2^{1/2}\bar{H}_6^{1/2}(dr^2+r^2\Omega_2^2) + V^{1/2}\bar{H}_2^{1/2}\bar{H}_6^{-1/2}ds_{\mathrm{K3}}^2\Big]\,, \end{aligned} \tag{5.48}$$

dilaton

$$\bar{\phi} = \phi + \delta\xi, \tag{5.49}$$

and R–R fields

$$\bar{C}_{(3)} = C_{(3)} + \delta C_{(3)}, \quad \bar{C}_{(7)} = C_{(7)} + \delta C_{(7)}. \tag{5.50}$$

Here

$$\gamma_1 = \phi + \delta\gamma_1,\ \bar{H}_2 = H_2(1+\delta H_2),\ \bar{H}_6 = H_6(1+\delta H_6), \tag{5.51}$$

H_2, H_6 are as in (3.30), (3.31) respectively and the unperturbed dilaton ϕ and the R–R potentials are as in (3.29). The difference with the case without D2–branes is that now there are D2–brane sources in the interior plus wrapped D6–brane sources, which can migrate inside due to the presence of the extra branes. The interior space is not flat.

We can analyse the perturbations of the interior geometry following the same route used above for the exterior geometry. The diffeomorphisms preserving the form of our ansatz are now

$$\delta r = cr, \qquad \delta t = \sigma c r^2 H_2(r)\left(\frac{r_6 - r_6'}{2r_{\mathrm{e}}} + \frac{r_6'}{r}\right) + \sigma d. \tag{5.52}$$

We can write

$$\begin{aligned} \delta\gamma_1 &= \delta\gamma_1^d(c(r), d(r)), \\ \delta\gamma_2 &= \delta\gamma_2^d(c(r), d(r)) + \Gamma_2, \\ \delta H_6 &= \delta H_6^d(c(r), d(r)) + \mathcal{H}_6, \\ \delta H_2 &= \delta H_2^d(c(r), d(r)), \\ \delta\xi &= \delta\xi^d(c(r), d(r)) + \Xi, \end{aligned} \tag{5.53}$$

and then we find that the equations for the free perturbation functions are

$$\begin{aligned} D\left(\chi_1'' + \frac{2}{r}\chi_1'\right) + \tilde{\omega}\chi_1 &= 0 &(5.54)\\ D\left(\chi_2'' + \frac{2}{r}\chi_2'\right) + \tilde{\omega}\chi_2 &= 0 &(5.55)\\ D\left(\chi_3'' + \frac{2}{r}\chi_3'\right) - 10A\chi_3' + (\tilde{\omega} - 10B)\chi_3 &= 10A(\chi_1' + \chi_2') &(5.56)\end{aligned}$$

where $\chi_1 = \Xi + 3\mathcal{H}_6$, $\chi_2 = \Gamma_2$, $\chi_3 = \mathcal{H}_6 - 3\Xi$ and

$$\begin{aligned} v &= \frac{V}{V_*}, \qquad n = \frac{M}{N}\\ A &= 4r_6 nv(n-2)^3(nv - v - 1), \qquad B = -3r_6 nv(n-2)^4\\ D &= v(n-2)^2[5r_6 n(n-2) - 8(1+v-nv)r][3r_6 n(n-2) - 4(1+v-nv)r]\\ \tilde{\omega} &= \frac{D}{rV(n-2)^2}(1 - n - 3v + 2nv)[r_6 n(n-2) - (1+v-nv)r]. \qquad (5.57)\end{aligned}$$

We see that (5.54), (5.55) decouple and can be solved analytically in terms of Whittaker functions. The solution regular at $r = 0$ is:

$$\chi_{1,2} = \frac{C_{1,2}}{r}\mathcal{M}_{\nu,\frac{1}{2}}\left(\sqrt{\frac{(3v - 2nv + n - 1)(1 + v - nv)}{v(2-n)}}r\right) \qquad (5.58)$$

where $C_{1,2}$ are constants of integration and ν in the subscript is:

$$\nu = -\frac{r_6(2-n)}{2}\sqrt{\frac{(3v - 2nv + n - 1)}{v(1+v-nv)(2-n)}} \qquad (5.59)$$

5.4.2 Junction conditions

Again we would like to match the perturbations in the interior and the exterior at the shell in a way similar to the case with no extra D2–branes (Sec. 5.2). We will not be able to complete the program with the same success because we cannot solve analytically the system of differential equations in the interior.

Continuity of the metric and fields at the shell implies

$$\begin{aligned} &\delta\phi(r_e) = \delta\xi(r_e), \quad \delta\psi_1(r_e) = \delta\gamma_1(r_e), \quad \delta\psi_2(r_e) = \delta\gamma_2(r_e), \qquad (5.60)\\ &\delta Z_2(r_e) = \delta H_2(r_e), \quad \delta Z_6(r_e) = \delta H_6(r_e). \end{aligned}$$

To relate the first derivatives, we compute the discontinuity in the extrinsic curvature at the surface $r = r_e$ when we patch the two geometries together. This allows us to infer the stress tensor of the perturbed shell from the supergravity point of view, with the result

$$S_{tt} = \frac{1}{2\kappa^2\sqrt{g_{rr}}}\left[2\frac{\bar{Z}_2'}{\bar{Z}_2} - 2\frac{\bar{Z}_6'}{\bar{Z}_6} - 4\psi_1' - \delta\psi_2' - 2\frac{\bar{H}_2'}{\bar{H}_2} + 2\frac{\bar{H}_6'}{\bar{H}_6} + 4\gamma_1' + \delta\gamma_2'\right] g_{tt}, \qquad (5.61)$$

$$S_{\rho\sigma} = \frac{1}{2\kappa^2\sqrt{g_{rr}}}\left[2\frac{\bar{Z}_2'}{\bar{Z}_2} - 2\frac{\bar{Z}_6'}{\bar{Z}_6} - 4\psi_1' + \frac{1}{2}\delta\psi_2' - 2\frac{\bar{H}_2'}{\bar{H}_2} + 2\frac{\bar{H}_6'}{\bar{H}_6} + 4\gamma_1' - \frac{1}{2}\delta\gamma_2'\right] g_{\rho\sigma}, \qquad (5.62)$$

$$S_{ij} = \frac{1}{2\kappa^2\sqrt{g_{rr}}}\left[\frac{\bar{Z}_2'}{\bar{Z}_2} - 3\frac{\bar{Z}_6'}{\bar{Z}_6} - 4\psi_1 - \frac{\bar{H}_2'}{\bar{H}_2} + 3\frac{\bar{H}_6'}{\bar{H}_6} + 4\gamma_1'\right] g_{ij}, \qquad (5.63)$$

$$S_{ab} = \frac{1}{2\kappa^2\sqrt{g_{rr}}}\left[\frac{\bar{Z}_2'}{\bar{Z}_2} - 2\frac{\bar{Z}_6'}{\bar{Z}_6} - 4\psi_1' - \frac{\bar{H}_2'}{\bar{H}_2} + 2\frac{\bar{H}_6'}{\bar{H}_6} + 4\gamma_1'\right] g_{ab} \qquad (5.64)$$

(coordinates ρ, σ run over $t, 1, 2$, i, j over θ, ϕ, and a, b over the K3). Considering the discussion in the beginning of Section 5.4, concerning the stress–energy tensor of the shell, we will assume that the S_{MN} is still sourced by a collection of BPS branes. The pair of D2–anti–D2 branes does not couple to the Ramond–Ramond fields and so does not contribute to the Wess–Zumino action. Using the worldvolume action for a wrapped D6–brane,

$$S = -\int_{\mathcal{M}_2} d^3\xi e^{-\phi}(\mu_6 V(r) - \mu_2)(-\det G_{\mu\nu})^{1/2} + \mu_6\int_{\mathcal{M}_2\times K3} C_{(7)} - \mu_2\int_{\mathcal{M}_2} C_{(3)}, \qquad (5.65)$$

where $G_{\mu\nu}$ is the induced string-frame metric, and the string-frame volume $V(r) = Ve^{\bar{\phi}-\psi_1}\bar{Z}_2\bar{Z}_6^{-1}$, one easily obtains the Einstein-frame stress-energy for a single brane in the exterior geometry,

$$S_{\mu\nu}^{brane} = -e^{3\bar{\phi}/4}(\mu_6 - \mu_2 V(r)^{-1})g_{\mu\nu}, \qquad (5.66)$$

$$S_{ab}^{brane} = -e^{3\bar{\phi}/4}\mu_6 g_{ab} \qquad (5.67)$$

(where μ, ν run over $t, 1, 2$). In the above action we have to add also the contribution coming from $2(M - N)$ D2 and anti–D2-branes. As we saw earlier, it seems that there is such a contribution for the problem at hand. We cannot see a reason why these branes do not annihilate with each other but we have to account for them in the description of the shell since by including them we can have a successful model describing the microphysics of the shell. These branes contribute to the DBI part of the action, while the Ramond–Ramond parts cancel:

$$S = -2(N-M)\int_{\mathcal{M}_2} d^3\xi e^{-\phi}\mu_2(-\det G_{\mu\nu})^{1/2} \tag{5.68}$$

If we use (5.66), (5.67) and (5.68) to calculate the stress-energy of the shell, we find that the value the stress tensor can be written as

$$S^{shell}_{\mu\nu} = \frac{1}{2\kappa^2\sqrt{g_{rr}}}\frac{e^{3\bar{\phi}/4+\psi_1/4}}{\bar{Z}_2^{1/4}\bar{Z}_6^{-3/4}}\left[\left(\frac{Z_2'}{\bar{Z}_2}-\frac{H_2'}{\bar{H}_2}\right)e^{-\bar{\phi}+\psi_1}+\frac{Z_6'}{\bar{Z}_6}-\frac{H_6'}{\bar{H}_6}\right]g_{\mu\nu}, \tag{5.69}$$

$$S^{shell}_{ij} = 0, \tag{5.70}$$

$$S^{shell}_{ab} = \frac{1}{2\kappa^2\sqrt{g_{rr}}}\frac{e^{3\bar{\phi}/4+\psi_1/4}}{\bar{Z}_2^{1/4}\bar{Z}_6^{-3/4}}\left[\frac{Z_6'}{\bar{Z}_6}-\frac{H_6'}{\bar{H}_6}\right]g_{ab}. \tag{5.71}$$

The matching conditions for first derivatives of the metric are then obtained by setting this brane stress tensor equal to the stress tensor calculated from the supergravity point of view above. Similarly, matching the discontinuity in the dilaton to the brane source gives

$$\phi'_{out}-\phi'_{in} = \frac{e^{3\bar{\phi}/4+\psi_1/4}}{4\bar{Z}_2^{1/4}\bar{Z}_6^{-3/4}}\left[e^{\psi_1-\bar{\phi}}\left(\frac{Z_2'}{\bar{Z}_2}-\frac{H_2'}{\bar{H}_2}\right)-3\left(\frac{Z_6'}{\bar{Z}_6}-\frac{H_6'}{\bar{H}_6}\right)\right]. \tag{5.72}$$

Taking the first–order part of all these equations gives us five equations relating the derivatives of $\delta\phi, \delta\psi_1, \delta\psi_2, \delta Z_2, \delta Z_6$ to the corresponding interior quantities.

We then have ten matching equations at the shell. However, we only have nine quantities to specify: we want to solve for the three free interior functions $\Xi, \Gamma_2, \mathcal{H}_6$ and their first derivatives at the shell in terms of Φ, Ψ_2, $\mathcal{Z}_6$ and their first derivatives, and we also have four undetermined constants in the diffeomorphisms to fix. Remarkably one can solve this system with respect to the exterior functions, their derivatives, the position of the shell and two of the diffeomorphism constants. The solution is an arbitrary function of the position of the shell. We can substitute in the rest of the solution and we have the exterior functions depending only in the interior ones and not in the diffeomorphism constants.

In principle we can solve this problem. This is because we have a microphysical model describing the degrees of freedom of the shell. This is something that we unfortunately lack for the non–extremal case. We will see in the next chapter that in the case of the shell branch, such a model cannot be constructed.

5.5 Summary

In this chapter we studied the stability of the extremal enhançon against small perturbations. Following the techniques introduced in the previous chapter we briefly sketched how to produce the equations which govern the perturbations, in the interior and the exterior geometry. Again we used residual diffeomorphism freedom in order to reduce the system of differential equations.

Initially we considered the boundary conditions at the shell. We had to match the interior with the exterior perturbations at the shell. We did that by computing the stress–energy tensor of the perturbed shell from the Israel junction conditions and kept terms in linear order in the perturbed modes. We did the same for the dilaton discontinuity. As we saw in the review chapter on the enhançon, the BPS shell is modelled by a collection of wrapped D6–branes over a two sphere. The natural choice is to use this model in order to calculate the stress–energy tensor of the perturbed shell. Of course this is valid as long as we keep the perturbations small, so that the branes do not get excited. The matching conditions for the perturbation modes were obtained by setting this brane stress–energy tensor equal to the stress–energy tensor calculated from supergravity. Finally we produced the three boundary conditions that we needed at the shell. It is remarkable that, although the location of the shell is also perturbed, we can use some of the diffeomorphism freedom to fix the coordinate position of the shell at the enhançon radius.

Having all the ingredients, perturbation equations and boundary conditions at the shell, we tried to find an instability using a Relaxation Method. This is a method for solving boundary value problems, as the one at hand. The differential equations are replaced by finite difference equations over a grid of points. A trial solution is used and then corrections are computed and added to it iteratively up until it finally 'relaxes' to the true solution, if one exists.

We studied these equations numerically for a wide range of the parameters r_2 and r_6, and failed to find a solution which rendered the shell unstable. Although the perturbation ansatz that we used is very restricted and we are far from proving gravitational stability of the extremal enhançon we believe that this result can be generalised. This is based on the fact that the extremal enhançon is a BPS object, conserving supersymmetry and in general such objects are believed to be stable. This result comes in support of the supergravity description of the enhançon shell as being made from wrapped D6–branes.

Finally we studied the $r_0 \to 0$ limit of the horizon branch with extra D2–branes. This is not exactly the same as the extremal enhançon with extra D2–branes. This can be seen from the stress–energy tensor calculated using the Israel junction conditions. We expect the shell to consist of $N - N'$ wrapped D6–branes and no extra D2–branes at all. However, such a model does not agree with the supergravity stress–energy tensor for the shell. We made a conjecture that we have some number $2(N - M)$ of unwrapped extra D2–branes, which do not couple with any Ramond–Ramond field. This could be the case if there is an equal number of extra D2–branes and anti–D2–branes. Although we can not explain the origin of the anti–D2–branes in this setup and the reason why they do not annihilate with the ordinary D2–branes, we use this setup in order to model the shell.

We derived the perturbation equations in the interior space. This time the interior was not flat as in the extremal case. Two out of the three modes decoupled and could be solved in terms of Whittaker functions. As in the original extremal case we calculated the stress–energy tensor using the Israel junction conditions and matched it with the stress–energy tensor from a model of $N - N'$ wrapped D6–branes plus the additional $2(M - N)$ D2–anti–D2–branes. We could not find an equally convenient set of boundary conditions at the shell, mainly because we could not solve analytically all of the perturbation equations in the interior. However calculations showed that the exterior modes can be written at the shell as functions of the interior modes without being functions of the position of the shell. The importance of this study is that even at this slightly more complicated version of the problem we were able to find a nice model to describe the degrees of freedom of the shell and use it to find the boundary conditions on the shell for the linear perturbations.

Before we continue to the study of the stability of the non–extremal enhançons, we must stress that the result from the stability analysis of the extremal enhançon does not settle the issue of stability. Although it is expected from supersymmetry that it is stable, we did not prove that it is stable. The perturbation ansatz that we used (4.1) is not the most general, so our analysis is incomplete.

Chapter 6

Non-extremal enhançon

In the review of the non-extremal enhançon in Chapter 3, we mentioned that there are actually two branches of solutions arising from an ambiguity of a choice of sign in the solution of the supergravity equations. One branch joins on to the extremal enhançon solution, the repulson singularity always lies outside the would-be horizon, and the geometry will be corrected by an enhançon shell; this is the shell branch. The other branch appears at a finite value of the mass and there is no repulson singularity. The solution has a regular horizon at $r = r_0$; this is the horizon branch. Depending on the number of extra D2–branes it may or may not have a shell outside the horizon.

The shell branch has two puzzling features, namely the exterior never contains an event horizon and in the large $K3$ volume limit it does not reproduce the expected non–extremal D6–branes. Taken together, the two statements above imply an interesting phase structure, with different solution families providing the physical description in different regimes of parameters. It would be interesting to see if there is a phase transition between the two branches. There might be a classical instability which could provide the mechanism for transitions between them.

In this chapter we will investigate further the physics of the non–extremal solutions in supergravity, improving our understanding of their structure. We will try to find such an instability extending the methods we used to study the stability of the extremal enhançon.

We will begin by discussing the thermodynamic aspects of the two branches. We will compare the entropies of the two solutions, and see that the horizon branch has larger entropy at large mass, as we would expect. We can also calculate the specific heat for the horizon branch; for the branch with a shell, the ambiguity in the division of energy between the shell and the black hole prevent us from obtaining a well-defined answer for the specific heat.

After discussing the thermodynamical properties of the two branches, we continue by investigating the stability of the horizon branch. Since there is no shell present we have only to take regular boundary conditions on the horizon. We will study numerically the system of coupled differential equations, describing the perturbation modes. We will show that the horizon branch solution is stable throughout the range of parameters.

Finally we turn to the shell branch of solutions. The shell branch of the non–extremal enhançon violates the Weak Energy Condition. We therefore regard that branch as completely unphysical; that is, we conclude that it does not model the geometry sourced by some collection of smeared branes for any values of the parameters, as we expect the fundamental D6-branes always to have positive energy densities. Thus we cannot study its stability.

6.1 Thermodynamics

We would like to briefly compare the behaviours of the two branches. The ADM energy density for these solutions is

$$E = \frac{(2r_0 + \hat{r}_2 + \hat{r}_6)}{4G}, \tag{6.1}$$

where G is Newton's constant. For the horizon branch, this gives

$$E_{hb} = \frac{1}{4G}\left(r_0 + \sqrt{\frac{r_0^2}{4} + r_2^2} + \sqrt{\frac{r_0^2}{4} + r_6^2}\right), \tag{6.2}$$

while for the shell branch,

$$E_{sb} = \frac{1}{4G}\left(r_0 - \sqrt{\frac{r_0^2}{4} + r_2^2} + \sqrt{\frac{r_0^2}{4} + r_6^2}\right). \tag{6.3}$$

The difference between the $r_0 = 0$ solutions is $\Delta E = |r_2|/2G$[1]. For $M < N$, we need to add this much energy to the extremal solution before we can get solutions on the horizon branch.

The entropy and temperature on the horizon branch are easily obtained from the metric (3.32)[2], giving

$$S_{hb} = \frac{A}{4G} = \frac{\pi r_0}{G}(r_0 + \hat{r}_2)^{3/8}(r_0 + \hat{r}_6)^{7/8}, \tag{6.4}$$

$$T_{hb} = \frac{1}{4\pi(r_0 + \hat{r}_2)^{1/2}(r_0 + \hat{r}_6)^{1/2}}. \tag{6.5}$$

For the shell branch, we must use the interior solution (3.38), which gives

$$S_{sb} = \frac{A}{4G} = \frac{\pi r_0'^2}{G} H_2(r_0')^{3/8} H_6(r_0')^{7/8}, \tag{6.6}$$

$$T_{sb} = \frac{1}{4\pi r_0'} \left(\frac{K(r_e)}{L(r_e) H_2(r_0') H_6(r_0')} \right)^{1/2}. \tag{6.7}$$

On the horizon branch, we see that the temperature is a monotonic function of r_0, and hence the specific heat is always negative. For the shell branch, we cannot evaluate the specific heat, as we do not know $r_0'(r_0)$.

The ambiguity in the interior solution on the shell branch prevents us from comparing the entropies of the two solutions for most values of the parameters. However, we can make a comparison at large energies, when $r_0 \gg r_2, r_6$. Then

$$E_{hb} \approx \frac{r_0}{2G}, \quad S_{hb} \approx \frac{\pi r_0^2}{G} \approx 4\pi G E_{hb}^2, \tag{6.8}$$

as for an uncharged black hole, while for the shell branch,

$$E_{sb} \approx \frac{r_0}{4G}, \quad S_{sb} \approx \frac{\pi r_0'^2}{G} \left(\frac{V_*}{V}\right)^{3/8} \approx 16\pi G E_{sb}^2 \frac{r_0'^2}{r_0^2} \left(\frac{V_*}{V}\right)^{3/8}. \tag{6.9}$$

Since $r_0' < r_0$ and V_*/V is a small parameter, we conclude that the entropy is larger on the horizon branch at large mass. Thus, at least for large fixed mass, we would expect the horizon branch to dominate.

[1]This seems to fit nicely with the result obtained in Section 5.4.

[2]More details on the temperature calculation can be gound in Appendix D.

It would also be interesting to compare the entropies at fixed low temperature (so again $r_0 \gg r_2, r_6$). Unfortunately, this is not so straightforward. On the horizon branch,

$$T_{hb} \approx \frac{1}{4\pi r_0}, \quad S_{hb} \approx \frac{1}{16\pi G T_{hb}^2}, \tag{6.10}$$

but on the shell branch,

$$T_{sb} \approx \frac{1}{4\pi r_0'} \left(1 - \frac{r_0'}{r_e}\right)^{-1/2}, \tag{6.11}$$

so

$$S_{sb} \approx \frac{\pi r_0'^2}{G} \left(1 - \frac{r_0}{r_e}\right)^{3/8} \approx \frac{1}{16\pi G T^2} \left(1 - \frac{r_0}{r_e}\right)^{3/8} \left(1 - \frac{r_0'}{r_e}\right)^{-1}. \tag{6.12}$$

Thus, whether S_{sb} is smaller or larger than S_{hb} in this regime depends on how close r_0' can be to r_0. Surprisingly, if it is sufficiently close, S_{sb} can be the larger.

Thus, we see that thermodynamic considerations suggest that at least for large masses, the horizon branch should be the preferred one. Detailed investigation of the thermodynamics is hampered by the fact that we don't know how r_0' varies with r_0. Black hole thermodynamics depends on studying the static vacuum solutions as functions of the parameters, so the presence of an unphysical one-parameter ambiguity in our family of solutions is a serious impediment.

The thermodynamic structure here fits nicely with an interesting suggestion in [149]. In some cases, black hole solutions should exist only for temperatures greater than a critical value. We saw that for the non-extremal enhançon, solutions with a regular event horizon exist only for values of the non-extremality parameter greater than a critical value—that is, for sufficiently large energies. There also appears to be a maximum temperature for these solutions, but no minimum.

6.2 Horizon-branch stability

Let us study the perturbations for the horizon branch solutions. The appropriate boundary conditions are then just that the linearised perturbations should be regular on the horizon $r = r_0$ and at infinity. The solutions of the equations (5.3,5.8,5.13) behave as

$$\Phi, \Psi_2, \mathcal{Z}_6 \to (r - r_0)^{\pm\bar{\sigma}}, \bar{\sigma} = (r_0 + \hat{r}_2)^{1/2}(r_0 + \hat{r}_6)^{1/2}\sigma \tag{6.13}$$

as $r \to r_0$, and they behave as

$$\Phi, \Psi_2, \mathcal{Z}_6 \to e^{\pm\sigma r} \tag{6.14}$$

as $r \to \infty$. We wish to know if there is some σ such that we obtain a solution where $\Phi, \Psi_2, \mathcal{Z}_6$ all have decaying behaviour both at infinity and the horizon.

We have investigated this question numerically, using the same relaxation method as for the extremal case, to search for solutions satisfying the boundary conditions. We start from a trial solution satisfying the falloff conditions at the horizon and infinity, with a smooth interpolation with no nodes (as we are most interested in the instability with largest σ, which we would expect to have no nodes). We then relax $\Phi, \Psi_2, \mathcal{Z}_6, \sigma$ to see if we can reach a solution of the equations of motion. We have explored a wide range of the free parameters $\hat{r}_6, \hat{r}_2, r_0$ of the background solution, and we never find any instability. The relaxation process fails to converge.

This is the expected result for large non-extremality; in this limit, the horizon branch solutions approach a four-dimensional Schwarzschild metric smeared over the K3 and longitudinal x_1, x_2 directions, and this Schwarzschild metric is known to be stable against the kind of perturbations we are considering [196] (note that our perturbations are assumed independent of the longitudinal coordinates, so the Gregory-Laflamme instability [204, 205] which will appear if the x_1, x_2 are non-compact is absent from this analysis).

The non-trivial result is that this stability persists over the whole of the horizon branch. Thus, the linearised stability analysis has revealed no sign of any transition from this branch of solutions to any other solution as the mass decreases. This is very interesting; although it does not rule out such a transition, the horizon branch has passed the first test we could subject it to, and provides the best available description of the non-extremal enhançon physics in the region where it is available. This leads us to suspect that there is no other supergravity solution describing enhançon physics for the range of parameters where the horizon branch solution exists. In the next Chapter we will find that the horizon branch is the only solution of the supergravity equations preserving the appropriate charges and symmetries, with a horizon.

6.3 Shell branch violates weak energy condition

When we reviewed the shell branch of the non–extremal enhançon solutions we showed that there were two features of this solution which we could not explain. One was the fact that when the volume of the compactification manifold went to infinity, the solution instead of reproducing the usual unwrapped non–extremal D6–branes it reproduces a solution of non–extremal D6–branes with additional dilaton hair. One other fact was a free parameter r_0' which could not be specified by the physics of the shell.

In fact it turns out that it is not just this freedom to specify r_0' which is unphysical: the shell branch solution given above is unphysical for any value of r_0', as the stress tensor of the shell required to match the exterior and interior solutions violates the weak energy condition.

This is easily seen by considering the tt component of the stress tensor of the thin shell (3.60), resulting from the Israel junction conditions [129]:

$$2\kappa^2 S_{tt} = \frac{1}{\sqrt{G_{rr}}}\left[\frac{\hat{Z}_2'}{\hat{Z}_2} + \frac{\hat{Z}_6'}{\hat{Z}_6} + \frac{4}{r_{\rm i}}\left(1 - \sqrt{\frac{L(r)}{K(r)}}\right)\right] G_{tt} \tag{6.15}$$

This determines the energy density ρ of the thin shell, which scales as

$$\rho \sim -\frac{\hat{Z}_2'}{\hat{Z}_2} - \frac{\hat{Z}_6'}{\hat{Z}_6} + \frac{4}{r_{\rm i}}\left(\sqrt{\frac{L(r)}{K(r)}} - 1\right) \tag{6.16}$$

The second term is always positive, as $\hat{r}_6 > 0$, implying that $\hat{Z}_6' < 0$ (that is, $\hat{Z}_6$ is decreasing as r increases). We generally assume that $r_0' < r_0$, so $L(r) > K(r)$, implying that the third term is positive. However, for solutions on the shell branch, $\hat{r}_2 < 0$, so the first term is negative.

If we consider a shell at large radius,

$$\rho \sim \frac{\hat{r}_2 + \hat{r}_6 + 2(r_0 - r_0')}{r^2}, \tag{6.17}$$

and the negative contribution from $\hat{r}_2$ is always balanced by the positive contributions from the other terms, to give a positive answer. This is just another way of saying that the exterior solution has a positive ADM mass (in fact, its ADM mass is greater than the mass of the extremal solution).

However, this is not what we want to consider. The solution is only supposed to model physical D6-branes, by the argument reviewed in Chapter 3, if the radius of the shell is close to the enhançon radius (3.37). In the non-extremal case, the branes feel an attractive force in the exterior geometry [129], so they will again not stop until they start to smear out at the enhançon radius.

When we consider a shell at the enhançon radius, the energy density ρ will be negative. At the enhançon radius, $\frac{\hat{Z}_2}{\hat{Z}_6} = \frac{V_*}{V}$, so ρ in (6.16) can be rewritten as

$$\rho \sim \frac{\hat{r}_2}{r_{\rm e}} \frac{1}{\hat{Z}_2} \left(1 + \frac{V_*}{V} \frac{\hat{r}_6}{\hat{r}_2}\right) + \frac{4}{r_{\rm e}} \left(\sqrt{\frac{L(r_{\rm e})}{K(r_{\rm e})}} - 1\right). \tag{6.18}$$

On the shell branch, $\hat{r}_2$ is negative, and $|\hat{r}_6/\hat{r}_2| < V/V_*$, so the first term is negative. When V_*/V is small, $\hat{Z}_2$ is small, and the first term will dominate over the second, so that the overall energy density of the shell will be negative. Now we need $V \gg V_*$ for this supergravity analysis to be relevant; so in the regime where this description is supposed to apply, the energy density of the shell is negative.

One can extend this discussion to consider solutions on the shell branch with additional D2-brane charge. The expression for the energy density of the shell becomes more complicated in this case, and we have not been able to find a simple argument that it will always be negative, but numerical investigation shows that the energy density of the shell is negative for all values of the parameters that we tried also in this more general case.

Thus, the weak energy condition is violated on the shell branch. Since the D6-branes which this shell is supposed to model have positive energy densities, this implies that the shell branch solution does not correctly describe small perturbations away from the enhançon solution.

One possibility is that this signals a breakdown of the thin-shell approximation for small departures from extremality. There is some evidence for this interpretation coming from the study of probe branes. In the BPS case considered previously, we had a moduli space of solutions of the classical equations of motion, and we argued that we could choose all the sources to lie at as small a radius as possible, justifying the thin shell picture. In thermal equilibrium at some non-zero temperature, the constituent branes will carry thermal kinetic energy, and it is not clear that the inter-brane interactions will be sufficient to restrain the branes within a narrow range in r. Near extremality, the average extra energy per brane scales as r_0/N, while the typical scale of the effective potential seen by a probe brane in the exterior region is $V_{eff} \sim r_0/r_e \sim r_0/N$, so it is not clear that branes in the enhançon shell will remain confined to a thin layer when we add some thermal energy.

6.4 Summary

In this chapter, we have investigated the physics of non-extremal enhançon solutions. We have found that the shell branch of non-extremal repulson solutions appears to be generically unphysical. The singularity in this solution cannot be removed by excising the region inside the enhançon radius and matching to a smooth interior across a physical enhançon shell. If we attempt to impose such a matching, the shell required to achieve it will violate the Weak Energy Condition. The puzzling features of the shell branch reviewed in Chapter 3, have found their explanation through this result. Since the supergravity solutions with these features violate the Weak Energy Condition, these properties do not represent the real physics of wrapped D6-branes.

Regarding the horizon branch, the numerical investigation showed that it is stable under the linearised perturbations described by the ansatz (4.1). Its stability persisted over a wide range of the parameters r_2, r_6 and r_0. This result comes as no surprise, just as in the extremal case. The reason is that the horizon branch resembles a four–dimensional Schwarzschild black hole (in the large mass limit) smeared over the $K3$ and the two longitudinal directions. Four–dimensional Schwarzschild is known to be stable under linear perturbations [196].

There is an interesting point in the stability analysis of the horizon branch. Because it is stable over the whole range of parameters, there is no potential instability which would signal the existence of a new family of solutions which might connect to the extremal enhançon. While this is not a proof, it is a plausible scenario.

What of small perturbations away from the extremal enhançon solution, where there is no horizon branch? We do not have a supergravity solution which describes them, but we do not feel this implies some pathology in the physics. It may be that the physics of non-extreme enhançons is not captured by a purely supergravity solution. They could involve non-trivial non-abelian gauge fields [147], or branes distributed in a 'thick shell' over some finite range in the radial coordinate. Alternatively, it may be that the appropriate solutions lie outside the ansatz we have considered here. So we need to find more general solutions describing non–extremal enhançons. This will be the subject of the next chapter.

Chapter 7

General enhançon solutions

In Chapter 3 we saw that there are non–extremal versions of the enhançon and it was noted that there are two different branches of solutions: the horizon branch, which always has a regular event horizon, and the shell branch, which always has an enhançon shell outside of the horizon (if any). The horizon branch approaches an uncharged black hole at large masses, so it is clearly physically relevant in this regime, but no solution on this branch exists for a finite range of masses above the BPS solution. Furthermore, the horizon branch solution does not exhibit the same physics as the extreme case, as it does not necessarily involve an enhançon shell. The shell branch, on the other hand, approaches the BPS solution as a parameter goes to zero, and always involves an enhançon shell. It thus represents a non-extremal generalisation of the singularity resolution in the BPS metric.

However, as shown in the previous chapter, this geometry is unphysical, as it violates the Weak Energy Condition (WEC). Thus, to find a non-extremal generalisation of the enhançon, we must look for more general solutions. A further motivation for looking for more general solutions is the confusing two-branch structure in the existing solutions: near extremality, the only solution is the shell branch, which smoothly approaches the BPS solution of [127]. However, far from extremality, we would expect the horizon branch, which approaches an uncharged black hole solution for large masses, to be the correct solution. The transition between these two branches is an important unresolved problem.

In this chapter, we will extend our investigation of non-extremal solutions, by finding the most general solution of the supergravity equations of motion with the correct symmetry and charges to correspond to a non-extremal enhançon solution. We will show that there are two families of asymptotically flat solutions, corresponding to extensions of the horizon branch and shell branch found previously. We demonstrate that the only solution with a regular event horizon is the horizon branch solution. Considering the shell branch, we will show that the general family of solutions we construct satisfies the WEC for certain ranges of parameters. We then discuss the additional input that would be required to fix these parameters to obtain a physical solution describing a real non-extreme generalisation of the enhançon.

We start by giving a brief description of the supergravity equations. We Kaluza–Klein reduce to four dimensions and specify an ansatz for the four dimensional solution. We write down the equations of motion for the metric components and the additional fields. Although it looks like a complicated system of differential equations, we can solve them analytically. We provide the most general solutions.

Then we try to see if there are any solutions to these equations that could look like enhançons. By imposing the appropriate boundary conditions we found the solutions that describe the horizon branch. Imposing regularity of the solution at the event horizon fixes the remaining free parameters, showing that the unique solution with a regular horizon is, as expected, the horizon branch solution.

Then we turn to the shell branch. Initially we study the extremal case. We find generalised solutions but they are not physical. We expect that the enhançon shell should be modelled by wrapped D6–branes over a two sphere, and studying the Israel junction conditions, we find that this model is correct only for the original BPS solution.

Turning to the non–extremal case, we find general solutions with additional hair. The freedom to add 'hair' to the exterior solution arises because the form of the shell stress tensor is not completely fixed. In this way we can circumvent the violation of the Weak Energy Condition that was the case for the original shell branch solution. Unfortunately, we need more input from physics beyond supergravity to determine the stress–energy tensor, which we do not have available for the non-extreme cases.

7.1 Supergravity equations

Our aim is to extend previous studies of the extreme and non–extreme enhançon solutions, by finding the most general solutions of the supergravity equations consistent with the appropriate symmetries. In this section, we will write the metric in a convenient way, and reduce the supergravity equations of motion to a simple system of equations for the free functions in the metric.

We want to describe a system built up from excited D-branes wrapped on K3. As usual, we will focus mainly on the case of D6-branes, to simplify formulae. We describe the results of the analysis for wrapped D4- and D5-branes at the end of this section. For D6-branes, we should consider ten-dimensional metrics which are static and have two flat non-compact directions and a compact K3 factor along the branes. We assume that the metric is independent of the non-compact longitudinal directions, and that only the overall volume of the K3 varies over the transverse space. It is then natural to proceed by Kaluza-Klein reducing from ten to four dimensions.

In ten dimensions, we have the Type IIA 10D supergravity action (in string frame)

$$\mathcal{S}_{10} = \frac{1}{2\kappa_{10}^2}\int d^{10}x\sqrt{-G_{10}}\left(e^{-2\Phi_{10}}\left[R_{10} + 4(\partial\Phi_{10})^2\right] - |F_{(2)}|^2 - |F_{(6)}|^2\right) . \qquad (7.1)$$

In Kaluza-Klein reducing, we write the ten-dimensional metric in an ansatz

$$dS_{10}^2 = dS_4^2 + e^B dx_{\|}^2 + e^{D/\sqrt{2}}ds_{K3}^2, \qquad (7.2)$$

where $dx_{\|}^2 = dx_1^2 + dx_2^2$ is a flat metric on the non-compact longitudinal directions, we assume that $F_{(6)} = f_2 \wedge \epsilon_{K3}$, where ϵ_{K3} is the volume form determined by the unit K3 metric ds_{K3}^2, and we assume that f_2 and $F_{(2)}$ are non-zero only in the four dimensions contained in dS_4^2. Then, following the classic technique of Maharana & Schwarz [221], we can obtain an action for the four-dimensional fields,

$$\begin{aligned} \mathcal{S}_4 &= \frac{1}{2\kappa_4^2}\int d^4x\sqrt{-G_4}(e^{-2\phi_4}\left[R_4 + 4(\partial\phi_4)^2 - \frac{1}{2}(\partial B)^2 - \frac{1}{2}(\partial D)^2\right]) &(7.3)\\ &\quad -e^{B+\sqrt{2}D}|F_2|^2 - e^{B-\sqrt{2}D}|f_2|^2), &(7.4)\end{aligned}$$

where the four-dimensional dilaton $\phi_4 = \Phi_{10} - B/2 - D/\sqrt{2}$. We can convert this 4D action to Einstein frame by writing

$$g_{\mu\nu} = e^{-2\phi_4} G_{\mu\nu}\,. \tag{7.5}$$

The result is

$$\begin{aligned} S_{4E} &= \frac{1}{2\kappa_4^2}\int d^4x\sqrt{-g_4}(R_{4E} - \frac{1}{2}(\partial\Phi_4)^2 - \frac{1}{2}(\partial B)^2 - \frac{1}{2}(\partial D)^2 & (7.6)\\ &-e^{B+\sqrt{2}D}|F_2|^2 - e^{B-\sqrt{2}D}|f_2|^2), & (7.7)\end{aligned}$$

where we have defined $\Phi_4 = 2\phi_4$ to obtain canonically normalised kinetic terms. Henceforth, we will work in Einstein frame for the 4D metric.

This process of Kaluza-Klein reduction has already led to one striking simplification: the dilaton is completely decoupled,

$$\nabla^2\Phi_4 = 0\,. \tag{7.8}$$

The other two scalars have slightly more complicated behaviour:

$$\nabla^2 B = e^B[|F_2|^2 e^{\sqrt{2}D} + |f_2|^2 e^{-\sqrt{2}D}], \tag{7.9}$$

$$\nabla^2 D = \frac{1}{\sqrt{2}} e^B[|F_2|^2 e^{\sqrt{2}D} - |f_2|^2 e^{-\sqrt{2}D}]\,. \tag{7.10}$$

The equations of motion for the gauge fields take the usual form,

$$\nabla_\mu(e^{B+\sqrt{2}D}F^{\mu\nu}) = 0, \quad \nabla_\mu(e^{B-\sqrt{2}D}f^{\mu\nu}) = 0. \tag{7.11}$$

We now wish to specify our ansatz for the four-dimensional metric. We assume that the metric is spherically symmetric in the three-dimensional space transverse to the branes, so the metric and scalar fields will only depend on the radial coordinate r in the transverse space. Thus, we take the metric ansatz

$$ds_{4E}^2 = -e^{2A(r)}dt^2 + e^{2C(r)}(dr^2 + r^2 d\Omega_2^2), \tag{7.12}$$

choosing an isotropic gauge for the radial coordinate. Since we wish to consider a system of D6-branes, which are magnetically charged under $F_{(2)}$, and carry an induced D2-brane charge, which is a magnetic charge under $F_{(6)}$, we take the ansätze for the field strengths to be

$$F_2 = Q_2\epsilon_{S^2}, \quad f_2 = q_2\epsilon_{S^2}, \tag{7.13}$$

where ϵ_{S^2} is the volume form corresponding to the unit sphere metric $d\Omega_2^2$. As the D2-brane charge arises from a curvature coupling of the D6-branes wrapped on K3, it is related to the D6-brane charge through $|q_2| = (V_*/V)|Q_2|$ [127]. These ansätze satisfy the gauge field equations of motion (7.11).

With this ansatz, the Einstein equations for the four-dimensional metric reduce to (where $'$ denotes ∂_r)

$$\begin{aligned} 2C'' + (C')^2 + \frac{4}{r}C' &= -\frac{1}{4}((\Phi_4')^2 + (B')^2 + (D')^2) \\ &\quad -\frac{1}{4}\frac{e^{B-2C}}{r^4}(e^{\sqrt{2}D}Q_2^2 + e^{-\sqrt{2}D}q_2^2), \end{aligned} \tag{7.14}$$

$$\begin{aligned} (C')^2 + \frac{2}{r}(C' + A') + 2A'C' &= \frac{1}{4}((\Phi_4')^2 + (B')^2 + (D')^2) \\ &\quad -\frac{1}{4}\frac{e^{B-2C}}{r^4}(e^{\sqrt{2}D}Q_2^2 + e^{-\sqrt{2}D}q_2^2), \end{aligned} \tag{7.15}$$

$$\begin{aligned} A'' + C'' + (A')^2 + \frac{1}{r}(A' + C') &= -\frac{1}{4}((\Phi_4')^2 + (B')^2 + (D')^2) \\ &\quad +\frac{1}{4}\frac{e^{B-2C}}{r^4}(e^{\sqrt{2}D}Q_2^2 + e^{-\sqrt{2}D}q_2^2), \end{aligned} \tag{7.16}$$

and the scalar equations become

$$\Phi_4'' + \Phi_4'(\frac{2}{r} + A' + C') = 0, \tag{7.17}$$

$$B'' + B'(\frac{2}{r} + A' + C') = \frac{1}{2}\frac{e^{B-2C}}{r^4}(e^{\sqrt{2}D}Q_2^2 + e^{-\sqrt{2}D}q_2^2), \tag{7.18}$$

and

$$D'' + D'(\frac{2}{r} + A' + C') = \frac{1}{\sqrt{2}}\frac{e^{B-2C}}{r^4}(e^{\sqrt{2}D}Q_2^2 - e^{-\sqrt{2}D}q_2^2). \tag{7.19}$$

We have reduced the problem of finding the general solution subject to the assumed symmetries to solving this system of equations for the five unknown functions A, B, C, D, Φ_4. This seems like a complicated coupled system of equations, but in fact it conceals some remarkable simplifications. If we introduce new functions $a(r) = A + C$, $c(r) = C + B/2$, (7.15) + (7.16) gives

$$a'' + (a')^2 + \frac{3}{r}a' = 0, \tag{7.20}$$

a completely decoupled equation for a. Similarly, (7.14)+(7.15)+(7.18) gives

$$c'' + c'\left[\frac{2}{r} + a'\right] + \frac{1}{r}a' = 0, \tag{7.21}$$

which can be rearranged to write

$$[c'r^2e^a]' = -re^a a'. \tag{7.22}$$

Similarly, (7.17) can be rewritten as

$$[\Phi_4' r^2 e^a]' = 0. \tag{7.23}$$

These equations are solvable once we know a. Furthermore, if we define $x_6 = -B - D/\sqrt{2}$ and $x_2 = -B + D/\sqrt{2}$, then $-2(7.18)$ $-\sqrt{2}(7.19)$ becomes

$$[x_6' r^2 e^a]' = -\frac{e^{a-2c}}{r^2} Q_2^2 e^{-2x_6}. \tag{7.24}$$

We choose to rewrite this as

$$r^2 e^a [x_6' r^2 e^a]' = -e^{2(a-c)} Q_2^2 e^{-2x_6}. \tag{7.25}$$

Similarly, $-2(7.18)$ $+\sqrt{2}(7.19)$ can be rewritten as

$$r^2 e^a [x_2' r^2 e^a]' = -e^{2(a-c)} q_2^2 e^{-2x_2}. \tag{7.26}$$

We now have a much simplified system of equations in terms of the functions a, c, x_2, x_6, Φ_4. Before proceeding to solve these equations, let us express our ansatz for the ten-dimensional fields in terms of these variables for future reference:

$$\begin{aligned} dS_{10}^2 &= -e^{\Phi_4+2(a-c)} e^{-\frac{x_6}{2}-\frac{x_2}{2}} dt^2 + e^{-\frac{x_6}{2}-\frac{x_2}{2}} dx_{\|}^2 + e^{\Phi_4+2c} e^{\frac{x_6}{2}+\frac{x_2}{2}} (dr^2 + r^2 d\Omega_2^2) \\ &\quad + e^{\frac{x_2}{2}-\frac{x_6}{2}} ds_{K3}^2, \end{aligned} \tag{7.27}$$

with ten-dimensional dilaton

$$\Phi_{10} = \frac{\Phi_4}{2} + \frac{x_2}{4} - \frac{3x_6}{4} \tag{7.28}$$

and gauge fields

$$F_{(2)} = Q_2 \epsilon_{S^2}, \quad F_{(6)} = q_2 \epsilon_{S^2} \wedge \epsilon_{K3}. \tag{7.29}$$

Note the familiar way in which the functions x_2, x_6 appear in the metric and dilaton.

7.1.1 General solutions of the field equations

We now proceed to solve the equations. The solution of (7.20) is

$$a = \ln\left(1 - \frac{r_h^2}{r^2}\right) + C_1. \tag{7.30}$$

Then $r^2 e^a = (r^2 - r_h^2)e^{C_1}$, and we can easily see that the solution of (7.23) is

$$\Phi_4 = A_1 \ln\left(\frac{r + r_h}{r - r_h}\right) + C_2, \tag{7.31}$$

and (7.22) is solved by

$$c = 2\ln\left(1 + \frac{r_h}{r}\right) + A_2 \ln\left(\frac{r + r_h}{r - r_h}\right) + C_3. \tag{7.32}$$

Then

$$e^{2(a-c)} = \frac{r^4}{(r + r_h)^4}\left(\frac{r - r_h}{r + r_h}\right)^{2A_2} e^{-2C_3}\left(\frac{r^2 - r_h^2}{r^2}\right)^2 e^{2C_1} = \left(\frac{r - r_h}{r + r_h}\right)^{2(A_2+1)} e^{2(C_1 - C_3)}. \tag{7.33}$$

Plugging this into (7.25) gives

$$(r^2 - r_h^2)\partial_r((r^2 - r_h^2)\partial_r x_6)e^{2x_6} = -Q_2^2 e^{-2C_3}\left(\frac{r - r_h}{r + r_h}\right)^{2(A_2+1)}, \tag{7.34}$$

and similarly

$$(r^2 - r_h^2)\partial_r((r^2 - r_h^2)\partial_r x_2)e^{2x_2} = -q_2^2 e^{-2C_3}\left(\frac{r - r_h}{r + r_h}\right)^{2(A_2+1)}. \tag{7.35}$$

These are non-linear equations, but nonetheless they have a closed-form solution. To solve them, it is convenient to introduce a new independent variable,

$$z = \ln\left(\frac{r - r_h}{r + r_h}\right), \tag{7.36}$$

so that these equations become

$$\partial_z^2 x_6 e^{2x_6} = -\frac{Q_2^2 e^{-2C_3}}{4r_h^2} e^{2(A_2+1)z}, \tag{7.37}$$

$$\partial_z^2 x_2 e^{2x_2} = -\frac{q_2^2 e^{-2C_3}}{4r_h^2} e^{2(A_2+1)z}. \tag{7.38}$$

The general solutions of these equations is

$$x_6 = \ln\left(\alpha - \frac{Q_2^2 e^{-2C_3}}{16r_h^2(A_2 + \gamma + 1)^2\alpha} e^{2(A_2+\gamma+1)z}\right) - \gamma z, \tag{7.39}$$

$$x_2 = \ln\left(\beta - \frac{q_2^2 e^{-2C_3}}{16r_h^2(A_2 + \kappa + 1)^2\beta} e^{2(A_2+\kappa+1)z}\right) - \kappa z. \tag{7.40}$$

7.1.2 Other cases

We can carry out a similar analysis for the cases of D4-branes wrapped on K3 in IIA and D5-branes wrapped on K3 in IIB. We will just briefly state the results, pointing out a few minor differences relative to the D6-brane case discussed in detail above.

For the D4-branes, we write the ten-dimensional string frame metric in the form

$$\begin{aligned} dS_{10}^2 &= -e^{2a-6c}e^{-\frac{x_4}{2}-\frac{x_0}{2}}dt^2 + e^{2c}e^{\frac{x_4}{2}+\frac{x_0}{2}}(dr^2 + r^2 d\Omega_4^2) \\ &+e^{\frac{x_0}{2}-\frac{x_4}{2}}ds_{K3}^2, \end{aligned} \tag{7.41}$$

and write the ten-dimensional dilaton as

$$\Phi_{10} = -\frac{x_4}{4} + \frac{3x_0}{4} \tag{7.42}$$

and gauge fields as

$$F_{(4)} = Q_4 \epsilon_{S^4}, \quad F_{(8)} = q_4 \epsilon_{S^4} \wedge \epsilon_{K3}. \tag{7.43}$$

We then obtain simple equations for the functions a, c, x_4, x_0, as in the previous case. Note that the absence of any unwrapped directions along the brane implies that there is one less scalar field in the dimensional reduction here; it is the decoupled scalar that we lose.

The general solution is

$$a(r) = \ln\left(1 - \frac{r_h^6}{r^6}\right) + C_1\,, \tag{7.44}$$

$$c(r) = \frac{1}{3}\left[2\ln\left(1 + \frac{r_h^3}{r^3}\right) + A_1 \ln\left(\frac{r^3 + r_h^3}{r^3 - r_h^3}\right) + C_2\right], \tag{7.45}$$

$$x_4(r) = \ln\left(\alpha - \frac{Q_4^2 e^{-2C_2}}{144 r_h^6 (A_1 + \gamma + 1)^2 \alpha} e^{2(A_1+\gamma+1)z}\right) - \gamma z\,, \tag{7.46}$$

$$x_0(r) = \ln\left(\beta - \frac{q_4^2 e^{-2C_2}}{144 r_h^6 (A_1 + \kappa + 1)^2 \beta} e^{2(A_1+\kappa+1)z}\right) - \kappa z, \tag{7.47}$$

where

$$z = \ln\left(\frac{r^3 - r_h^3}{r^3 + r_h^3}\right). \tag{7.48}$$

For the case of D5-branes in type IIB, we write the ten-dimensional string frame metric in the form

$$\begin{aligned} dS_{10}^2 &= -e^{2\varphi+2a-4c}e^{-\frac{x_5}{2}-\frac{x_1}{2}}dt^2 + e^{-\frac{x_5}{2}-\frac{x_1}{2}}dx^2 + e^{2\varphi+2c}e^{\frac{x_5}{2}+\frac{x_1}{2}}(dr^2 \\ &+r^2 d\Omega_3^2) + e^{\frac{x_1}{2}-\frac{x_5}{2}}ds_{K3}^2; \end{aligned} \tag{7.49}$$

where x is the single unwrapped brane direction, and write the ten-dimensional dilaton as

$$\Phi_{10} = \frac{3}{2}\varphi - \frac{x_5}{2} + \frac{x_1}{2} \tag{7.50}$$

and gauge fields as

$$F_{(3)} = Q_3 \epsilon_{S^3}, \quad F_{(7)} = q_3 \epsilon_{S^3} \wedge \epsilon_{K3}. \tag{7.51}$$

We then obtain simple equations for the functions a, c, φ, x_5, x_1. In this case, the combination φ which decouples is not the same as the five-dimensional dilaton.

The general solution is

$$\begin{aligned}
a(r) &= \ln\left(1 - \frac{r_h^4}{r^4}\right) + C_1\,, & (7.52)\\
\varphi(r) &= A_1 \ln\left(\frac{r^2 + r_h^2}{r^2 - r_h^2}\right) + C_2 & (7.53)\\
c(r) &= \frac{1}{2}\left[2\ln\left(1 + \frac{r_h^2}{r^2}\right) + A_2 \ln\left(\frac{r^2 + r_h^2}{r_2 - r_h^2}\right) + C_3\right]\,, & (7.54)\\
x_5(z) &= \ln\left(\alpha - \frac{Q_3^2 e^{-2C_3 - C_2}}{64 r_h^4 (A_2 + A_1 + \gamma + 1)^2 \alpha} e^{2(A_2 + A_1 + \gamma + 1)z}\right) - \gamma z\,, & (7.55)\\
x_1(z) &= \ln\left(\beta - \frac{q_3^2 e^{-2C_3 - C_2}}{64 r_h^4 (A_2 + A_1 + \kappa + 1)^2 \beta} e^{2(A_2 + A_1 + \kappa + 1)z}\right) - \kappa z\,, & (7.56)
\end{aligned}$$

where

$$z = \ln\left(\frac{r^2 - r_h^2}{r^2 + r_h^2}\right)\,. \tag{7.57}$$

We see that the solutions obtained in both these cases are very similar in form to the case of D6-branes.

7.2 New enhançons?

In the last section, we found the general solution of the supergravity equations of motion subject to the symmetries associated with an enhançon-like solution. The solution has a simple closed form. It generalises the known solutions, introducing a number of constants of integration. We would now like to see if this leads to any new physical enhançon solutions.[1] We will just discuss the D6-brane case; the other

[1] Note that we have not introduced any enhançon shells, so at this stage we are really looking for more general analogues of the repulson solution—that is, what we are discussing is the solution exterior to any enhançon shell.

cases will clearly be very similar.

We first need to impose the condition of asymptotic flatness, which will fix some of the constants. To impose asymptotic flatness, we require that all the functions fall off as $1/r$ at large r. In the case of Φ_4, this corresponds to a choice of gauge, defining the ten-dimensional dilaton so that $\Phi_{10}(\infty) = 0$. Examining (7.30,7.31,7.32), we see that this fixes $C_1 = C_2 = C_3 = 0$. From (7.39,7.40), we obtain non-trivial equations for α and β,

$$\alpha - \frac{Q_2^2}{16r_h^2(A_2+\gamma+1)^2\alpha} = 1, \tag{7.58}$$

$$\beta - \frac{q_2^2}{16r_h^2(A_2+\kappa+1)^2\beta} = 1, \tag{7.59}$$

with solutions

$$\alpha = \frac{1}{2}(1 \pm \sqrt{1+\frac{Q_2^2}{4r_h^2(A_2+\gamma+1)^2}}), \quad \beta = \frac{1}{2}(1 \pm \sqrt{1+\frac{q_2^2}{4r_h^2(A_2+\kappa+1)^2}}). \tag{7.60}$$

It turns out to be convenient to rewrite these as

$$\alpha = \frac{1}{4r_h(A_2+\gamma+1)}\left(2r_h(A_2+\gamma+1) \pm \sqrt{Q_2^2+4r_h^2(A_2+\gamma+1)^2}\right), \tag{7.61}$$

$$\beta = \frac{1}{4r_h(A_2+\kappa+1)}\left(2r_h(A_2+\kappa+1) \pm \sqrt{q_2^2+4r_h^2(A_2+\kappa+1)^2}\right). \tag{7.62}$$

Thus, the most general asymptotically flat solution is

$$a = \ln\left(1-\frac{r_h^2}{r^2}\right), \tag{7.63}$$

$$\Phi_4 = A_1 \ln\left(\frac{r+r_h}{r-r_h}\right), \tag{7.64}$$

$$c = 2\ln\left(1+\frac{r_h}{r}\right) + A_2 \ln\left(\frac{r+r_h}{r-r_h}\right), \tag{7.65}$$

$$x_6 = \ln\left(\alpha-(\alpha-1)\left(\frac{r+r_h}{r-r_h}\right)^{-2(A_2+\gamma+1)}\right) + \gamma\ln\left(\frac{r+r_h}{r-r_h}\right), \tag{7.66}$$

$$x_2 = \ln\left(\beta-(\beta-1)\left(\frac{r+r_h}{r-r_h}\right)^{-2(A_2+\kappa+1)}\right) + \kappa\ln\left(\frac{r+r_h}{r-r_h}\right), \tag{7.67}$$

with α and β given by (7.61,7.62).

To begin to analyse the physics of these solutions, we note that there are two kinds of potential singularities in the solution (7.63-7.67). There is a singularity at

$r = r_h$, where $a \to -\infty$, and other functions may diverge. Since $a \to -\infty$ gives $g_{00} \to 0$ in (7.27), this singularity could correspond to an event horizon, if we choose other constants of integration appropriately. However, there is another possible singularity; if we choose the lower sign in either (7.61) or (7.62), there will be a singularity in (7.66) or (7.67) respectively at some $r > r_h$. This type of singularity is the analogue of the repulson singularity in the original enhançon story [127]. We see that, as in the discussion of non–extreme enhançons in [129], it arises from a discrete choice: there are different branches of solutions. Henceforth, we will assume that we take the positive sign in (7.61), and we will refer to the solution where we take the positive sign in (7.62) as the horizon branch, and to the solution where we take the negative sign in (7.62) as the shell branch. The shell branch solutions will only be valid outside of an enhançon shell.[2]

7.2.1 Uniqueness of the horizon branch

Addressing first the horizon branch, we will see that the only solution where the coordinate singularity at $r = r_h$ is a regular event horizon is the horizon branch solution found previously in [129]. For $r = r_h$ to be a regular horizon, we clearly need the ten-dimensional dilaton Φ_{10} to remain finite at $r = r_h$. We should also require that the volume of the two-sphere and K3 components of the metric remain finite there, to avoid any diverging curvature invariants. Furthermore, we must require that the factor in front of the $dx_{\|}^2$ directions remain finite: as argued in [222], a divergence of such a component may not lead to diverging curvature invariants, but it does cause a divergence in components of the curvature in a suitable orthonormal frame. Taken together, these conditions require that c, Φ_4, x_2 and x_6 are finite at $r = r_h$. That is, they impose $A_1 = A_2 = \gamma = \kappa = 0$.

[2]Solutions on the horizon branch do not have a repulson singularity, but they may nonetheless have a non-trivial enhançon shell appearing in them, if the $K3$ volume in (7.27) reaches string-scale outside the horizon (see [129] for details). We will ignore this issue in what follows; similar general remarks to those we make for the non–extremal solutions on the shell branch will apply in this case.

Thus, we have a unique solution with a regular horizon. It has

$$a = \ln\left(1 - \frac{r_h^2}{r^2}\right), \Phi_4 = 0, c = 2\ln\left(1 + \frac{r_h}{r}\right), \tag{7.68}$$

$$x_6 = \ln\left(\alpha - (\alpha - 1)\left(\frac{r + r_h}{r - r_h}\right)^{-2}\right) = \ln\left(\frac{r^2 + (Q_2^2 + 4r_h^2)^{1/2} r + r_h^2}{(r + r_h)^2}\right), \tag{7.69}$$

$$x_2 = \ln\left(\beta - (\beta - 1)\left(\frac{r + r_h}{r - r_h}\right)^{-2}\right) = \ln\left(\frac{r^2 + (q_2^2 + 4r_h^2)^{1/2} r + r_h^2}{(r + r_h)^2}\right), \tag{7.70}$$

where in the above we have used the values of α, β from (7.61,7.62), taking the positive sign in both equations. Using (7.27), this can be easily shown to be identical to the horizon branch solution (3.32) written in isotropic coordinates.

Thus, we find that the unique solution consistent with the symmetries we expect the enhançon to have possessing a regular event horizon is the horizon-branch solution found before. This is perhaps not a surprising result, but it is quite satisfying to be able to extend the analysis of a particular ansatz undertaken in [129] to a consideration of the most general form of non–extreme enhançon metric.

7.2.2 Shell branch: Extremal solutions

We turn now to a discussion of the shell branch. As usual in discussions of the enhançon mechanism, it is useful to first consider the extreme case, and then extend this to non–extreme solutions. Let us therefore consider what happens to the general solution (7.63-7.67) if we take $r_h = 0$.

This will depend on how we take the limit. If we take $r_h \to 0$ with A_1, A_2, κ, γ held fixed, then we recover the usual extremal solution. We will get $a = \Phi_4 = c = 0$,

$$\alpha \approx \frac{|Q_2|}{4r_h(A_2 + \gamma + 1)}, \quad \beta \approx \frac{-|q_2|}{4r_h(A_2 + \kappa + 1)} \tag{7.71}$$

(recalling that we are considering the shell branch, so we take the negative sign in (7.62)), which gives

$$x_6 \approx \ln\left(1 + \alpha\frac{4(A_2 + \gamma + 1)r_h}{r}\right) \approx \ln\left(1 + \frac{|Q_2|}{r}\right), \tag{7.72}$$

$$x_2 \approx \ln\left(1 + \beta\frac{4(A_2 + \kappa + 1)r_h}{r}\right) \approx \ln\left(1 - \frac{|q_2|}{r}\right), \tag{7.73}$$

which gives us the exterior metric of the BPS enhançon solution of [127].

On the other hand, we could take the limit $r_h \to 0$ with $\tilde{A}_1 = A_1 r_h$ etc held fixed, which will give a more general extremal solution. This still has $a = 0$, but now

$$c = \frac{2\tilde{A}_2}{r}, \tag{7.74}$$

$$\Phi_4 = \frac{2\tilde{A}_1}{r}, \tag{7.75}$$

and

$$x_6 = \ln\left(\alpha - (\alpha - 1)e^{\frac{-4(\tilde{A}_2+\tilde{\gamma})}{r}}\right) + 2\frac{\tilde{\gamma}}{r} \tag{7.76}$$

$$x_2 = \ln\left(\beta - (\beta - 1)e^{\frac{-4(\tilde{A}_2+\tilde{\kappa})}{r}}\right) + 2\frac{\tilde{\kappa}}{r}. \tag{7.77}$$

In this limit, (7.61,7.62) become

$$\alpha = \frac{1}{4(\tilde{A}_2 + \tilde{\gamma})}\left(2(\tilde{A}_2 + \tilde{\gamma}) + \sqrt{Q_2^2 + 4(\tilde{A}_2 + \tilde{\gamma})^2}\right), \tag{7.78}$$

$$\beta = \frac{1}{4(\tilde{A}_2 + \tilde{\kappa})}\left(2(\tilde{A}_2 + \tilde{\kappa}) - \sqrt{q_2^2 + 4(\tilde{A}_2 + \tilde{\kappa})^2}\right). \tag{7.79}$$

These additional solutions look similar to the exterior solution in the familiar BPS enhançon to some extent; they have a singularity at some $r > 0$, where $x_2 \to -\infty$, implying that the volume of the K3 goes to zero. We wish to ask if we can build a physical solution where this singularity is resolved. To resolve the singularity, we need to be able to consistently excise the region inside the radius where the K3 volume reaches the self-dual point, replacing it with flat space by introducing a shell of branes at this radius.

If we consider the junction between this solution and flat space, we can define the shell stress tensor in terms of the discontinuity in the extrinsic curvature [129, 193], as we did in Chapter 3.

Assuming the interior metric is flat, $K^-_{AB} = 0$, so $\gamma_{AB} = K^+_{AB}$. The components of the stress tensor for a general metric of the form (7.27) are then

$$S_{tt} = \frac{1}{\kappa^2\sqrt{G_{rr}}}(4c' + x_2' + x_6')G_{tt}, \tag{7.80}$$

$$S_{\mu\nu} = \frac{1}{\kappa^2\sqrt{G_{rr}}}(2a' + 2c' + \Phi_4' + x_2' + x_6')G_{\mu\nu}, \tag{7.81}$$

$$S_{ij} = \frac{1}{\kappa^2\sqrt{G_{rr}}} 2a' G_{ij}, \tag{7.82}$$

$$S_{ab} = \frac{1}{\kappa^2\sqrt{G_{rr}}} (2a' + 2c' + \Phi_4' + x_6')G_{ab}, \tag{7.83}$$

where indices μ, ν run over the non-compact longitudinal directions, i, j run over the S^2 directions, and a, b run over the K3 directions. We thus see that $S_{ij} = 0$ for any solution with $r_h = 0$, as we would expect for an extremal solution.

Since the stress tensor in the sphere directions vanishes, it is natural to see what happens if we try to model the source for this shell by a collection of fundamental branes, generalising the BPS enhançon solution. The DBI action for wrapped D6-branes is the same as earlier (3.53) and plugging in the metric (7.27), we obtain

$$S = -\int d^3\xi e^{a-c}(\mu_6 e^{-x_6} - \mu_2 e^{-x_2}). \tag{7.84}$$

Since the action does not couple to the 4d dilaton Φ_4, it cannot source a discontinuity in this field; thus, we must set $\tilde{A}_1 = 0$. The action has a Lorentz symmetry relating the time direction and the non-compact spatial directions; we can therefore only use it as the source if the shell stress tensor also respects this symmetry, which forces us to set $\tilde{A}_2 = 0$. We are then just left with the terms coming from x_2' and x_6' in the stress-energy. If these are to be sourced by the brane action, these functions need to satisfy $x_2' e^{x_2} =$ constant, $x_6' e^{x_6} =$ constant. These constraints force us to set $\tilde{\gamma} = \tilde{\kappa} = 0$. This gives us back the usual BPS enhançon solution.

Thus, while we have found additional solutions with $r_h = 0$, these are not physical extreme enhançon solutions, in the sense that they do not correspond to the geometry sourced by a collection of BPS branes. Requiring that the shell stress tensor have the appropriate form to correspond to the brane sources completely fixes the constants of integration in the solution. That is, in the extreme case at least, our usual no-hair intuition continues to hold. The additional parameters do not actually correspond to a family of generalised physical solutions; the only truly physical solution is the usual one.

In passing, it is interesting to note the effect of the deformations in the more general solution on the asymptotics of the solution—in particular, on the ADM mass. If we just consider turning the $\tilde{\kappa}$ parameter on slightly, modifying the behaviour of

x_2, its asymptotics will be

$$e^{x_2} \approx \left(1 + \frac{4(\beta-1)\tilde{\kappa}}{r}\right)\left(1 + \frac{2\tilde{\kappa}}{r}\right). \tag{7.85}$$

Assuming $\tilde{\kappa} \ll q_2^2$,

$$\beta \approx \frac{-|q_2|}{4\kappa}\left(1 - 2\frac{\tilde{\kappa}}{|q_2|}\right), \tag{7.86}$$

so

$$e^{x_2} \approx 1 - \frac{|q_2|}{r} + \frac{4\tilde{\kappa}}{r}. \tag{7.87}$$

The effect of this will be that positive values of $\tilde{\kappa}$ increase the ADM mass. This teaches us two things: first, the solutions with $\tilde{\kappa} \neq 0$ are clearly not supersymmetric, since they do not saturate the BPS bound. Second, this suggests a potentially useful way to correct the problem with the WEC in the non–extreme case.

7.2.3 Shell branch: Non–Extremal solutions

Let us now consider the non–extreme shell branch, where we take $r_h \neq 0$. We have the freedom to consider any solution in the general family (7.63-7.67). However, in this section, we will focus just on the effects of turning on the parameter κ which modifies the behaviour of x_2. The philosophy underlying this approach is that we need to focus on a subset of the possible deformations to keep the formulae arising in the discussion of manageable complexity, and this seems to be the most natural deformation to consider, since it is x_2 which already has 'unusual' behaviour in any shell branch solution. We will show that turning on this deformation is sufficient to produce solutions which do not violate the WEC.

Let us first review the argument that the WEC is violated in the usual non-extremal shell branch solution using the notation of this chapter. The non-extremal solution considered in Chapter 6 is the special case of the general asymptotically flat solution (7.63-7.67) where $A_1 = A_2 = \gamma = \kappa = 0$, and we take the negative sign in (7.62). From the metric (7.27) we see that the enhançon radius is given by

$$e^{x_2 - x_6} = \frac{V_*}{V}. \tag{7.88}$$

For the non–extreme shell branch solution of [129] in our coordinates, this becomes

$$\frac{(\beta - (\beta-1)e^{2z})}{(\alpha - (\alpha-1)e^{2z})} = \frac{V_*}{V}. \tag{7.89}$$

We assume that we excise the portion of the solution inside this radius and replace it with either flat space or a horizon branch solution. There is then a discontinuity at this radius, corresponding to a shell whose stress tensor is calculated as in the extremal case in the previous subsection. Assuming the interior solution is still flat (which maximises the shell's contribution to the overall ADM mass), we see from (7.80) that the shell energy density is

$$\rho \propto -x_2' - x_6' - 4c'. \tag{7.90}$$

The x_6' and c' terms make positive contributions to the energy density. However, the choice of the negative sign in (7.62) implies that $\beta < 0$, and as a consequence the first term is negative;

$$-x_2' = -\frac{2(1-\beta)e^{2z}}{(\beta - (\beta-1)e^{-2z})}\partial_r z < 0. \tag{7.91}$$

To see that this negative term dominates, we first write the first two terms together, using (7.89),

$$-x_2' - x_6' = -\frac{2(1-\beta)e^{2z_e}}{(\beta-(\beta-1)e^{2z_e})}\left(1 - \frac{(\alpha-1)}{(1-\beta)}\frac{V_*}{V}\right)\partial_r z. \tag{7.92}$$

This expression is valid only at the enhançon radius $z = z_e$, where (7.89) is satisfied. Now

$$\frac{(\alpha-1)}{(1-\beta)} = \frac{\sqrt{Q_2^2+4r_h^2} - 2r_h}{\sqrt{q_2^2+4r_h^2}+2r_h} < \frac{V}{V_*}, \tag{7.93}$$

since $|Q_2|/|q_2| = V/V_*$. Thus, the first two terms together give a negative answer. Furthermore, for this supergravity analysis to be relevant, we need to assume that $V_* \gg V$, so that higher-order corrections involving the K3 curvature are suppressed. This implies by (7.89) that $(\beta - (\beta-1)e^{2z_e}) \ll 1$, so these terms will dominate over the remaining positive term, $-4c' = \frac{8r_h}{r_e(r_e+r_h)}$. Thus, $\rho < 0$, and the shell violates the WEC. The usual non–extreme enhançon solution thus cannot correspond to the geometry sourced by a physical collection of branes.

A primary motivation for looking for more general solutions was to see how general this problem is. We will now show that we can produce solutions where the shell satisfies the WEC by generalising to non-zero values of κ. First, we note that changing κ will change the enhançon radius; (7.88) now implies

$$\frac{(\beta-(\beta-1)e^{2(\kappa+1)z})}{(\alpha-(\alpha-1)e^{2z})}e^{-\kappa z} = \frac{V_*}{V}. \tag{7.94}$$

The first two terms in the energy density are then

$$-x_2' - x_6' = \left[\frac{2(\kappa+1)(\beta-1)e^{2(\kappa+1)z}}{(\beta-(\beta-1)e^{2(\kappa+1)z})} + \kappa + \frac{2(\alpha-1)e^{2z}}{(\alpha-(\alpha-1)e^{2z})}\right]\partial_r z. \tag{7.95}$$

Using (7.94), we can rewrite this as

$$-x_2' - x_6' = \frac{-2(\kappa+1)(1-\beta)e^{2(\kappa+1)z}}{(\beta-(\beta-1)e^{2(\kappa+1)z})}\left[1 - \frac{(\alpha-1)}{(\kappa+1)(1-\beta)}\frac{V_*}{V}e^{-\kappa z}\right]\partial_r z + \kappa\partial_r z. \tag{7.96}$$

In this generalisation, it is still true that

$$\frac{(\alpha-1)}{(\kappa+1)(1-\beta)} = \frac{\sqrt{Q_2^2+4r_h^2}-2r_h}{\sqrt{q_2^2+4(\kappa+1)^2r_h^2}+2(\kappa+1)r_h} < \frac{V}{V_*}. \tag{7.97}$$

However, this does not imply that the factor in square brackets in (7.95) is positive. For positive κ, the factor of $e^{-\kappa z} > 1$, and it can easily be made sufficiently large to make this factor negative, at least for small values of r_h. Note also that the additional $\kappa\partial_r z$ term is also acting in the same direction for positive κ. Thus, the contribution of the x_6' term can dominate over that of the x_2' term for suitable values of κ, leading to a shell stress energy which satisfies the WEC.[3]

However, we still have the problem that the solution depends on constants of integration, which seem to represent an unphysical freedom to modify the geometry. Simply imposing the WEC cannot completely fix the constants of integration in the solution. These parameters are best thought of as parameterising the shell stress tensor, and are not wholly fixed at the supergravity level, because supergravity on its own cannot completely determine the shell stress tensor. At the fundamental level, there should be a definite form for this stress tensor, which will fix these parameters (possibly up to some discrete choices). However, this will require some input from physics beyond supergravity, which provides a real microphysical model for the shell stress tensor, as the DBI action did in the BPS case.

Thus, we have a complete description of the solutions at the supergravity level which satisfy the appropriate symmetry assumptions, and we can see that some of them will satisfy the WEC, which is our primary physics constraint on them at this

[3]This seems a natural way to modify the solution to satisfy the WEC; however, other possibilities certainly exist. For example, turning on a positive γ will modify the stress-energy in a very similar way, and can also lead to solutions which satisfy the WEC.

level. However, since we do not have a microphysical model for the shells in the non–extremal cases, we cannot determine which (if any) of this family of solutions actually correspond to physical non–extreme generalisations of the enhançon mechanism.

7.3 Summary

We have been studying the extension of the enhançon mechanism to non-extremal, finite temperature geometries. There are non-extremal versions of the enhançon geometry, and there are two different branches of solutions: the horizon branch, which always has a regular event horizon, and the shell branch, which always has an enhançon shell outside of the horizon (if any).

In this chapter, we have extended this work by finding the most general solution consistent with the symmetries and charges associated with the enhançon. These solutions represent generalisations of the exterior geometry in the enhançon solution. One of the constants of integration, r_h, can be interpreted as a non-extremality parameter, so these are generally non-extremal solutions. We find that the branch structure noted in [129] and reviewed in Chapter 3 arises when we impose asymptotic flatness: this results in a quadratic equation for one of the constants of integration, with the two roots corresponding to the horizon branch and the shell branch.

Considering the horizon branch, and assuming that there is no shell outside of the horizon, we showed that imposing regularity of the solution at the event horizon fixes the remaining free parameters, showing that the unique solution with a regular horizon is, as expected, the horizon branch solution. This solution reduces to an uncharged black hole at large mass.

Considering the shell branch, we saw that we had a family of solutions at $r_h = 0$. On the shell branch, we are considering singular supergravity metrics (there is a delta-function singularity at the location of the shell), so we can no longer fix these constants of integration by imposing regularity of the solution. However, the only solution in this family for which the stress tensor of the shell inferred from the supergravity solution is of the form predicted for a collection of wrapped branes by the DBI action was the familiar BPS solution. Thus, we find that if we specify a particular form for the shell stress tensor, then as expected, there is no remaining freedom in the form of the solution; the solution is completely described by giving its conserved charges and ADM mass.

In the non-extreme case, the shell branch solution obtained in [129] is unphysical, as it violates the weak energy condition. We have shown that this problem can be circumvented by considering more general solutions. This provides us with a multi-parameter family of solutions which satisfy all the constraints on physical solutions at the supergravity level. This freedom to add 'hair' to the exterior solution arises because the form of the shell stress tensor is not completely fixed. Indeed, the four free parameters in the exterior solution correspond precisely to the freedom to specify three components of the shell stress tensor and the discontinuity in the dilaton, although the translation between the parameters and the stress tensor is quite non-trivial. (The freedom to specify the shell stress in the sphere directions, which is not affected by these parameters, corresponds to the further ambiguity previously noted in [129], in the division of the energy above extremality between the shell itself and a black hole inside the shell.) Thus, if we had a microphysical model of the shell, we would expect to be able to fix all of this freedom. However, this requires further input from physics beyond supergravity, which we do not have available for the non-extreme cases.

Let us reiterate the essential difference between the two branches: on the horizon branch, we seek a smooth supergravity solution. We can then determine the solution uniquely without requiring additional input, as it does not involve explicit sources. On the shell branch, the singularity can never be clothed by a horizon; we want to describe its resolution by the expansion of the branes sourcing the geometry. We cannot determine the appropriate geometry uniquely, as it involves explicit sources, and we do not have a fundamental description of those sources for the non-extremal case.

In fact, our lack of understanding of the non-extremal physics goes deeper: we cannot exclude the possibility that none of these solutions provide an appropriate physical description of a non-extremal enhançon. It is possible that the shell thickens once we add some energy to it, invalidating the thin-shell approximation used here;

alternatively, the non-abelian gauge fields which become light near the shell may become important (this may even lead to violations of spherical symmetry) [147].

Conclusion

One of the main problems of classical gravity and the theory by which it is described (General Relativity), is the existence of curvature singularities. One of the motivations of a quantum theory of gravity is the resolution of these singularities. By resolution we mean that quantum gravity should render as physical these singularities and explain the way we can do that. Nowadays string theory is the most promising candidate of a quantum theory of gravity. String theory has a way to resolve singularities in certain spaces such as orbifolds and conifolds. This happens because there are extra degrees of freedom, coming from the strings, which resolve the singularity. We would like to do something similar with other spacetime singularities.

A new mechanism for singularity resolution in string theory is the enhançon mechanism [127]. This resolves a class of singularities dubbed the repulson [223], [224]. This kind of spacetime preserves eight supercharges and has a naked singularity. A test particle feels a repulsive force near the singularity, hence the name repulson.

One can naively construct this spacetime using D–branes. In the prototype example [127], one uses D6–branes wrapped on a $K3$ manifold. This manifold has a non–trivial curvature which induces a negative D2–brane effective charge on the unwrapped part of the worldvolume [177]. This brane is a composite object with a modified effective tension, which can become zero or even negative. Using such an object as a probe we see that the effective tension becomes zero at a special value of the radius, called the enhançon radius, which is always 'outside' the singularity, and is negative below that radius. This means that the probe cannot move further to the origin. Trying to construct the repulson spacetime by bringing individual branes from infinity fails, because the branes cannot move further then the enhançon radius. At that radius they stop being pointlike, in the transverse directions, and smear around over a two-sphere forming a locus.

New degrees of freedom become massless at this locus which are not described by the supergravity. Since there are no brane sources in the interior of this locus the spacetime must be flat to a first approximation. Therefore, the repulson singularity gets excised as it was a remnant of the inability of the supergravity to describe the new light degrees of freedom. These are described by string theory and are needed in order to determine the correct geometry.

This excision is consistent with supergravity [129]. The stress–energy tensor of the thin shell, separating the interior flat space and the exterior repulson–like geometry, using Israel's junction conditions, is equal to the stress–energy tensor of a thin shell of wrapped D6–branes smeared over a two sphere. Although supergravity can not grasp the string physics needed to describe the enhançon mechanism properly, it displays some awareness of the behaviour of the branes that source this geometry.

Non–extremal generalisations of the enhançon can be written using the harmonic function rule. These are difficult to study from the string theory point of view, mainly because they break all the supersymmetry. There are two branches of solutions, arising from an ambiguity of a choice of sign in the solution of the supergravity equations. One branch has a regular horizon and it looks like a black hole with R–R charges. This branch, known as horizon branch, appears above a finite value of mass. The other branch always has a shell of branes outside the horizon and in the extremal limit joins on to the BPS solution. This is the shell branch. Different solution families provide the physical description in different regimes of parameters. There might be a classical instability which could provide the mechanism for transitions between them. This would an interesting phase structure of the dual gauge theory.

We can further examine the physics of the enhançon mechanism using supergravity. For this reason we study its stability under small linear perturbations. We can write down the most general radial perturbation ansatz that respects the symmetries of the extremal an non–extremal solutions. Of course this is still very limited but the instabilities that we expected to find were not breaking the symmetries of the enhançon solution. This ansatz produces an over determined system of equations, which we can simplify considerably by using some diffeomorphism invariance left, to determine a certain gauge.

We can also find more generalised supergravity solutions that describe non–extremal enhançon. We compactify supergravity on the $K3$ and the two longitudinal directions and solve the equations of motion for an ansatz that satisfies the symmetries of the enhançon.

Regarding the extremal enhançon both investigations give pleasing results. Starting from the stability analysis, we find that it is , for the whole range of parameters, stable under perturbations described by a sufficiently general but still quite limited ansatz. This strengthens the case of the excision. Although far from completely proving gravitational stability, we believe on the ground of supersymmetry that this solution will be stable. The extremal enhançon shell is constructed by BPS objects and we expect this to be stable.

The initial enhançon solution was first written using the harmonic function rule, that is using a restricted ansatz for the metric. Actually the supergravity equations of motion can be solved explicitly, with the appropriate conditions, and give a family of extremal solutions resembling the enhançon. The only solution in this family, for which the stress tensor of the shell inferred from the supergravity solution, is of the form predicted for a collection of wrapped branes by the DBI action, was the familiar BPS solution.

So the enhançon solution not only is consistent with supergravity, but it is also a unique solution of the equations of motion. This solution is supersymmetric, so it seems that supergravity can grasp the physics, without any additional data from string theory.

As for the horizon branch the situation is almost similar. A numerical investigation has shown that it is stable, under perturbations described by a quite general ansatz. Again this is something expected, because for very large masses, the horizon branch looks like a four–dimensional Schwarzschild black hole smeared over the $K3$ and longitudinal directions, and we know this to be stable.

What is quite interesting is that stability of the horizon branch persists over the whole range of parameters. An instability of the horizon branch could have been interpreted as evidence for the existence of a new family of solutions, which might connect to the extremal enhançon solution. While absence of evidence is not evidence of absence, the stability of the horizon branch makes it seem plausible that it provides the full description of non-extremal enhançon physics for the range of parameters where it exists.

We can find generalised solutions of the horizon branch, by solving the equations of motion. If we assume that there is no shell outside the horizon, then the unique solution is the horizon branch. All the free parameters are fixed once we impose regularity of the solution at the event horizon.

In order to understand the horizon branch better, we can add extra D2-branes and take the extremal limit. In this limit there is an enhançon shell. We can model it by wrapped D6–branes. As we saw earlier, when extra D2–branes are present, some of the wrapped D6–branes are allowed to move in the interior. A straightforward calculation of the Israel junction conditions shows that the stress–energy tensor of the shell is not exactly that of the wrapped D6–branes. It seems as if there are also pairs of D2 and anti–D2–branes, which contribute. There is a finite difference in the energy in the extremal limit of the shell and the horizon branches of solutions. It might be that such a difference could be explained by such an argument. Unfortunately there is no physical interpretation of the existence of these pairs. This is just a conjecture based on the results of a supergravity calculation, which lacks any physical input.

Supergravity also succeeds in describing the horizon branch as it did for the extremal enhançon. Unfortunately this is not the case with the shell branch of solutions.

The shell branch has various puzzling features. First the solution depends on a free parameter r_0', which can not be calculated from the other parameters of the solution. We do not know the physics of the shell in this case in order to determine it. A more important problem is that in the large $K3$ volume limit the solution does not reproduce the unusual non–extremal D6–branes.

The shell branch of non-extremal repulson solutions appears to be generically unphysical. If we remove the singularity in this solution by excising the region inside the enhançon radius and matching to a smooth interior across an enhançon shell, then this shell violates the Weak Energy Condition.

We can find more general solutions of the shell branch of the non–extremal solutions. These solutions have additional parameters ('hair') which can be used in order to solve the problem of the WEC violation. The freedom to add hair in these solutions comes from the fact that the stress–energy of the shell is not completely fixed. We do not have a fundamental description of the physics of the shell in this case, which could determine all parameters. This requires information from physics beyond the reach of supergravity, which is not available for non–extremal cases.

In fact it is possible that the thin-shell approximation breaks down for small departures from extremality. There is some evidence coming from the study of probe branes. In the BPS case considered previously, we had a moduli space of solutions of the classical equations of motions, and we argued that we could choose all the sources to lie at as small a radius as possible, justifying the thin shell picture. In thermal equilibrium at some non-zero temperature, the constituent branes will carry thermal kinetic energy, and it is not clear that the inter-brane interactions will be sufficient to restrain the branes within a narrow range. It is not clear that branes in the enhançon shell will remain confined to a thin layer when we add some thermal energy.

Thus we conclude the study of the enhançon mechanism in general and the non–extremal enhançon in particular. We found that the extremal enhançon solution and the horizon branch of the non–extremal solution are unique solutions and moreover stable to small linearised perturbations. Although the ansatz that we used was quite restricted, this results were expected and can, we think, be trusted.

Regarding the shell branch of the non–extremal enhançon solution, we saw that the initial solution [127], [129] is unphysical because it violates the Weak Energy Condition. We constructed more general solutions and saw that this problem can be circumvented by the addition of 'hair' at the exterior. Unfortunately, we can not say anything more on the subject because we do not understand the physics of the shell completely.

So there go our hopes to try and use supergravity to understand non–extremal solutions. Regarding the extremal enhançon, supergravity described the wrong solution but still one could see that the excision was sensible from its point of view. It did not describe or explain the physics behind the excision but one could use supergravity arguments to see that it is consistent. In the case of the shell branch of the non–extremal enhançon, supergravity alone is unable to give even a solution to the problem.

It is also worth noting that our study of more general solutions has not resolved the issue of the branch structure and phase transitions. Assuming the near-extremal behaviour is described by some shell branch solution, while the behaviour at large masses should be described by the horizon branch, one expects that there will be some phase transition between the two branches as a function of mass. Unfortunately, since we are unable to identify the correct shell branch solution on the basis of supergravity information alone, we cannot even set up the problem of studying this phase transition.

Appendix A

The $K3$ manifold

A.1 Features of the $K3$

$K3$ is a four dimensional, Ricci flat, simply connected, compact Kähler manifold with $SU(2)$ holonomy [225]. It has the orbifolds $T^4/\mathbb{Z}_N$, $N \in 2,3,4,6$ as geometrical limits [226, 227]. It contains one four–cycle and twenty two independent two–cycles. Nineteen of them are self–dual and three are anti–self–dual.

Although the metric of the $K3$ is not known, the properties of the manifold can be determined. Such a quantity which we will use later is the Euler characteristic which can be computed using the orbifold limits of the manifold,

$$\begin{aligned}
\chi(K3) &= \frac{1}{32\pi^2}\int_{K3}\sqrt{g}\left(R_{abcd}R^{abcd} - 4R_{ab}R^{ab} + R^2\right) \\
&= \frac{1}{32\pi^2}\int_{K3}\sqrt{g}\epsilon_{abcd}R^{ab}R_{cd} \\
&= -\frac{1}{16\pi^2}\int_{K3}\mathrm{Tr}R\wedge R \\
&= 24. \qquad \text{(A.1.1)}
\end{aligned}$$

A.2 Type IIA on $K3$

Compactification of type IIA superstrings on K3 breaks half of the supersymmetry and gives the following massless fields. The six–dimensional metric $g_{\mu\nu}$ and anti-symmetric tensor field $B_{\mu\nu}$ from direct dimensional reduction of the NS–NS sector. From the R–R sector we get the one-form $C_{(1)}$ and three–form $C_{(3)}$. In addition we have fields coming from the dimensional reduction on the various cycles of the manifold. Starting with the ten–dimensional R–R three–form we get twenty two six–dimensional one–forms by integrating on the various two cycles of the $K3$. In six dimensions a three–form field is dual to a one–form field. In total we have twenty four massless one–form fields in six dimensions. In addition we get eighty one scalars: fifty eight moduli parameterising the $K3$ metric (corresponding to independent deformations of Kähler structure and complex structure), twenty two moduli from integrating the B-field over twenty two two-cycles, and finally the dilaton.

Appendix B

Type IIA Supergravity

The bosonic part of the type IIA action in Einstein frame is

$$\frac{1}{2\kappa^2}\int d^{10}x(-G)^{1/2}R - \frac{1}{4\kappa^2}\int\Big(d\Phi\wedge *d\Phi + g_s e^{-\Phi}H_3\wedge *H_3$$
$$+g_s^{1/2}e^{3\Phi/2}F_2\wedge *F_2 + g_s^{3/2}e^{\Phi/2}\tilde{F}_4\wedge *\tilde{F}_4 + g_s^2 B_2\wedge F_4\wedge F_4\Big), \qquad \text{(B.0.1)}$$

where

$$\tilde{F}_4 = F_4 - C_1\wedge H_3 \quad , \quad F_4 = dC_3 \quad , \quad F_2 = dC_1. \qquad \text{(B.0.2)}$$

We define the Einstein metric by $(G_{\mu\nu})_{\mathrm{Einstein}} = g_s^{1/2}e^{-\Phi/2}(G_{\mu\nu})_{\mathrm{string}}$. As a result g_s appears in the action, explicitly and also through $2\kappa^2 = (2\pi)^7\alpha'^4 g_s^2$. The field equations are [228]

$$\begin{aligned}
d{*}d\Phi &= -\frac{g_s e^{-\Phi}}{2}H_3\wedge *H_3 + \frac{3g_s^{1/2}e^{3\Phi/2}}{4}F_2\wedge *F_2 + \frac{g_s^{3/2}e^{\Phi/2}}{4}\tilde{F}_4\wedge *\tilde{F}_4 \\
d(e^{3\Phi/2}{*}F_2) &= g_s e^{\Phi/2}H_3\wedge *\tilde{F}_4 \\
d(e^{\Phi/2}{*}\tilde{F}_4) &= -g_s^{1/2}F_4\wedge H_3 \\
\frac{g_s}{2}F_4\wedge F_4 &= d(e^{-\Phi}{*}H_3 + g_s^{1/2}e^{\Phi/2}C_1\wedge *\tilde{F}_4) \\
R_{MN} &= \frac{1}{2}\partial_M\Phi\partial_N\Phi + \frac{g_s e^{-\Phi}}{4}(H_M{}^{PQ}H_{NPQ} - \frac{1}{12}G_{MN}H^{PQR}H_{PQR}) \\
&\quad + \frac{g_s^{1/2}e^{3\Phi/2}}{2}(F_M{}^P F_{NP} - \frac{1}{16}G_{MN}F^{PQ}F_{PQ}) \\
&\quad + \frac{g_s^{3/2}e^{\Phi/2}}{12}(\tilde{F}_M{}^{PQR}\tilde{F}_{NPQR} - \frac{3}{32}G_{MN}\tilde{F}^{PQRS}\tilde{F}_{PQRS})e^{\Phi/2}. \qquad \text{(B.0.3)}
\end{aligned}$$

We use indices $M, N, \ldots$ in ten dimensions. The Bianchi identities are

$$d\tilde{F}_4 = -F_2\wedge H_3 \quad , \quad dF_2 = 0.$$

Appendix C

Relaxation Method

We have to solve a system of ordinary differential equations which satisfy boundary conditions both at the beginning and at the end of the range of the independent variable. This type of problem is called a two point boundary value problem. In order to solve it numerically we will use the techniques and routines described in [210].

The basic idea as explained in Section 5.3.1 is quite simple. We replace the continuum of the range of r, the independent variable, with a lattice of points. We then write the differential equations as an approximate algebraic system of finite difference equations on each point of the lattice. Similarly we replace the boundary conditions with such an algebraic system. Then we use a test solution for the dependent functions. This solution does not satisfy the equations and it does not have to satisfy the boundary conditions. Using this test solution and the finite difference equations in the interior and at the boundaries one can calculate corrections which are then added to the test solution. If the problem has a solution satisfying the boundary conditions, then this corrected solution is closer to it than the initial test one. If this procedure is iterated, then the final result is very close to the true solution (if there is one) satisfying the correct boundary conditions (even though we started with one that did not) to a degree of accuracy that we can control. It is necessary that a good initial guess should be made so that the method is quick and efficient.

In the following we will give some technical details about the method and we will present the source code of the programs that we used.

C.1 The method

We have a general set of N first order coupled differential equations in matrix form

$$\frac{d\mathbf{y}}{dx} = \mathbf{g}(x, \mathbf{y}) \tag{C.1.1}$$

that satisfy n_1 boundary conditions at the one end of the range and $n_2 = N - n_1$ boundary conditions at the other end. We first define a grid by a set of $k = 0, \ldots, M-1$ points at which we supply values for the independent variable x_k. x_0 is the initial boundary, while x_{M-1} is the final one. $\mathbf{y}_k$ is the entire set of dependent variables $y_0, \ldots, y_{N-1}$ at point x_k. At an arbitrary point k we approximate the system of ODEs by algebraic relations of the form

$$\mathbf{E}_k = \mathbf{y}_k - \mathbf{y}_{k-1} - (x_k - x_{k-1})\mathbf{g}_k(x_k, x_{k-1}\mathbf{y}_k, \mathbf{y}_{k-1}) = 0, \quad k = 1, \ldots, M-1. \tag{C.1.2}$$

$\mathbf{g}_k$ can be evaluated using information from both points $k, k-1$. These are N equations coupling $2N$ variables at points $k, k-1$.

At the first boundary we have

$$\mathbf{E}_0 = \mathbf{B}(x_0, \mathbf{y}_0) = 0. \tag{C.1.3}$$

These vectors have only n_1 non zero components corresponding to the initial n_1 boundary conditions. At the second boundary we have

$$\mathbf{E}_M = \mathbf{C}(x_{M-1}, \mathbf{y}_{M-1}) \tag{C.1.4}$$

where again only n_2 components of these vectors are non zero, corresponding to the boundary conditions at the second boundary.

The solutions of the finite difference equations problem in the above equations consists of a set of variables $y_{j,k}$, the values of the N variables y_j at the M points x_k. We provide an initial guess solution to this problem. Then we determine increments $\Delta y_{j,k}$ such that $y_{j,k} + \Delta y_{j,k}$ is an improved approximation to the solution.

We can find the equations that the increments should satisfy by expanding the FDEs in first order Taylor series with respect to small changes $\Delta\mathbf{y}_k$. At an interior point this gives

$$\mathbf{E}_k(\mathbf{y}_k+\Delta\mathbf{y}_k, \mathbf{y}_{k-1}k+\Delta\mathbf{y}_{k-1}) \simeq \mathbf{E}_k(\mathbf{y}_k, \mathbf{y}_{k-1})+\sum_{n=0}^{N-1}\frac{\partial \mathbf{E}_k}{\partial y_{n,k-1}}\Delta y_{m,k-1}+\sum_{n=0}^{N-1}\frac{\partial \mathbf{E}_k}{\partial y_{n,k}}\Delta y_{m,k} \tag{C.1.5}$$

For a solution we want the updated value to zero so the general set of equations at the interior can be written in matrix form as

$$\sum_{n=0}^{N-1} S_{j,n}\Delta y_{n,k-1} + \sum_{n=N}^{2N-1} S_{j,n}\Delta y_{n-N,k} = -E_{j,k}, \quad j = 0, \ldots, N-1, \tag{C.1.6}$$

where

$$S_{j,n} = \frac{\partial E_{j,k}}{\partial y_{n,k-1}}, \quad S_{j,n+N} = \frac{\partial E_{j,k}}{\partial y_{n,k}}, \quad n = 0, \ldots, N-1. \tag{C.1.7}$$

Similarly the algebraic relations at the boundaries can be expanded in Taylor series for increments that improve the solution. At the first boundary we have

$$\sum_{n=0}^{N-1} S_{j,n}\Delta y_{n,0} = -E_{j,0}, \quad j = n_2, n_2+1, \ldots, N-1 \tag{C.1.8}$$

where

$$S_{j,n} = \frac{\partial E_{j,0}}{\partial y_{n,0}}. \tag{C.1.9}$$

At the second boundary

$$\sum_{n=0}^{N-1} S_{j,n}\Delta y_{n,M-1} = -E_{j,M-1}, \quad j = n_2, n_2+1, \ldots, N-1 \tag{C.1.10}$$

where

$$S_{j,n} = \frac{\partial E_{j,M}}{\partial y_{n,M-1}}. \tag{C.1.11}$$

We have the system of equations (C.1.6-C.1.11) to solve for the corrections $\Delta\mathbf{y}$, iterating until the corrections are sufficiently small. Then we have the solution to our problem.

C.2 The routines

We use the routines provided in [210]. They are the routines which solve the algebraic system. We have to provide them with two additional routines. The one is the main program which controls the whole process, gives the initial guess and calls the solving routines. We also have to provide a function which is called by the solving routines in which we store the information in equations (C.1.6-C.1.11), representing the differential equations to be solved and the boundary conditions.

C.2.1 Extremal enhançon

```
const int M=10000;
int mpt=M+1;
DP h,a,r6,re,r0=0.0;
Vec_DP *x_p;

int main(void)
{
  const int NE=7,NB=3,NYJ=NE,NYK=M+1;
  int itmax,k;
  DP conv,slowc;

  Vec_INT indexv(NE);
  Vec_DP scalv(NE);
  Mat_DP y(NYJ,NYK);
  x_p=new Vec_DP(M+1);
  Vec_DP &x=*x_p;

  itmax=50;
  conv=1.0e-15;
  slowc=1.0;

  cout<<endl<<"Input r6, a:"<<endl;
  cin>>r6>>a;

  re=2.0*r6/(a-1.0);
  h=100.0*r6/M;

```

```
indexv[0]=0;
indexv[1]=1;
indexv[2]=2;
indexv[3]=3;
indexv[4]=4;
indexv[5]=5;
indexv[6]=6;

for (k=0;k<M+1;k++) {
  x[k]=k*h+re;
  y[6][k]=1.0/r6;
  y[0][k]=exp(-y[6][k]*x[k])*(1-re/x[k]);
  y[1][k]=-(y[6][k]+y[6][k]*re/x[k]+re/x[k]/x[k])*y[0][k];
  y[2][k]=exp(-y[6][k]*x[k])*(1-re/x[k]);
  y[3][k]=-(y[6][k]+y[6][k]*re/x[k]+re/x[k]/x[k])*y[2][k];
  y[4][k]=exp(-y[6][k]*x[k])*(1-re/x[k]);
  y[5][k]=-(y[6][k]+y[6][k]*re/x[k]+re/x[k]/x[k])*y[4][k];

}

scalv[0]=1.0/r6;
scalv[1]=(y[1][M] > scalv[0]*r6 ? y[1][M] : scalv[0]);
scalv[2]=(y[2][M] > 1.0 ? y[2][M] : 1.0);
scalv[3]=(y[3][M] > scalv[2] ? y[3][M] : scalv[2]);
scalv[4]=(y[4][M] > 1.0 ? y[4][M] : 1.0);
scalv[5]=(y[5][M] > scalv[4] ? y[5][M] : scalv[4]);
scalv[6]=1.0;

for (;;) {
cout << endl << "Enter V/V* or 999 to end" << endl;
cin >> a;
if (a == 999) {
 delete x_p;
```

```
61     return 0;
62    }
63
64    NR::solvde(itmax,conv,slowc,scalv,indexv,NB,y);
65    cout << endl << "r0 = ";
66    cout << fixed << setprecision(3) << setw(7) << r0;
67    cout << " omega = " << setprecision(6) << y[6][0];
68    cout << endl;
69   }
70  }
```

We will briefly explain the structure, the constants and the functions of the program. Starting from line 01, M is the number of the points of the grid. The more we have, the more accurate, but slower, our calculation.

In line 18, itmax is the number of maximum iterations. If the program can not find a solution after that many iterations it stops. In line 19, conv is the convergence criterion. In line 20, slowc controls the fraction of corrections used after each iteration.

In lines 21–22, the program asks for initial values of r_6 and $a = V/V^*$. These are the parameters of the program. Then in line 26 r_e is calculated.

In lines 28–34, indexv lists the column ordering of variables used to construct the matrix s of equations (C.1.7, C.1.9, C.1.11)

In lines 36–46, we write initial random guess for the functions. The program assigns a value for the functions y[j] at every point k. The program starts to relax from here. y[6][k] is σ, y[0][k] is Φ, y[1][k] is Φ', y[2][k] is Ψ_2, y[3][k] is Ψ_2', y[4][k] is Z_6, y[5][k] is Z_6', all calculated at the grid point x[k].

In lines 48–54, the typical values of the variables are set. These are used to calculate the errors and to check convergence.

Finally in lines 56–70 is the main loop. It calls the function that calculates the corrections (solvde line 64), applies them and checks them if they converge. In case they do it returns here, prints the value of σ (line 67) and asks for another value of the parameter a to restart or 999 to finish. In case there is no solution the program stops after a pre–arranged number of iterations.

C.2.2 Horizon branch

```
int mpt=M+1;
DP h,r0,a,r6;
Vec_DP *x_p;

int main(void)
{
  const int NE=7,NB=3,NYJ=NE,NYK=M+1;
  int itmax,k;
  DP conv,slowc,rsig;

  Vec_INT indexv(NE);
  Vec_DP scalv(NE);
  Mat_DP y(NYJ,NYK);
  x_p=new Vec_DP(M+1);
  Vec_DP &x=*x_p;

  itmax=100;
  conv=1.0e-15;
  slowc=1.0;
  cout<<endl<<"Input r6, r0, a:"<<endl;
  cin>>r6>>r0>>a;

  rsig=sqrt(r0-r0*0.5+sqrt(r6*r6/a/a+r0*r0*0.25))
   *sqrt(r0-r0*0.5+sqrt(r6*r6+r0*r0*0.25));

  h=100.0*rsig/M;
  indexv[0]=0;
  indexv[1]=4;
  indexv[2]=2;
  indexv[3]=3;
  indexv[4]=1;
  indexv[5]=5;
```

```
indexv[6]=6;
for (k=0;k<M+1;k++) {
  x[k]=k*h+r0;
  y[6][k]=1.0/rsig;
  y[0][k]=(1.0-r0/x[k])*exp(-y[6][k]*x[k]);
  y[1][k]=
=(1.0-r0/x[k])*exp(-y[6][k]*x[k])*(r0/x[k]/x[k]+y[6][k]*r0/x[k]-y[6][k]);
  y[2][k]=(1.0-r0/x[k])*exp(-y[6][k]*x[k]);
  y[3][k]=
=(1.0-r0/x[k])*exp(-y[6][k]*x[k])*(r0/x[k]/x[k]+y[6][k]*r0/x[k]-y[6][k]);
  y[4][k]=(1.0-r0/x[k])*exp(-y[6][k]*x[k]);
  y[5][k]=
=(1.0-r0/x[k])*exp(-y[6][k]*x[k])*(r0/x[k]/x[k]+y[6][k]*r0/x[k]-y[6][k]);
}
scalv[0]=1.0;
scalv[1]=(y[1][M] > scalv[0] ? y[1][M] : scalv[0]);
scalv[2]=(y[2][M] > 1.0 ? y[2][M] : 1.0);
scalv[3]=(y[3][M] > scalv[0] ? y[3][M] : scalv[2]);
scalv[4]=(y[4][M] > 1.0 ? y[4][M] : 1.0);
scalv[5]=(y[5][M] > scalv[0] ? y[5][M] : scalv[4]);
scalv[6]=1.0/rsig;
for (;;) {
cout << endl << "Enter V/V* or 999 to end" << endl;
cin >> a;
if (a == 999) {
 delete x_p;
```

```
62     return 0;
63   }
64
65   NR::solvde(itmax,conv,slowc,scalv,indexv,NB,y);
66   cout << endl << "r0 = ";
67   cout << fixed << setprecision(3) << setw(7) << r0;
68   cout << " omega = " << setprecision(6) << y[6][0];
69   cout << endl;
70  }
71 }
```

The structure of this program is the same as with the previous one. The difference now is that there is another parameter r_0, the mass of the black hole. It is needed as additional input in line 20. rsig in line 23 is actually $\bar{\sigma}$ in (6.2.13).

It must be repeated that these two programs must by accompanied by two functions (one each), which have all the problem specific information about the differential equations and the boundary conditions. We do not present these programs here.

Appendix D

Black hole temperature

In this appendix we will give a few details concerning the calculation of the temperature of the horizon (6.5) and shell (6.7) branch solutions of the the non–extremal enhançon in Section 6.1[1].

We will first calculate the temperarture of the horizon branch solution. We can obtain the Euclidean horizon branch solution by analytically continuing t to to real values of $\tau = it$ in equation (3.32):

$$\begin{aligned} g_s^{1/2}\, ds_E^2 &= Z_2^{-5/8} Z_6^{-1/8} (K d\tau^2 + dx_1^2 + dx_2^2) + Z_2^{3/8} Z_6^{7/8} (K^{-1} dr^2 + r^2 d\Omega_2^2) \\ &\qquad + V^{1/2} Z_2^{3/8} Z_6^{-1/8} ds_{\mathrm{K3}}^2 \,. \end{aligned} \tag{D.0.1}$$

In the Euclidean space we encounter a singularity at $r = r_0$. To examine the region near $r = r_0$ we set

$$r - r_0 = \frac{R^2}{4 r_0 Z_2(r_0)^{3/8} Z_6(r_0)^{1/8}}. \tag{D.0.2}$$

Then we have

$$\begin{aligned} g_s^{1/2}\, ds_E^2 &= R^2 d\left(\frac{\tau}{2 r_0 \sqrt{Z_2 Z_6}}\right)^2 + dR^2 + Z_2^{-5/8} Z_6^{-1/8} (dx_1^2 + dx_2^2) + Z_2^{3/8} Z_6^{7/8} r^2 d\Omega_2^2 \\ &\qquad + V^{1/2} Z_2^{3/8} Z_6^{-1/8} ds_{\mathrm{K3}}^2 \,, \end{aligned} \tag{D.0.3}$$

where r is a function of R. It can be seen from (D.0.3), that the coordinate singularity at $R = 0$ ($r = r_0$) is of the same nature as the coordinate singularity at the

[1] [14] for more details.

origin of the polar coordinates on the plane. R plays the role of the radial coordinate, and $\frac{\tau}{2r_0\sqrt{Z_2Z_6}}$ plays the role of the angular coordinate. In order to avoid this singularity we periodically identify the 'angular' coordinate with period 2π, in the region $r > r_0$ and then add a point in the plane $R-\tau$ to extend the space at $R=0$. The temperature of the black hole is the period of the imaginary time coordinate, which is

$$T_{hb} = \frac{1}{4\pi r_0\sqrt{Z_2(r_0)Z_6(r_0)}}, \tag{D.0.4}$$

which reduces to (6.5).

Similarly we can obtain the Euclidean shell branch solution by analytically continuing t to to real values of $\tau = it$ in equation (3.38):

$$\begin{aligned} g_s^{1/2}\,ds_E^2 &= H_2^{-5/8}H_6^{-1/8}\left(\frac{K(r_e)}{L(r_e)}Ldt^2 + dx_1^2 + dx_2^2\right) + H_2^{3/8}H_6^{7/8}(L^{-1}dr^2 + r^2d\Omega) \\ &\quad + V^{1/2}H_2^{3/8}H_6^{-1/8}ds_{K3}^2\,. \end{aligned} \tag{D.0.5}$$

In the Euclidean space we encounter a singularity at $r = r_0'$. To examine the region near $r = r_0'$ we set

$$r - r_0' = \frac{R^2}{4r_0'H_2(r_0')^{3/8}H_6(r_0')^{1/8}}. \tag{D.0.6}$$

Then we have

$$\begin{aligned} g_s^{1/2}\,ds_E^2 &= R^2 d\left(\frac{\tau}{2r_0'\sqrt{\frac{L(r_e)}{K(r_e)}H_2H_6}}\right)^2 + dR^2 + H_2^{-5/8}H_6^{-1/8}(dx_1^2+dx_2^2) + \\ &\quad H_2^{3/8}H_6^{7/8}r^2d\Omega_2^2 + V^{1/2}H_2^{3/8}H_6^{-1/8}ds_{K3}^2\,, \end{aligned} \tag{D.0.7}$$

where again r is a function of R. The procedure is essentially the same. The coordinate singularity at $R = 0$ ($r = r_0'$) is of the same nature as the coordinate singularity at the origin of the polar coordinates on the plane. In order to avoid this singularity we periodically identify the 'angular' coordinate with period 2π, in the region $r > r_0'$ and then add a point in the plane $R-\tau$ to extend the space at $R=0$. The temperature of the black hole is the period of the imaginary time coordinate, which is

$$T_{sb} = \frac{1}{4\pi r_0'}\left(\frac{K(r_e)}{L(r_e)H_2(r_0')H_6(r_0')}\right)^{1/2}. \tag{D.0.8}$$

Bibliography

[1] A. Dimitriadis and S. F. Ross, "Stability of the non-extremal enhancon solution. I: Perturbation equations," *Phys. Rev. D* **66** (2002) 106003, `hep-th/0207183`.

[2] A. Dimitriadis and S. F. Ross, "Properties of non-extremal enhancons," `hep-th/0307216`.

[3] A. Dimitriadis, A. W. Peet, G. Potvin, and S. F. Ross, "Enhancon Solutions: Pushing Supergravity to its Limits," `hep-th/0311271`.

[4] **Particle Data Group** Collaboration, K. Hagiwara *et al.*, "Review of particle physics," *Phys. Rev.* **D66** (2002) 010001.

[5] G. L. Smith *et al.*, "Short range tests of the equivalence principle," *Phys. Rev.* **D61** (2000) 022001.

[6] C. D. Hoyle *et al.*, "Sub-millimeter tests of the gravitational inverse-square law: A search for 'large' extra dimensions," *Phys. Rev. Lett.* **86** (2001) 1418–1421, `hep-ph/0011014`.

[7] R. Penrose, "Gravitational collapse and space-time singularities," *Phys. Rev. Lett.* **14** (1965) 57–59.

[8] S. W. Hawking, "The occurrence of singularities in cosmology III. causality and singularities," *Proc. Roy. Soc. Lond.* **A300** (1967) 182.

[9] S. W. Hawking and R. Penrose, "The singularities of gravitational collapse and cosmology," *Proc. Roy. Soc. Lond.* **A314** (1970) 529–548.

[10] S. Weinberg, "The quantum theory of fields. 3 vol. set,". Cambridge, UK: Univ. Pr. (1995).

[11] T. P. Cheng and L. F. Li, "Gauge theory of elementary particle physics,". Oxford, Uk: Clarendon (1984) 536 P. (Oxford Science Publications).

[12] J. Polchinski, "Dirichlet-branes and Ramond-Ramond charges," *Phys. Rev. Lett.* **75** (1995) 4724–4727, `hep-th/9510017`.

[13] C. Misner, K. Thorne, and J. Wheeler, *Gravitation.* Freeman, 1973.

[14] R. M. Wald, "General Relativity,". Chicago, Usa: Univ. Pr. (1984) 491p.

[15] V. Mukhanov and R. H. Brandenberger, "A nonsingular universe," *Phys. Rev. Lett.* **68** (1992) 1969–1972.

[16] R. H. Brandenberger, V. Mukhanov, and A. Sornborger, "A cosmological theory without singularities," *Phys. Rev.* **D48** (1993) 1629–1642, `gr-qc/9303001`.

[17] G. W. Gibbons, G. T. Horowitz, and P. K. Townsend, "Higher dimensional resolution of dilatonic black hole singularities," *Class. Quant. Grav.* **12** (1995) 297–318, `hep-th/9410073`.

[18] G. T. Horowitz and R. C. Myers, "The value of singularities," *Gen. Rel. Grav.* **27** (1995) 915–919, `gr-qc/9503062`.

[19] G. 't Hooft and M. J. G. Veltman, "One loop divergencies in the theory of gravitation," *Annales Poincare Phys. Theor.* **A20** (1974) 69–94.

[20] M. H. Goroff and A. Sagnotti, "The ultraviolet behavior of einstein gravity," *Nucl. Phys.* **B266** (1986) 709.

[21] A. E. M. van de Ven, "Two loop quantum gravity," *Nucl. Phys.* **B378** (1992) 309–366.

[22] P. Van Nieuwenhuizen, "Supergravity," *Phys. Rept.* **68** (1981) 189–398.

[23] N. Marcus and A. Sagnotti, "The ultraviolet behavior of N=4 yang-mills and the power counting of extended superspace," *Nucl. Phys.* **B256** (1985) 77.

[24] Z. Bern, L. J. Dixon, D. C. Dunbar, M. Perelstein, and J. S. Rozowsky, "On the relationship between Yang-Mills theory and gravity and its implication for ultraviolet divergences," *Nucl. Phys.* **B530** (1998) 401–456, `hep-th/9802162`.

[25] S. W. Hawking, "Particle creation by black holes," *Commun. Math. Phys.* **43** (1975) 199–220.

[26] T. Banks, "Lectures on black holes and information loss," *Nucl. Phys. Proc. Suppl.* **41** (1995) 21–65, `hep-th/9412131`.

[27] J. D. Bekenstein, "Black holes and the second law," *Nuovo Cim. Lett.* **4** (1972) 737–740.

[28] J. D. Bekenstein, "Black holes and entropy," *Phys. Rev.* **D7** (1973) 2333–2346.

[29] J. D. Bekenstein, "Generalized second law of thermodynamics in black hole physics," *Phys. Rev.* **D9** (1974) 3292–3300.

[30] R. M. Wald, "The thermodynamics of black holes," *Living Rev. Rel.* **4** (2001) 6, `gr-qc/9912119`.

[31] T. Padmanabhan, "Gravity and the thermodynamics of horizons," `gr-qc/0311036`.

[32] G. 't Hooft, "Dimensional reduction in quantum gravity," `gr-qc/9310026`.

[33] L. Susskind, "The World as a hologram," *J. Math. Phys.* **36** (1995) 6377–6396, `hep-th/9409089`.

[34] D. Bigatti and L. Susskind, "TASI lectures on the holographic principle," `hep-th/0002044`.

[35] R. Bousso, "The holographic principle," *Rev. Mod. Phys.* **74** (2002) 825–874, hep-th/0203101.

[36] T. Thiemann, "Lectures on loop quantum gravity," *Lect. Notes Phys.* **631** (2003) 41–135, gr-qc/0210094.

[37] T. Thiemann, "Introduction to modern canonical quantum general relativity," gr-qc/0110034.

[38] C. Rovelli, "Loop quantum gravity," *Living Rev. Rel.* **1** (1998) 1, gr-qc/9710008.

[39] J. B. Hartle and S. W. Hawking, "Wave function of the universe," *Phys. Rev.* **D28** (1983) 2960–2975.

[40] Stephen Hawking in S. Hawking and W. Israel, *General Relativity, an Einstein Centenary Survey.* Cambridge, Uk: Univ. Pr., 1979.

[41] R. Loll, "Discrete approaches to quantum gravity in four dimensions," *Living Rev. Rel.* **1** (1998) 13, gr-qc/9805049.

[42] C. J. Isham, "Topos theory and consistent histories: The internal logic of the set of all consistent sets," *Int. J. Theor. Phys.* **36** (1997) 785–814, gr-qc/9607069.

[43] R. Penrose, "Twistor theory and the Einstein vacuum," *Class. Quant. Grav.* **16** (1999) A113–A130.

[44] R. D. Sorkin, "Causal sets: Discrete gravity (notes for the valdivia summer school)," gr-qc/0309009.

[45] M. B. Green, J. H. Schwarz, and E. Witten, *Supestring theory vol.1 Introduction and vol.2 Loop amplitudes, anomalies and phenomenology.* Cambridge, Uk: Univ. Pr., 1987. Cambridge Monographs On Mathematical Physics.

[46] J. Polchinski, *String theory vol.1 An introduction to the bosonic string and vol.2 Superstring theory and beyond.* Cambridge, Uk: Univ. Pr., 1998. Cambridge Monographs On Mathematical Physics.

[47] M. F. Sohnius, "Introducing supersymmetry," *Phys. Rept.* **128** (1985) 39–204.

[48] M. B. Green and J. H. Schwarz, "Anomaly cancellation in supersymmetric D=10 gauge theory and superstring theory," *Phys. Lett.* **B149** (1984) 117–122.

[49] D. J. Gross, J. A. Harvey, E. J. Martinec, and R. Rohm, "The heterotic string," *Phys. Rev. Lett.* **54** (1985) 502–505.

[50] C. M. Hull and P. K. Townsend, "Unity of superstring dualities," *Nucl. Phys.* **B438** (1995) 109–137, `hep-th/9410167`.

[51] P. K. Townsend, "The eleven-dimensional supermembrane revisited," *Phys. Lett.* **B350** (1995) 184–187, `hep-th/9501068`.

[52] E. Witten, "String theory dynamics in various dimensions," *Nucl. Phys.* **B443** (1995) 85–126, `hep-th/9503124`.

[53] P. K. Townsend, "Four lectures on M-theory," `hep-th/9612121`.

[54] A. Sen, "An introduction to non-perturbative string theory," `hep-th/9802051`.

[55] J. Callan, Curtis G., E. J. Martinec, M. J. Perry, and D. Friedan, "Strings in background fields," *Nucl. Phys.* **B262** (1985) 593.

[56] M. Natsuume, "The singularity problem in string theory," `gr-qc/0108059`.

[57] L. J. Dixon, J. A. Harvey, C. Vafa, and E. Witten, "Strings on orbifolds," *Nucl. Phys.* **B261** (1985) 678–686.

[58] L. J. Dixon, J. A. Harvey, C. Vafa, and E. Witten, "Strings on orbifolds. 2," *Nucl. Phys.* **B274** (1986) 285–314.

[59] P. S. Aspinwall, B. R. Greene, and D. R. Morrison, "Multiple mirror manifolds and topology change in string theory," *Phys. Lett.* **B303** (1993) 249–259, `hep-th/9301043`.

[60] P. S. Aspinwall, B. R. Greene, and D. R. Morrison, "Calabi-Yau moduli space, mirror manifolds and spacetime topology change in string theory," *Nucl. Phys.* **B416** (1994) 414–480, `hep-th/9309097`.

[61] E. Witten, "Phases of N = 2 theories in two dimensions," *Nucl. Phys.* **B403** (1993) 159–222, `hep-th/9301042`.

[62] P. Candelas, P. S. Green, and T. Hubsch, "Finite distances between distinct Calabi-Yau vacua: (other worlds are just around the corner)," *Phys. Rev. Lett.* **62** (1989) 1956.

[63] A. Strominger, "Massless black holes and conifolds in string theory," *Nucl. Phys.* **B451** (1995) 96–108, `hep-th/9504090`.

[64] B. R. Greene, D. R. Morrison, and A. Strominger, "Black hole condensation and the unification of string vacua," *Nucl. Phys.* **B451** (1995) 109–120, `hep-th/9504145`.

[65] A. E. Lawrence and E. J. Martinec, "String field theory in curved spacetime and the resolution of spacelike singularities," *Class. Quant. Grav.* **13** (1996) 63–96, `hep-th/9509149`.

[66] E. Witten, "Noncommutative geometry and string field theory," *Nucl. Phys.* **B268** (1986) 253.

[67] C. B. Thorn, "String field theory," *Phys. Rept.* **175** (1989) 1–101.

[68] B. Zwiebach, "Closed string field theory: Quantum action and the B-V master equation," *Nucl. Phys.* **B390** (1993) 33–152, `hep-th/9206084`.

[69] R. H. Brandenberger and C. Vafa, "Superstrings in the early universe," *Nucl. Phys.* **B316** (1989) 391.

[70] G. T. Horowitz and A. R. Steif, "Singular string solutions with nonsingular initial data," *Phys. Lett.* **B258** (1991) 91–96.

[71] M. Gasperini and G. Veneziano, "Pre - big bang in string cosmology," *Astropart. Phys.* **1** (1993) 317–339, hep-th/9211021.

[72] R. Brustein and R. Madden, "Graceful exit and energy conditions in string cosmology," *Phys. Lett.* **B410** (1997) 110–118, hep-th/9702043.

[73] J. Khoury, B. A. Ovrut, N. Seiberg, P. J. Steinhardt, and N. Turok, "From big crunch to big bang," *Phys. Rev.* **D65** (2002) 086007, hep-th/0108187.

[74] N. Seiberg, "From big crunch to big bang - is it possible?," hep-th/0201039.

[75] V. Balasubramanian, S. F. Hassan, E. Keski-Vakkuri, and A. Naqvi, "A space-time orbifold: A toy model for a cosmological singularity," *Phys. Rev.* **D67** (2003) 026003, hep-th/0202187.

[76] L. Cornalba and M. S. Costa, "A new cosmological scenario in string theory," *Phys. Rev.* **D66** (2002) 066001, hep-th/0203031.

[77] N. A. Nekrasov, "Milne universe, tachyons, and quantum group," *Surveys High Energ. Phys.* **17** (2002) 115–124, hep-th/0203112.

[78] S. Elitzur, A. Giveon, D. Kutasov, and E. Rabinovici, "From big bang to big crunch and beyond," *JHEP* **06** (2002) 017, hep-th/0204189.

[79] H. Liu, G. Moore, and N. Seiberg, "Strings in a time-dependent orbifold," *JHEP* **06** (2002) 045, hep-th/0204168.

[80] H. Liu, G. Moore, and N. Seiberg, "Strings in time-dependent orbifolds," *JHEP* **10** (2002) 031, hep-th/0206182.

[81] L. Cornalba, M. S. Costa, and C. Kounnas, "A resolution of the cosmological singularity with orientifolds," *Nucl. Phys.* **B637** (2002) 378–394, hep-th/0204261.

[82] B. Craps, D. Kutasov, and G. Rajesh, "String propagation in the presence of cosmological singularities," *JHEP* **06** (2002) 053, hep-th/0205101.

[83] S. Kachru and L. McAllister, "Bouncing brane cosmologies from warped string compactifications," *JHEP* **03** (2003) 018, hep-th/0205209.

[84] G. T. Horowitz and J. Polchinski, "Instability of spacelike and null orbifold singularities," *Phys. Rev.* **D66** (2002) 103512, hep-th/0206228.

[85] G. T. Horowitz and A. Strominger, "Black strings and p-branes," *Nucl. Phys.* **B360** (1991) 197–209.

[86] D. J. Smith, "Intersecting brane solutions in string and M-theory," *Class. Quant. Grav.* **20** (2003) R233, hep-th/0210157.

[87] A. Strominger and C. Vafa, "Microscopic origin of the Bekenstein-Hawking entropy," *Phys. Lett.* **B379** (1996) 99–104, hep-th/9601029.

[88] J. M. Maldacena, "Black holes in string theory," hep-th/9607235.

[89] A. W. Peet, "The bekenstein formula and string theory (N-brane theory)," *Class. Quant. Grav.* **15** (1998) 3291–3338, hep-th/9712253.

[90] K. Skenderis, "Black holes and branes in string theory," *Lect. Notes Phys.* **541** (2000) 325–364, hep-th/9901050.

[91] A. W. Peet, "Tasi lectures on black holes in string theory," hep-th/0008241.

[92] J. R. David, G. Mandal, and S. R. Wadia, "Microscopic formulation of black holes in string theory," *Phys. Rept.* **369** (2002) 549–686, hep-th/0203048.

[93] J. M. Maldacena, "The large N limit of superconformal field theories and supergravity," *Adv. Theor. Math. Phys.* **2** (1998) 231–252, hep-th/9711200.

[94] S. S. Gubser, I. R. Klebanov, and A. M. Polyakov, "Gauge theory correlators from non-critical string theory," *Phys. Lett.* **B428** (1998) 105–114, hep-th/9802109.

[95] E. Witten, "Anti-de Sitter space and holography," *Adv. Theor. Math. Phys.* **2** (1998) 253–291, hep-th/9802150.

[96] O. Aharony, S. S. Gubser, J. M. Maldacena, H. Ooguri, and Y. Oz, "Large N field theories, string theory and gravity," *Phys. Rept.* **323** (2000) 183–386, hep-th/9905111.

[97] E. D'Hoker and D. Z. Freedman, "Supersymmetric gauge theories and the AdS/CFT correspondence," hep-th/0201253.

[98] J. M. Maldacena, "TASI 2003 lectures on AdS/CFT," hep-th/0309246.

[99] O. Aharony, "The non-AdS/non-CFT correspondence, or three different paths to QCD," hep-th/0212193.

[100] F. Bigazzi, A. L. Cotrone, M. Petrini, and A. Zaffaroni, "Supergravity duals of supersymmetric four dimensional gauge theories," *Riv. Nuovo Cim.* **25N12** (2002) 1–70, hep-th/0303191.

[101] S. S. Gubser, "Curvature singularities: The good, the bad, and the naked," *Adv. Theor. Math. Phys.* **4** (2002) 679–745, hep-th/0002160.

[102] J. Polchinski and M. J. Strassler, "The string dual of a confining four-dimensional gauge theory," hep-th/0003136.

[103] R. C. Myers, "Dielectric-branes," *JHEP* **12** (1999) 022, hep-th/9910053.

[104] C. P. Herzog, I. R. Klebanov, and P. Ouyang, "D-branes on the conifold and N = 1 gauge / gravity dualities," hep-th/0205100.

[105] I. R. Klebanov and M. J. Strassler, "Supergravity and a confining gauge theory: Duality cascades and χsb-resolution of naked singularities," *JHEP* **08** (2000) 052, hep-th/0007191.

[106] I. R. Klebanov and A. A. Tseytlin, "Gravity duals of supersymmetric SU(N) x SU(N+M) gauge theories," *Nucl. Phys.* **B578** (2000) 123–138, hep-th/0002159.

[107] K. Pilch and N. P. Warner, "$N = 1$ supersymmetric renormalization group flows from IIB supergravity," *Adv. Theor. Math. Phys.* **4** (2002) 627–677, `hep-th/0006066`.

[108] J. M. Maldacena and C. Nunez, "Towards the large N limit of pure $N = 1$ super Yang Mills," *Phys. Rev. Lett.* **86** (2001) 588–591, `hep-th/0008001`.

[109] K. Pilch and N. P. Warner, "N = 2 supersymmetric RG flows and the IIB dilaton," *Nucl. Phys.* **B594** (2001) 209–228, `hep-th/0004063`.

[110] A. Brandhuber and K. Sfetsos, "An N = 2 gauge theory and its supergravity dual," *Phys. Lett.* **B488** (2000) 373–382, `hep-th/0004148`.

[111] A. Buchel, A. W. Peet, and J. Polchinski, "Gauge dual and noncommutative extension of an $N = 2$ supergravity solution," *Phys. Rev. D* **63** (2001) 044009, `hep-th/0008076`.

[112] N. Evans, C. V. Johnson, and M. Petrini, "The enhancon and $N = 2$ gauge theory/gravity RG flows," *JHEP* **10** (2000) 022, `hep-th/0008081`.

[113] I. R. Klebanov and N. A. Nekrasov, "Gravity duals of fractional branes and logarithmic RG flow," *Nucl. Phys.* **B574** (2000) 263–274, `hep-th/9911096`.

[114] M. Grana and J. Polchinski, "Gauge / gravity duals with holomorphic dilaton," *Phys. Rev.* **D65** (2002) 126005, `hep-th/0106014`.

[115] M. Bertolini *et al.*, "Fractional D-branes and their gauge duals," *JHEP* **02** (2001) 014, `hep-th/0011077`.

[116] J. Polchinski, "N = 2 gauge-gravity duals," *Int. J. Mod. Phys.* **A16** (2001) 707–718, `hep-th/0011193`.

[117] O. Aharony, "A note on the holographic interpretation of string theory backgrounds with varying flux," *JHEP* **03** (2001) 012, `hep-th/0101013`.

[118] M. Petrini, R. Russo, and A. Zaffaroni, "N = 2 gauge theories and systems with fractional branes," *Nucl. Phys.* **B608** (2001) 145–161, `hep-th/0104026`.

[119] M. Billo, L. Gallot, and A. Liccardo, "Classical geometry and gauge duals for fractional branes on ALE orbifolds," *Nucl. Phys.* **B614** (2001) 254–278, hep-th/0105258.

[120] M. Bertolini, P. Di Vecchia, M. Frau, A. Lerda, and R. Marotta, "N = 2 gauge theories on systems of fractional D3/D7 branes," *Nucl. Phys.* **B621** (2002) 157–178, hep-th/0107057.

[121] C. P. Herzog, I. R. Klebanov, and P. Ouyang, "D-branes on the conifold and N= 1 gauge / gravity dualities," hep-th/0205100.

[122] A. Fayyazuddin and D. J. Smith, "Localized intersections of M5-branes and four-dimensional superconformal field theories," *JHEP* **04** (1999) 030, hep-th/9902210.

[123] A. Fayyazuddin and D. J. Smith, "Warped AdS near-horizon geometry of completely localized intersections of M5-branes," *JHEP* **10** (2000) 023, hep-th/0006060.

[124] J. P. Gauntlett, N. Kim, D. Martelli, and D. Waldram, "Wrapped fivebranes and N = 2 super Yang-Mills theory," *Phys. Rev.* **D64** (2001) 106008, hep-th/0106117.

[125] F. Bigazzi, A. L. Cotrone, and A. Zaffaroni, "N = 2 gauge theories from wrapped five-branes," *Phys. Lett.* **B519** (2001) 269–276, hep-th/0106160.

[126] P. Di Vecchia, A. Lerda, and P. Merlatti, "N = 1 and N= 2 super yang-mills theories from wrapped branes," *Nucl. Phys.* **B646** (2002) 43–68, hep-th/0205204.

[127] C. V. Johnson, A. W. Peet, and J. Polchinski, "Gauge theory and the excision of repulson singularities," *Phys. Rev. D* **61** (2000) 086001, hep-th/9911161.

[128] M. Bertolini, "Four lectures on the gauge-gravity correspondence," hep-th/0303160.

[129] C. V. Johnson, R. C. Myers, A. W. Peet, and S. F. Ross, "The enhançon and the consistency of excision," *Phys. Rev. D* **64** (2001) 106001, hep-th/0105077.

[130] C. V. Johnson, "Enhancons, fuzzy spheres and multi-monopoles," *Phys. Rev. D* **63** (2001) 065004, hep-th/0004068.

[131] C. V. Johnson, "The enhancon, multimonopoles and fuzzy geometry," *Int. J. Mod. Phys.* **A16** (2001) 990, hep-th/0011008.

[132] J. K. Barrett and C. V. Johnson, "Wrapped d-branes as bps monopoles: The moduli space perspective," hep-th/0312053.

[133] L. M. Dyson, L. Jarv, and C. V. Johnson, "Oblate, toroidal, and other shapes for the enhancon," *JHEP* **05** (2002) 019, hep-th/0112132.

[134] L. Jarv and C. V. Johnson, "Rotating black holes, closed time-like curves, thermodynamics, and the enhancon mechanism," *Phys. Rev.* **D67** (2003) 066003, hep-th/0211097.

[135] L. Jarv and C. V. Johnson, "Orientifolds, M-theory, and the ABCD's of the enhancon," *Phys. Rev.* **D62** (2000) 126010, hep-th/0002244.

[136] C. V. Johnson and R. C. Myers, "The enhancon, black holes, and the second law," *Phys. Rev. D* **64** (2001) 106002, hep-th/0105159.

[137] N. R. Constable, "The entropy of 4D black holes and the enhancon," *Phys. Rev. D* **64** (2001) 104004, hep-th/0106038.

[138] L. Järv, *The enhançon mechanism in string theory.* Ph.D thesis 2002, Centre for Particle Theory, University of Durham.

[139] A. Karch, D. Lust, and D. J. Smith, "Equivalence of geometric engineering and Hanany-Witten via fractional branes," *Nucl. Phys.* **B533** (1998) 348–372, hep-th/9803232.

[140] K. Dasgupta and S. Mukhi, "Brane constructions, fractional branes and anti-de Sitter domain walls," *JHEP* **07** (1999) 008, hep-th/9904131.

[141] P. Merlatti, "The enhancon mechanism for fractional branes," *Nucl. Phys.* **B624** (2002) 200–218, hep-th/0108016.

[142] M. Frau, A. Liccardo, and R. Musto, "The geometry of fractional branes," *Nucl. Phys.* **B602** (2001) 39–60, hep-th/0012035.

[143] M. Natsuume, "The heterotic enhancon," *Phys. Rev.* **D65** (2002) 086002, hep-th/0111044.

[144] R. Kallosh, T. Mohaupt, and M. Shmakova, "Excision of singularities by stringy domain walls," *J. Math. Phys.* **42** (2001) 3071–3081, hep-th/0010271.

[145] P. Berglund, T. Hubsch, and D. Minic, "Probing naked singularities in non-supersymmetric string vacua," *JHEP* **02** (2001) 010, hep-th/0012042.

[146] P. Berglund, T. Hubsch, and D. Minic, "On relativistic brane probes in singular spacetimes," *JHEP* **01** (2001) 041, hep-th/0012180.

[147] M. Wijnholt and S. Zhukov, "Inside an enhancon: Monopoles and dual Yang-Mills theory," *Nucl. Phys.* **B639** (2002) 343–369, hep-th/0110109.

[148] E. Witten, "Anti-de Sitter space, thermal phase transition, and confinement in gauge theories," *Adv. Theor. Math. Phys.* **2** (1998) 505–532, hep-th/9803131.

[149] D. Z. Freedman and J. A. Minahan, "Finite temperature effects in the supergravity dual of the $N = 1^*$ gauge theory," *JHEP* **01** (2001) 036, hep-th/0007250.

[150] A. Buchel, "Finite temperature resolution of the Klebanov-Tseytlin singularity," *Nucl. Phys.* **B600** (2001) 219–234, hep-th/0011146.

[151] A. Buchel, C. P. Herzog, I. R. Klebanov, L. A. Pando Zayas, and A. A. Tseytlin, "Non-extremal gravity duals for fractional D3-branes on the conifold," *JHEP* **04** (2001) 033, hep-th/0102105.

[152] S. S. Gubser, C. P. Herzog, I. R. Klebanov, and A. A. Tseytlin, "Restoration of chiral symmetry: A supergravity perspective," *JHEP* **05** (2001) 028, hep-th/0102172.

[153] C. P. Herzog and P. Ouyang, "Fractional D1-branes at finite temperature," *Nucl. Phys.* **B610** (2001) 97–116, hep-th/0104069.

[154] S. S. Gubser, A. A. Tseytlin, and M. S. Volkov, "Non-Abelian 4-d black holes, wrapped 5-branes, and their dual descriptions," *JHEP* **09** (2001) 017, hep-th/0108205.

[155] M. Bertolini, T. Harmark, N. A. Obers, and A. Westerberg, "Non-extremal fractional branes," *Nucl. Phys.* **B632** (2002) 257–282, hep-th/0203064.

[156] D. Lust and S. Theisen, "Lectures on string theory," *Lect. Notes Phys.* **346** (1989) 1–346.

[157] E. Kiritsis, "Introduction to superstring theory," hep-th/9709062.

[158] H. Ooguri and Z. Yin, "Lectures on perturbative string theories," hep-th/9612254.

[159] A. M. Polyakov, "Quantum geometry of bosonic strings," *Phys. Lett.* **B103** (1981) 207–210.

[160] F. Gliozzi, J. Scherk, and D. I. Olive, "Supergravity and the spinor dual model," *Phys. Lett.* **B65** (1976) 282.

[161] F. Gliozzi, J. Scherk, and D. I. Olive, "Supersymmetry, supergravity theories and the dual spinor model," *Nucl. Phys.* **B122** (1977) 253–290.

[162] J. Dai, R. G. Leigh, and J. Polchinski, "New connections between string theories," *Mod. Phys. Lett.* **A4** (1989) 2073–2083.

[163] C. V. Johnson, "D-branes,". Cambridge, USA: Univ. Pr. (2003) 548 p.

[164] J. Polchinski, S. Chaudhuri, and C. V. Johnson, "Notes on D-branes," hep-th/9602052.

[165] J. Polchinski, "Lectures on D-branes," hep-th/9611050.

[166] C. P. Bachas, "Lectures on D-branes," hep-th/9806199.

[167] I. Taylor, Washington, "Lectures on D-branes, gauge theory and M(atrices)," hep-th/9801182.

[168] P. Di Vecchia and A. Liccardo, "D branes in string theory. I," hep-th/9912161.

[169] P. Di Vecchia and A. Liccardo, "D-branes in string theory. II," hep-th/9912275.

[170] C. V. Johnson, "D-brane primer," hep-th/0007170.

[171] E. Witten, "Bound states of strings and p-branes," *Nucl. Phys.* **B460** (1996) 335–350, hep-th/9510135.

[172] A. Abouelsaood, J. Callan, Curtis G., C. R. Nappi, and S. A. Yost, "Open strings in background gauge fields," *Nucl. Phys.* **B280** (1987) 599.

[173] R. G. Leigh, "Dirac-born-infeld action from dirichlet sigma model," *Mod. Phys. Lett.* **A4** (1989) 2767.

[174] M. Li, "Boundary states of D-branes and Dy-strings," *Nucl. Phys.* **B460** (1996) 351–361, hep-th/9510161.

[175] M. R. Douglas, "Branes within branes," hep-th/9512077.

[176] K. Dasgupta, D. P. Jatkar, and S. Mukhi, "Gravitational couplings and Z(2) orientifolds," *Nucl. Phys.* **B523** (1998) 465–484, hep-th/9707224.

[177] C. P. Bachas, P. Bain, and M. B. Green, "Curvature terms in D-brane actions and their M-theory origin," *JHEP* **05** (1999) 011, hep-th/9903210.

[178] M. Bershadsky, C. Vafa, and V. Sadov, "D-branes and topological field theories," *Nucl. Phys.* **B463** (1996) 420–434, hep-th/9511222.

[179] M. B. Green, J. A. Harvey, and G. W. Moore, "I-brane inflow and anomalous couplings on D-branes," *Class. Quant. Grav.* **14** (1997) 47–52, hep-th/9605033.

[180] M. J. Duff, R. R. Khuri, and J. X. Lu, "String solitons," *Phys. Rept.* **259** (1995) 213–326, hep-th/9412184.

[181] K. S. Stelle, "BPS branes in supergravity," hep-th/9803116.

[182] G. Papadopoulos and P. K. Townsend, "Intersecting M-branes," *Phys. Lett.* **B380** (1996) 273–279, hep-th/9603087.

[183] A. A. Tseytlin, "Harmonic superpositions of M-branes," *Nucl. Phys.* **B475** (1996) 149–163, hep-th/9604035.

[184] J. P. Gauntlett, D. A. Kastor, and J. Traschen, "Overlapping branes in M-theory," *Nucl. Phys.* **B478** (1996) 544–560, hep-th/9604179.

[185] M. R. Douglas, "Gauge fields and D-branes," *J. Geom. Phys.* **28** (1998) 255–262, hep-th/9604198.

[186] M. R. Douglas, D. Kabat, P. Pouliot, and S. H. Shenker, "D-branes and short distances in string theory," *Nucl. Phys.* **B485** (1997) 85–127, hep-th/9608024.

[187] S. H. Shenker, "Another length scale in string theory?," hep-th/9509132.

[188] C. Bachas, "D-brane dynamics," *Phys. Lett.* **B374** (1996) 37–42, hep-th/9511043.

[189] J. Polchinski, "Tensors from K3 orientifolds," *Phys. Rev.* **D55** (1997) 6423–6428, hep-th/9606165.

[190] L. Alvarez-Gaume and D. Z. Freedman, "Geometrical structure and ultraviolet finiteness in the supersymmetric sigma model," *Commun. Math. Phys.* **80** (1981) 443.

[191] P. K. Townsend, "D-branes from m-branes," *Phys. Lett.* **B373** (1996) 68–75, hep-th/9512062.

[192] C. Schmidhuber, "D-brane actions," *Nucl. Phys.* **B467** (1996) 146–158, hep-th/9601003.

[193] W. Israel, "Singular hypersurfaces and thin shells in general relativity," *Nuovo Cim.* **B44S10** (1966) 1.

[194] E. J. Weinberg, "Black holes with hair," gr-qc/0106030.

[195] K. Maeda, T. Torii, M. Narita, and S. Yahikozawa, "The stability of the shell of D2-D6 branes in a $N = 2$ supergravity solution," *Phys. Rev. D* **65** (2002) 024030, hep-th/0107060.

[196] S. Chandrasekhar, *The Mathematical theory of black holes.* Oxford Univ. Press, New York, Oxford, 1992.

[197] J. M. Bardeen, K. S. Thorne, and D. W. Meltzer, "A catalogue of methods for studying the normal modes of radial pulsation of general-relativistic stellar models," *Astrophysical Journal* **145** (1966) 505–513.

[198] K. D. Kokkotas and B. G. Schmidt, "Quasi-normal modes of stars and black holes," *Living Rev. Rel.* **2** (1999) 2, gr-qc/9909058.

[199] T. Regge and J. A. Wheeler, "Stability of a Schwarzschild singularity," *Phys. Rev.* **108** (1957) 1063–1069.

[200] F. J. Zerilli, "Gravitational field of a particle falling in a Schwarzschild geometry analyzed in tensor harmonics," *Phys. Rev.* **D2** (1970) 2141–2160.

[201] K. S. Thorne, "Gravitational radiation damping," *Phys. Rev. Lett.* **21** (1968) 320–323.

[202] K. S. Thorne and A. Campolattaro, "Non-radial pulsation of general-relativistic stellar models. I. analytic analysis for $l >= 2$," *Astrophysical Journal* **158** (1969) 997–1019.

[203] R. J. Gleiser, C. O. Nicasio, R. H. Price, and J. Pullin, "Gravitational radiation from Schwarzschild black holes: The second order perturbation formalism," *Phys. Rept.* **325** (2000) 41–81, gr-qc/9807077.

[204] R. Gregory and R. Laflamme, "Black strings and p-branes are unstable," *Phys. Rev. Lett.* **70** (1993) 2837–2840, hep-th/9301052.

[205] R. Gregory and R. Laflamme, "The instability of charged black strings and p-branes," *Nucl. Phys.* **B428** (1994) 399–434, hep-th/9404071.

[206] C. F. E. Holzhey and F. Wilczek, "Black holes as elementary particles," *Nucl. Phys.* **B380** (1992) 447–477, hep-th/9202014.

[207] B. Xanthopoulos, "Reducible system of linear differential equations," *Proc. R. Soc. Lond.* **A378** (1981) 61–71.

[208] B. Xanthopoulos, "Metric and electromagnetic perturbations of the Reissner–Nordström black hole," *Proc. R. Soc. Lond.* **A378** (1981) 73–88.

[209] P. Kanti, N. E. Mavromatos, J. Rizos, K. Tamvakis, and E. Winstanley, "Dilatonic black holes in higher-curvature string gravity. II: Linear stability," *Phys. Rev.* **D57** (1998) 6255–6264, hep-th/9703192.

[210] W. H. Press, S. A. Teukolsky, W. T. Vetterling, and B. P. Flannery, *Numerical Recipes in C++: The Art of Scientific Computing.* Cambridge Univ. Press, Cambridge, UK, 2002.

[211] U. H. Danielsson, A. Guijosa, and M. Kruczenski, "Brane-antibrane systems at finite temperature and the entropy of black branes," *JHEP* **09** (2001) 011, hep-th/0106201.

[212] A. Sen, "Stable non-BPS states in string theory," *JHEP* **06** (1998) 007, hep-th/9803194.

[213] T. Banks and L. Susskind, "Brane - antibrane forces," hep-th/9511194.

[214] A. Sen, "Non-BPS states and branes in string theory," hep-th/9904207.

[215] A. Lerda and R. Russo, "Stable non-BPS states in string theory: A pedagogical review," *Int. J. Mod. Phys.* **A15** (2000) 771–820, `hep-th/9905006`.

[216] J. H. Schwarz, "TASI lectures on non-BPS D-brane systems," `hep-th/9908144`.

[217] M. R. Gaberdiel, "Lectures on non-BPS Dirichlet branes," *Class. Quant. Grav.* **17** (2000) 3483–3520, `hep-th/0005029`.

[218] K. Ohmori, "A review on tachyon condensation in open string field theories," `hep-th/0102085`.

[219] W. Taylor and B. Zwiebach, "D-branes, tachyons, and string field theory," `hep-th/0311017`.

[220] G. T. Horowitz, J. M. Maldacena, and A. Strominger, "Nonextremal black hole microstates and U-duality," *Phys. Lett.* **B383** (1996) 151–159, `hep-th/9603109`.

[221] J. Maharana and J. H. Schwarz, "Noncompact symmetries in string theory," *Nucl. Phys.* **B390** (1993) 3–32, `hep-th/9207016`.

[222] G. T. Horowitz and S. F. Ross, "Naked black holes," *Phys. Rev.* **D56** (1997) 2180–2187, `hep-th/9704058`.

[223] K. Behrndt, "About a class of exact string backgrounds," *Nucl. Phys.* **B455** (1995) 188–210, `hep-th/9506106`.

[224] R. Kallosh and A. D. Linde, "Exact supersymmetric massive and massless white holes," *Phys. Rev. D* **52** (1995) 7137–7145, `hep-th/9507022`.

[225] P. S. Aspinwall, "K3 surfaces and string duality," `hep-th/9611137`.

[226] T. Eguchi, P. B. Gilkey, and A. J. Hanson, "Gravitation, gauge theories and differential geometry," *Phys. Rept.* **66** (1980) 213.

[227] M. A. Walton, "The heterotic string on the simplest Calabi-Yau manifold and its orbifold limits," *Phys. Rev.* **D37** (1988) 377.

[228] L. J. Romans, "Massive N=2a supergravity in ten-dimensions," *Phys. Lett.* **B169** (1986) 374.